NEURAL NETWORK BASED HYBRID MODELLING AND MINLP BASED OPTIMISATION OF MSF DESALINATION PROCESS WITHIN gPROMS

Development of Neural Network based Correlations for Estimating Temperature Elevation due to Salinity, Hybrid Modelling and MINLP based Optimisation of Design and Operation Parameters of MSF Desalination Process within gPROMS

MD Tanvir Sowgath

Submitted for the Degree of Doctor of Philosophy

School of Engineering Design and Technology

University of Bradford, UK

2007

To my Parents

Abstract

Keywords: MSF Desalination Process, Neural Networks, Modelling, Simulation, Optimisation, Water Demand, Design, Operation, Flexible Scheduling

Desalination technology provides fresh water to the arid regions around the world. Multi-Stage Flash (MSF) distillation process has been used for many years and is now the largest sector in the desalination industry. Top Brine Temperature (TBT) (boiling point temperature of the feed seawater in the first stage of the process) is one of the many important parameters that affect optimal design and operation of MSF processes. For a given pressure, TBT is a function of Boiling Point Temperature (BPT) at zero salinity and Temperature Elevation (TE) due to salinity. Modelling plays an important role in simulation, optimisation and control of MSF processes and within the model, calculation of TE is therefore important for each stages (including the first stage, which determines the TBT).

Firstly, in this work, several Neural Network (NN) based correlations for predicting TE are developed. It is found that the NN based correlations can predict the experimental TE very closely. Also predictions of TE by the NN based correlations were found to be good when compared to those obtained using the existing correlations from the literature.

Secondly, a hybrid steady state MSF process model is developed using gPROMS modelling tool embedding the NN based correlation. gPROMS provides an easy and flexible platform to build a process flowsheet graphically. Here a *Master Model* connecting (automatically) the individual unit model (brine heater, stages, etc.) equations is developed which is used repeatedly during simulation and optimisation. The model is validated against published results. Seawater is the main source raw material for MSF processes and is subject to seasonal temperature variation. With fixed design the model is then used to study the effect of a number of parameters (e.g. seawater and steam temperature) on the freshwater production rate. It is observed that, the variation in the parameters affect the rate of production of fresh water. How the design and operation are to be adjusted to maintain a fixed demand of fresh water through out the year (with changing seawater temperature) is also investigated via repetitive simulation.

Thirdly, with clear understanding of the interaction of design and operating parameters, simultaneous optimisation of design and operating parameters of MSF process is considered via the application MINLP technique within gPROMS. Two types of optimisation problems are considered: (a) For a fixed fresh water demand throughout the year, the external heat input (a measure of operating cost) to the process is minimised; (b) For different fresh water demand throughout the year and with seasonal variation of seawater temperature, the total annualised cost of desalination is minimised. It is found that seasonal variation in seawater temperature results in significant variation in design and some of the operating parameters but with minimum variation in process temperatures. The results also reveal the possibility of designing stand-alone flash stages which would offer flexible scheduling in terms of the connection of various units (to build up the process) and efficient maintenance of the units throughout the year as the weather condition changes. In addition, operation at low temperatures throughout the year will reduce design and operating costs in terms of low temperature materials of construction and reduced amount of anti-scaling and anti-corrosion agents.

Finally, an attempt was made to develop a hybrid dynamic MSF process model incorporating NN based correlation for TE. The model was validated at steady state condition using the data from the literature. Dynamic simulation with step changes in seawater and steam temperature was carried out to match the predictions by the steady state model. Dynamic optimisation problem is then formulated for the MSF process, subjected to seawater temperature change (up and down) over a period of six hours, to maximise a performance ratio by optimising the brine heater steam temperature while maintaining a fixed water demand.

Acknowledgements

First, I would like to express my gratitude to my supervisor Professor Mujtaba for his care, support and valuable comments during the research. I am also grateful to my parents for their constant love, prayers, financial support and patience.

I also would like to take this opportunity to thank Mr. John Purvis and Mr. Kevin Knifton for their support.

Table of Contents

List of Tables

List of Figures

List of Papers Published from this Work

1. M.S. Tanvir and I.M. Mujtaba, MSF desalination process: development of neural network based seawater physical property models, In Proceeding of JICEC05 Jordan International Chemical Engineering Conference,2005, V 12-14 September, Amman, Jordan
2. M.S. Tanvir and I.M. Mujtaba, Neural Network based correlations for estimating temperature elevation for seawater in MSF desalination process, Desalination, 195, (2006), 251.
3. M.S. Tanvir and I.M. Mujtaba, Simulation of MSF Desalination Process for Fixed Water Demand using gPROMS and Neural Network based Temperature Elevation Correlation, In Proceeding of IWC2006 Conference, (2006), 300, 12-14 June, Portugal
4. M.S. Tanvir and I.M. Mujtaba, Modelling and Simulation of MSF Desalination Process using gPROMS and Neural Network based Physical Property Correlation, Computer Aided Chemical Engineering, 21B, (2006), 315.
5. M.S. Tanvir and I.M. Mujtaba, Optimisation of Design and Operation of MSF Desalination Process using MINLP Technique in gPROMS, Desalination, 222, (2007), 419
6. M.S. Tanvir and I.M. Mujtaba, Optimisation of MSF Desalination Process for Fixed Water Demand using gPROMS, Computer Aided Chemical Engineering, 24, (2007), 763.
7. M.S. Tanvir and I.M. Mujtaba, Reduce Fouling and Frequent Shutdown of MSF Desalination Plant by Flexible Design and Operation, submitted to TCE, IChemE, 2007

Chapter 1

Introduction

1.1 Introduction

The natural phenomenon of hydrology/water cycle (Figure 1.1), which occurs on the earth for millions of years to supply the fresh water to sustain the human and other lives on earth, is a combination of membrane and distillation process. In natural water cycle, water evaporated from the sea is ultimately returned to the earth as rain, surface water or underground flow thus it completes the distillation cycle of water. Groundwater flow infiltrates the surface water and groundwater returns to the sea/lakes through infiltration and thus it can be called natural membrane process.

Although seawater is abundant, it is too salty to sustain human life or farming/industrial potential and therefore the fresh water is mainly supplied by industrial desalination technology.

Water is the essence of life. Desalination technology provides fresh water to the arid regions and the gulf countries. Moreover, desalination technology is an alternative source of fresh water in many regions. To meet the demand fresh water for different human activities, reducing fresh water cost is also necessary. These can be achieved by improving desalination plants performance and operation.

There are several desalination processes including the Multi Stage Flash (MSF) process which is widely used and is most energy intensive. This process is the main focus of this study.

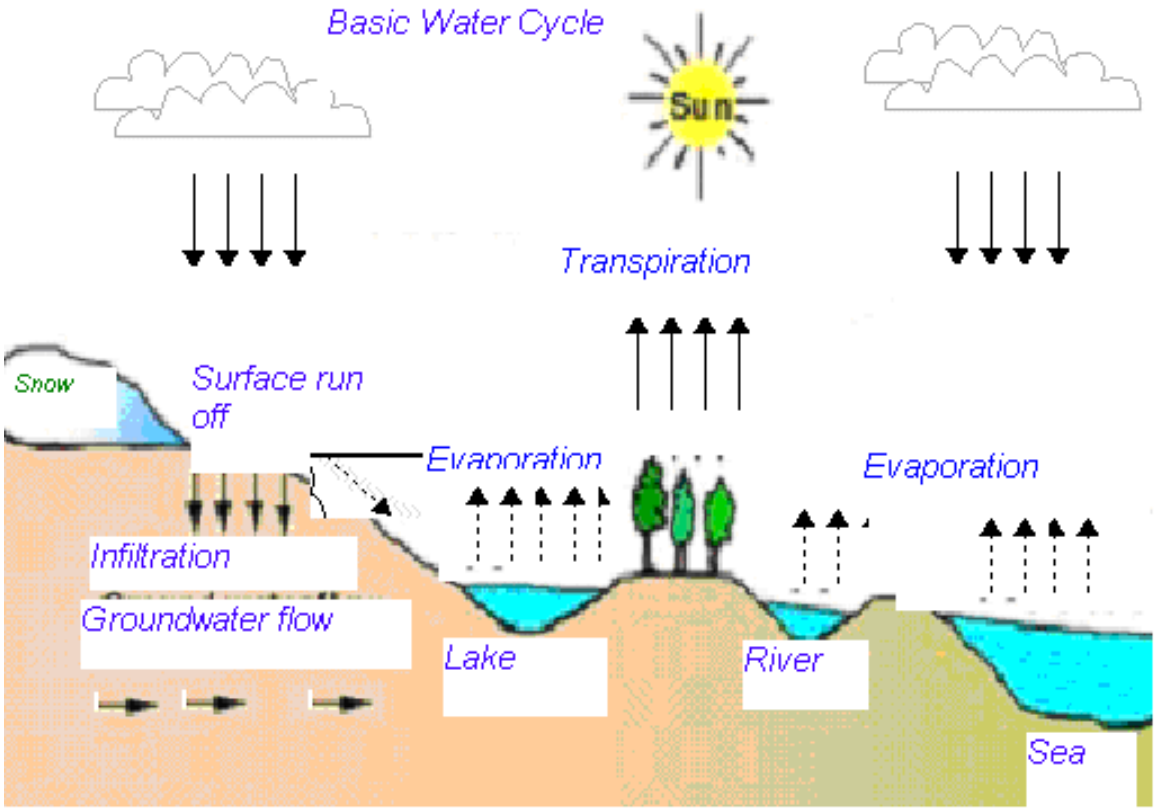

Figure 1.1 Basic Hydrology Cycle

1.2 Global Water Issues

Like most other natural resources, fresh water is not evenly distributed on earth. Although seawater is abundant, the available water in the ocean and sea is saline and is not suitable for normal human consumption. Moreover, only 2.5% of total water resource is fresh water and 80% of it is frozen in the icecaps. Twenty five percent (25%) is consumed by industry, 10% is consumed for drinking and 65% is used for agriculture. At present about 40% of world's population is suffering from water shortages and this is expected to increase to more than 60% (El-Dessouky and Ettouney, 2002).

The supply of fresh water around the world becomes tighter by the day due to the weather

pattern change, intense agricultural practice, industrialisation, population growth and above all to maintain the high living standard. Without supplying the adequate amount of fresh water, the sustainable industrial production will become impractical. Moreover, the continuous rise in world population, industrialisation and agricultural production and changes in the lifestyle makes the industrial desalination a major source for providing the water supply for arid regions of the world and during droughts.

1.3 The Role of Desalination for Combating Water Crisis

Desalination is a science where fresh water can be obtained from the saline water. However, the scope of desalination technology nowaday is not only a water treatment technology to produce the freshwater from the seawater but also water treatment technology for effluent waters and production of ultra pure water for modern electronic industry.

Over the recent decades, industrial scale desalination technology brings life to oil rich arid regions and the technology has been developed at a very high rate (Wangnick, 1991). Renewable water source will become scarce over the next century. The development of arid and semiarid region over the last decades depends on the desalination by supplying the fresh water.

Although, the desalination has some demerits from economical and environmental point of view such as high costs, energy intensity, this technology can provide the fresh water over the drought period and work as substitute for other water supply technologies in many regions. Technically advanced process makes the desalination process economically viable technology for supplying fresh water..

Desalination has a direct impact on combating the global problem of water shortage in the

last decades and it brings the life over the years in different parts of the world. Over the recent decades, it saves operational cost in the arid region for combating the water crisis. Moreover, many countries are experiencing water shortages because of growing demand of the fresh water and developed countries (USA, UK and Japan) as well as the developing countries (Pakistan, Malaysia and India) are using the desalination technology to provide freshwater. Note, desalination technology has fewer health risks compared to other alternative technologies for supplying water such as: water-recycling technology. The excessive use of underground water affects the ground water and contaminates the water. Also, the transportation of fresh water or other conventional ways to supply fresh water are not viable to provide the fresh water at a cheap rate in the arid regions, islands etc.

The study of water demand per head around the world shows that, in future, desalination will be a prominent means of supplying fresh water (El-Dessouky and Ettouney, 2002) for future generation and sustainable development. To make desalination as a sustainable technological option, the process needs to be improved in terms of better design and operation requiring as minimum energy as possible (which is the focus of this work).

1.4 Types of Desalination Processes

According to the type of energy it consumed and types of technology it used, the commonly used industrial desalination processes (Figure 1.2) can be classified broadly into two groups:

- Heat consuming or thermal process
- Power consuming or membrane process

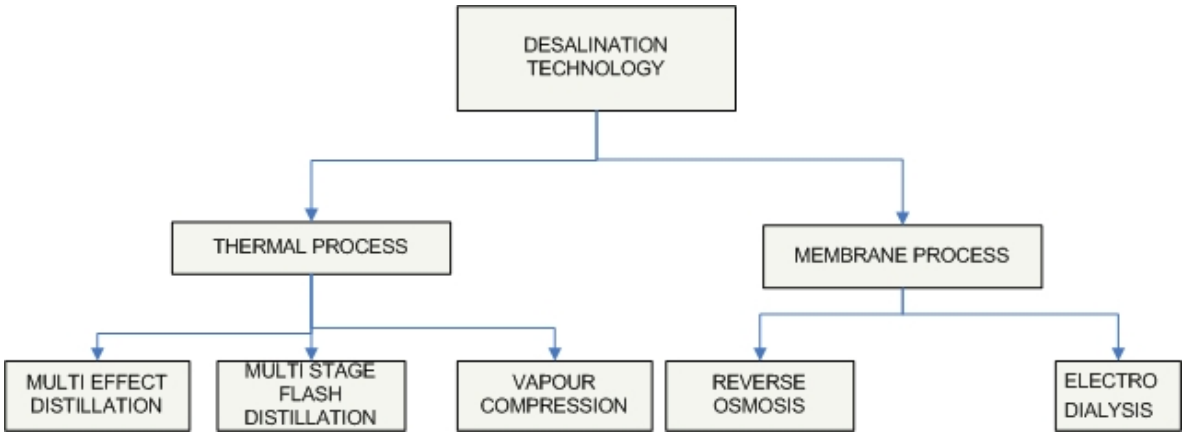

Figure 1.2 Common Industrial Desalination Processes

1.4.1 Thermal process

Thermal process is the oldest desalination technology and reliable process because of good amount of experience. Thermal process is the combination of evaporation of water from brine and condensation of water vapour.

According to the phase change of the thermal process, it can be divided into:

- Multi-Effect Evaporator (MEE)
- Multistage Flash Distillation (MSF)
- Thermal or Mechanical Vapour compression (TVC or MVC)

MEE and MSF are mainly dominant in the thermal desalination field. Vapour compression desalination uses power directly.

MSF process

MSF process (Figure 1.3) became popular as industrial desalination after 1960 because of its simple construction and control. About 56% of the total installed desalination process is MSF (Hussain, 2003). In MSF process, seawater evaporates into the vessel with lower pressure than the saturation pressure. The seawater is preheated by condensing vapour from the stage and then is superheated at an elevated temperature TBT (90-125^{o}C) according to the type of pre-treatment used and constituents present in the seawater. Flashing process is continued in each stage to achieve the equilibrium with current stage. See further details of MSF process in Chapter 2 (2.1).

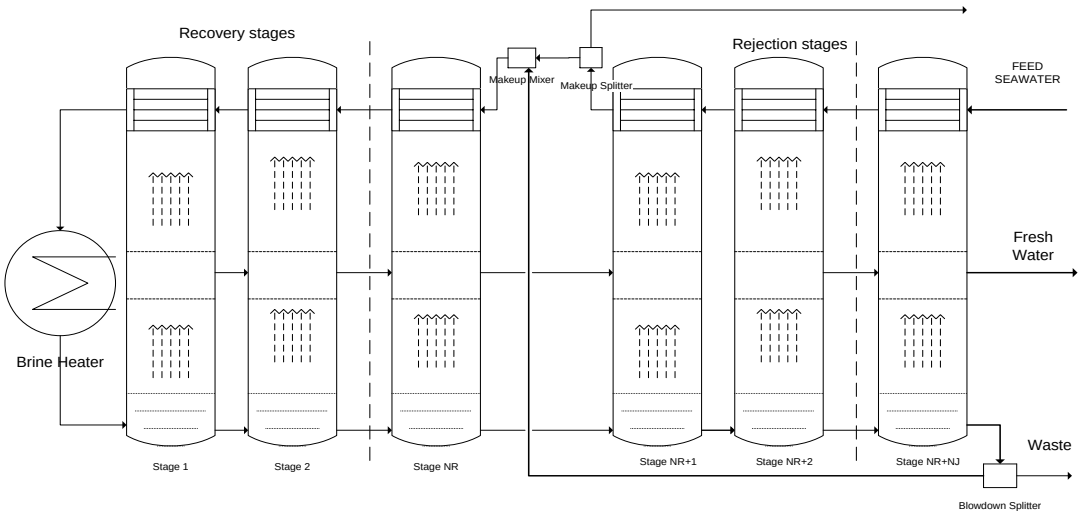

Figure 1.3 A Typical MSF Desalination Plant (source: Spiegler, 1977)

MEE process

MEE (Figure 1.4) was the first distillation process to produce fresh water from the seawater. Several configurations of evaporators are reported in the literature. Among them,

vertical and horizontal effects MEE are commonly used (El-Dessouky and Ettouney, 2002).

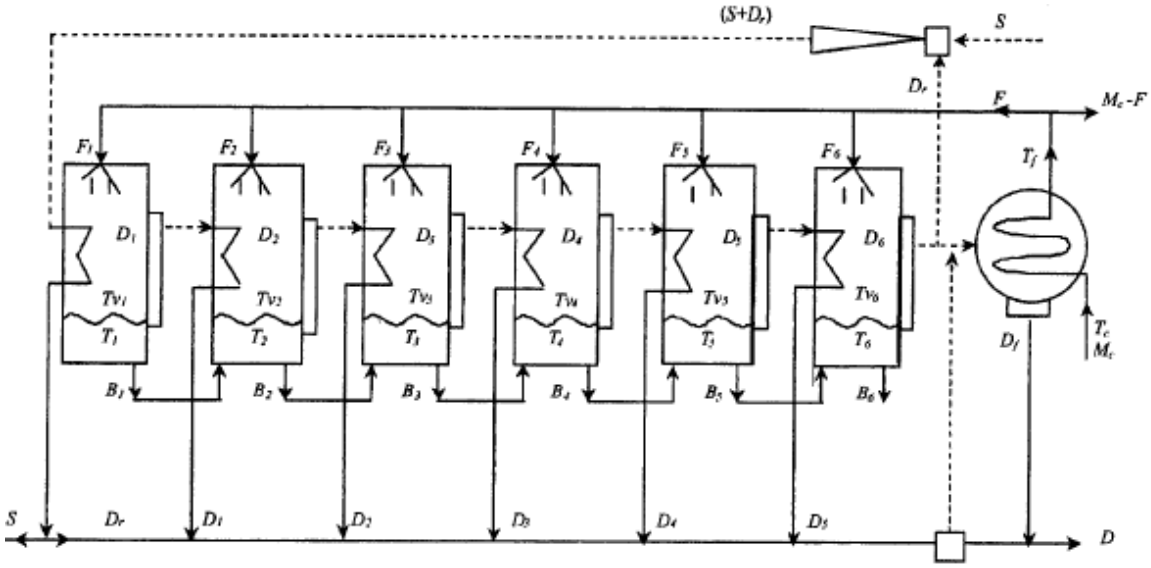

Figure 1.4 MEE (source: Alasfour et al., 2005)

1.4.2 Membrane process

In membrane process the composition of desalted water depends on the membrane characteristics, the feed composition and the amount of recycle steam.

Reverse Osmosis process

RO process is the dominant industrial membrane technology. In biological osmosis process, due to difference in osmotic pressure in two different concentrated solution, solvent flow through the membrane from the concentrated solution to diluted solution to achieve the equilibrium concentration. In Reverse Osmosis (RO) (Figure 1.5) process, much higher external pressure is used to reverse the process. Pure water is flown through the semi permeable membrane. The RO process depends on the quality of semi permeable membrane used and specific power consumption depends on the total dissolved solids in the seawater.

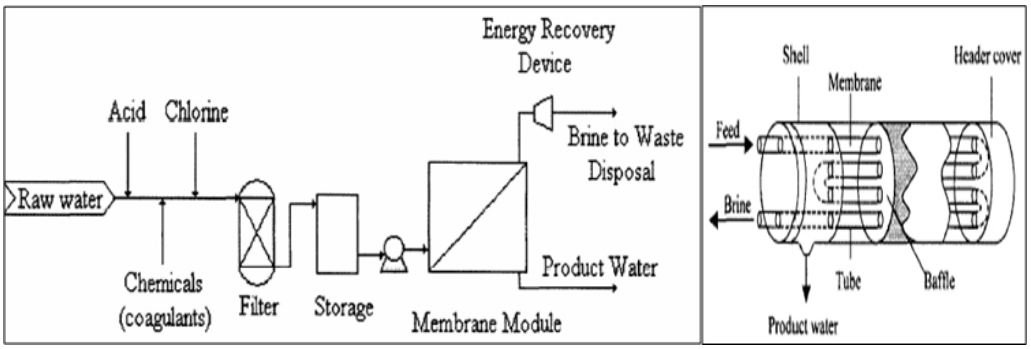

Figure 1.5 Reverse Osmosis (source: Villafafila and Mujtaba, 2003)

1.4.3 Complex plants

More complex process, as a combination of the basic processes, is found in the literature to optimise the efficiency of the energy and to minimise the cost (Marcovecchio et al., 2005). Hybrid process (MSF and RO) and dual purpose (cogeneration of fresh water and electricity production) are typical example of complex desalination processes. MSF-RO series will consume lower energy than the MSF-RO in parallel. Moreover, pre-treatment cost of plant in series will be reduced (Culotta et al. 2003). More successful complex plant examples are dual-purpose where considerable energy and pre-treatment cost is reduced.

1.5 The Choice of Desalination System

The selection of a particular desalination process depends on several factors. One desalting process may be viable to a particular situation, or conversely it is not a viable to other situation. There is no unique desalination process, which is economical / technical viable solution for any particular region. The decision to purify fresh water from the seawater depends on political decision as well as economic (construction costs, local labour costs and fuel costs, etc.), technical (the chemical constituents such as salinity) and environment

factors.

According to the Wangnick's inventory report (Wagnick, 1991) the MSF and RO processes are the pioneer in this field (86% of the total capacity). The remaining 14 percent is made up of other processes. However, thermal desalination process is more suitable for treating water with high salinity (Pearce, . The development of good quality and cheaper membrane and lower fuel consumption makes RO desalination more attractive. The cost of operation for membrane desalination such as electrodialysis and RO is proportional to the salinity of feed water. Reverse Osmosis technique is more suitable for lower salinity water. It is not suitable for electronic industries where high quality water (e.g. distilled water) is required. Water production cost of RO process is less sensitive to energy price than thermal process.

The limited use of RO process in Gulf countries is a result of higher salinity of the seawater. MSF desalination is dominant in Gulf region and it is mainly because of cogeneration of electricity and fresh water. Besides, it can produce large amount of fresh water at lower cost from higher salinity seawater. The RO process is dominant in USA, Japan and other countries where seawater salinity is lower than 35000 ppm and summer average temperature of air and water are below 25^{o}C (Hussain, 2003).

Although RO process is gaining popularity in recent years, the good quality technical water is still supplied by thermal processes to the different chemical industries and power industries for general cooling and boiling applications especially on coastal sites in the other regions of the world. European navy produces potable water form the heavily polluted water found in the commercial harbour by distillation process. The marine industry exercises this technology for their daily needs on board ship (Pearce, 2004).

The MSF technology is very robust technology of with minimal requirements of particle

sizes to enter the plant. The MEE plant constrains coarse particle filtration for water entering the condenser tubes. The RO plants need excellent seawater quality such that certain Silt Density Index (SDI) value has to be maintained before seawater is fed into the RO membrane. The conventional pre-treatment is satisfactory for deep seawater but open intake seawater often proves unreliable. Open seawater necessitates special treatment with UF membrane. Deep seawater intake has disadvantage of high investment cost and shallow seawater intake needs to treat the biologically active seawater (Gille, 2003). Several steps involved in industrial desalination project are shown in Figure 1.6. Raw seawater is pre-treated before entering one or more desalination process. The desalted water is then post treated according to the requirement. It is then pumped to the distribution system. The salts and residual brine are discharged back in the sea from the last step.

The cost associated with desalted water considers pre-treatment, post treatment of the seawater and distribution. Overall feasibility of desalination as a project depends on the specific site and types of desalination technology used and environmental factors such as: concentrate disposal, land use, noise, air quality and odour (AWWA, 2004). Desalination technology pollutes air, the nearby seas and land. For the production of freshwater, desalination produces air pollution (namely emission of NOx, SO_2, volatile compounds, particulate, CO_2) that is associated with energy production/consumption. The brine concentrate also contains chemicals (low concentrations of anti-scalants, surfactants, and acid) used in the pre-treatment of the feed water may damage marine life.

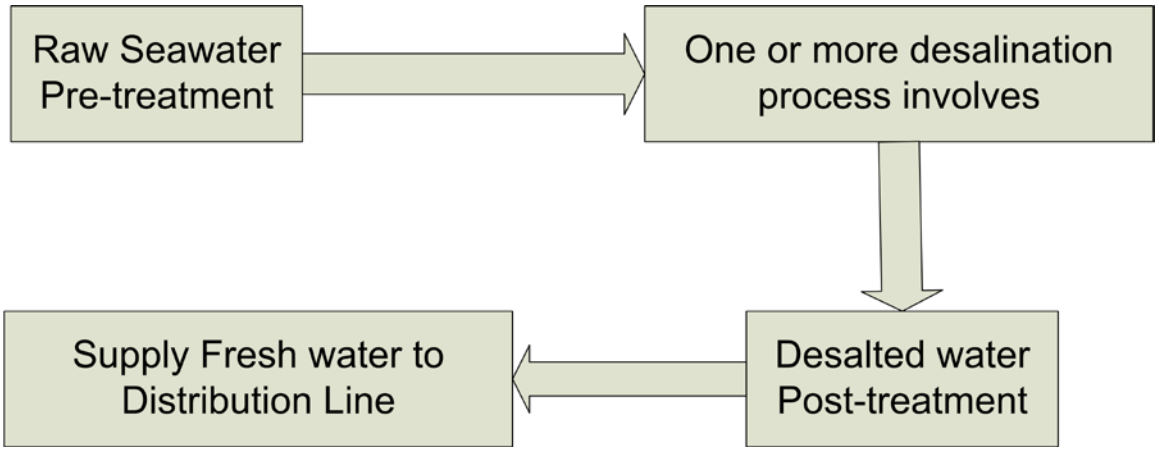

Figure 1.6 Typical Water Supply Steps for Industrial Desalination

(Adopted from AWWA, 2004)

1.6 Scope of this Research

Having given an introduction on (i) the importance of freshwater for life and sustainable development, (ii) the available technologies for making freshwater in the earlier sections, this section highlights the scope of this research. This work is focused on MSF distillation based technology for freshwater production. The ultimate goal is to develop a mathematical model based optimisation framework for optimisation of design and operation parameters of MSF processes.

Referring to Figure 1.2, the design parameters include: (a) number of flash units in the recovery and rejection section, (b) area of heat exchangers in the flash units to condense/recover heat from the flashed vapour, (c) area of heat exchanger of the brineheater, etc. The operating parameters include (a) steam temperature and flow rate to the brineheater, (b) flow rate recycled brine, (c) flow rate of rejected seawater, (d) flash chamber pressures, etc. The degrees of freedom in terms of deciding design and operating

parameters are very large and therefore understanding the interaction between the design and operating parameters is very important. These understandings will help the engineers to set physical bounds on different parameters within which the plant has to be optimised. However, understanding these interactions using a real plant is almost impossible, using a pilot plant would be quite expensive but using a process model is an alternative, cheap and attractive option. Therefore, this approach has been adopted in this work.

The accuracy of predictions from a process model depends largely on the accurate calculations of physical properties such as solubility, density, viscosity, and enthalpy. For MSF process TBT (Top Brine Temperature, described in the next chapter) is an important parameter affecting the design, operation and thus the economics of the process. Accurate calculation of TE (boiling point Temperature Elevation due to salinity, a physical property of saline water) is therefore important to estimate TBT accurately and the boiling point temperature of each flash chamber (Spiegler and Liard, 1980).

With these backdrops, this work focuses on developing several physical property correlations for TE, steady state and dynamic process model, steady state and dynamic optimisation framework. The modelling and optimisation framework is then used for better understanding, design and operation of MSF processes. The detailed aims and objectives of the thesis are outlined below.

1.7 Aims and Objectives of the Research

The aims and objectives of this thesis are summarised below:

- Several Neural Networks (NN) based correlations are developed for estimating TE for given salinity (in terms of weight percent) and BPT (in terms of degree

centigrade). Note, the use of NNs in all aspects of process engineering activities, such as modelling, design, optimisation and control, has considerably increased in recent years (Mujtaba and Hussain, 2001).

- A detailed MSF process model is developed using gPROMS modelling tool. One of the Neural Network based correlations developed above is used to determine the TE. This correlation is embedded in the gPROMS based process model, resulting the hybrid model. The above model is validated using the simulation results reported by Rosso et. al. (1996) before it is extensively used for further investigation.
- Investigations on how the design and operation are to be adjusted to maintain a fixed demand of fresh water through out the year for changing seawater temperature are carried out through repetitive simulation.
- Simultaneous optimisation of design and operating parameters of MSF desalination process is then considered via the application MINLP technique within gPROMS. For a fixed fresh water demand throughout the year, the external heat input (a measure of operating cost) to the process is minimised.
- For three different fixed water demand and for changing seawater temperature the total annualised cost of the desalination (investment and operation cost) required is minimised while optimising the design parameter such as Number of Stages and operating parameters such at Top Brine Temperature (TBT) Steam Temperature (reflects utility cost), Recycled Brine Flowrate and Rejected Seawater Flowrate (reflect pumping cost).
- Finally, a hybrid dynamic MSF process model is developed, validated and simulated with step changes in different parameters. A dynamic optimisation

problem is formulated to maximise the performance ratio of MSF process subject to seawater temperature variation by optimising the brine heater steam temperature.

1.8 Thesis Layout

The layout of this thesis is presented below.

Chapter 1: Introduction

A general introduction, global water crisis and the role of desalination technology on combating the water crisis are described in this chapter. Literature reviews on different commercial desalination processes, the selection of the particular desalination technology and the historical context of the industrial desalination technology are presented here with particular emphasis on MSF process. The aims and objectives of this research and the thesis layout are also presented.

Chapter 2: Literature Review

The aspects of modelling simulation and optimisation with reference to MSF process are reviewed. Brief description of the importance of the TBT in the MSF process modelling and different optimisation techniques and their solutions within gPROMS are also discussed.

Chapter 3: Neural Network based Correlation for TBT

A general overview of the neural network techniques and neural network based applications in process engineering is presented in this chapter. Several Neural network based correlations for predicting TE have been developed and validated with the different experimental data sets and compared with the different empirical

correlations from the literature.

Chapter 4: Modelling, Simulation and Optimisation in gPROMS

Important features of gPROMS model Builder software package that has been used for modelling, simulation and optimisation is discussed in this chapter. The brief description of the graphical user interface development and the connectivity to the different mathematical software and MS Office software through gPROMS foreign process and object interface is also highlighted.

Chapter 5: Simulation of MSF Process for Fixed Water Demand

A detailed steady state mathematical MSF process model is presented here with validation of results from the literature. The effect of changing process parameters on the MSF process performance to maintain the fixed water demand are presented and analysed in this chapter.

Chapter 6: Simultaneous Design and Operation Optimisation of MSF Process

An MINLP based graphical gPROMS model is developed here. Performance and economic optimisations are carried out for different seawater temperature for different fixed water demand. Sensitivity of the different cost parameters is also investigated.

Chapter 7: Dynamic Simulation and Optimisation of MSF process

A detailed dynamic MSF process model incorporating NN base correlation for predicting TE is presented in this chapter. The model prediction at the steady state condition is validated with those available in the literature. The dynamic responses of

the MSF process model are qualitatively analysed. Finally, dynamic optimisation within gPROMS for fixed water demand is carried out.

Chapter 8: Conclusions and Future Recommendations

The final conclusions and suggested future recommendations of this work are presented.

Chapter 2

Literature Review

2.1 Introduction

In this chapter, first, general literature reviews on MSF process, process modelling and simulation and process optimisation are presented. Then, a brief literature reviews on MSF process modelling, simulation and optimisation are presented. Detailed literature reviews on physical property correlations based on empirical methods, on Neural Network techniques and features and capabilities of gPROMS software are presented in Chapter 3 and 4 respectively. Further literatures relevant to this work on modelling; simulation and optimisation of MSF process are discussed in Chapters 5-7.

2.2 MSF Process

2.2.1 Introduction

Distillation is the oldest of all desalination technologies. Multi-Stage Flash (MSF) distillation process has been used for many years and is now the largest sector in the desalination industry. MSF process produces 56% of the total fresh water produced by desalination technologies (Hussain, 2003). An MSF process (Figure 2.1) mainly consists of brine heater section, recovery and rejection sections each with a number of flash chambers (stages). Seawater enters into the last stage of the rejection stages and passes through a series of tubes to remove heat from the stages. Before the rejection section seawater is partly discharged to the sea to balance the heat. The other part is mixed with recycled brine

form the last stage of the rejection section and fed before the last stage of the recovery section. Seawater flowing through the tubes in different stages to recover heat from the stages and the brine heater raises the seawater temperature to the maximum attainable temperature (also known as Top Brine Temperature, TBT). After that it enters into the first flashing stage and produce flashing vapour. This process continues until the last stage of the rejection section. The concentrated brine from the last stage is partly discharged to the sea and the remaining is recycled as mentioned before.

A typical MSF process model includes mass and energy balances and various physical properties.

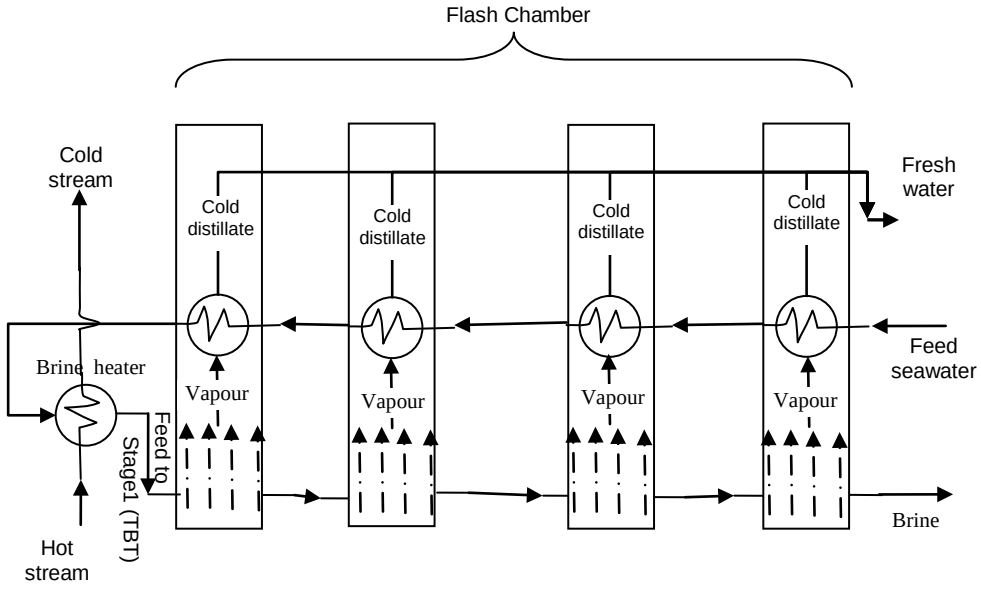

Figure 2.1. A Typical MSF Process

Adequate knowledge of the total heat transfer area, the length of the flash chamber, control of the corrosion and scale formation are needed for modelling, design and scale up of MSF processes. These parameters are dependent on/ inter-related with the TBT (also known as the maximum attainable temperature) (Spiegler and Liard, 1980). The optimum TBT is

controlled according to the types of pre-treatment in the process (Nada, 2002). The TBT is one of the important parameters needed for designing, modelling, simulation and optimisation of the process. In a typical MSF process model the TBT, which is the maximum attainable temperature of the MSF process, is the outlet temperature of brine heater or the feed entering into the first stage (Figure 2.1). This temperature is also the boiling point temperature (BPT) for seawater entering the first stage. According to the Dühring's rule (Foust et. al, 1980), the seawater BPT is usually calculated by summing up the BPT of pure water at a given pressure and the TE due to salinity. Note the TE is a function of the dissolved solids concentration and BPT. The accurate measurement or estimation of seawater physical properties (density, heat capacity, BPT, TE, etc.) is of considerable importance in the development, design and operation of desalination plants. For example, if more than 20 stages are connected in an MSF plant, small error in calculating TE can lead to considerable errors in the calculation of heat transfer area, length of the flash chambers, etc. (Spiegler and Liard, 1980).

Several correlations for estimating the TE exist in the literature (Bromley et al., 1974). The seawater composition (Total Dissolved Solid (TDS), different salts such as Boron, Calcium and the acidity of the seawater) varies for different plants located over various regions. As seawater compositions are subject to wide variations over a wide operating range and seawater condition for different plant, therefore, these correlations can lead to inaccurate predictions of physical property. Good correlations, which act over a wide range of operation and composition of seawater, are therefore necessary for modelling, simulation, and design of MSF processes.

Seawater undergoes seasonal temperature variation. For a given plant design (fixed configuration in terms of recovery and rejection stages, volume of stages, sizes of heat

exchangers, etc.) and operation (fixed TBT, flowrates, steam temperature, etc.) increasing seawater temperature (winter to summer) will certainly affect the performance of the MSF process. On the other hand, it is true that water consumption increases during the summer than in the winter.

Simulation and optimisation help achieving better design and operation of desalination processes leading to low cost production of fresh water. The cost of energy of MSF processes is almost equal to the total other cost. So, the energy optimisation in MSF processes is very important. Modelling of MSF processes played a very important role over the years in simulation, optimisation and control (Maniar and Deshpande, 1996).

Several configurations of the MSF desalination systems are found in the literature, which is developed over the year:

- Single stage Flash
- Once through MSF
- Simple mixer brine recirculation
- Conventional MSF (such as One Stage Heat rejection Brine Circulation MSF, Two Stage/Multiple Heat Rejection and Multiple Brine Recirculation)

As described earlier, Conventional MSF plant (Figure 2.2) consists of three major sections: the brine heater, the recovery section and the heat rejection section where several flash stages arranged in two separate groups, namely, the recovery and rejection stages and includes:

- A large brine pool
- The demister (is formed of the wired mesh)

- The tube bundle of the condenser and preheater.
- The distillate tray
- Water boxes at both ends of the tube bundle
- Connections for venting system.
- Instrumentation: thermocouple, level sensor and conductivity meter
- The number of stages in the heat recovery section is larger than the heat rejection section.
- The brine heater

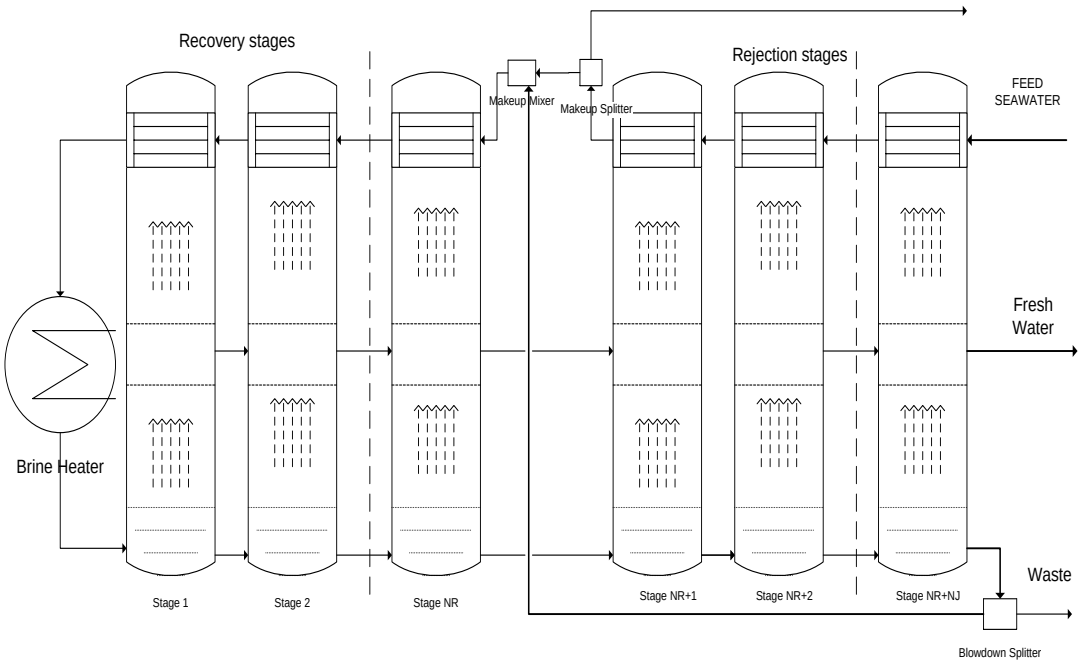

Figure 2.2 A Typical Conventional Multi Stage Distillation

Each stage consists of a flash chamber, vapour space, a tube bundle and a fresh water-collecting tray. Inside the tube bundle flows the cooling brine, which is heated by condensation of vapour outside the tubes.

2.2.2 The role of TBT in MSF process

Physical property of seawater plays an important part in designing thermal desalination plants. With the increase of number of stages connected into series, error in the boiling point calculation of each stage could make substantial differences in the results (Spiegler and Liard, 1980).

Since the early days of the commercial multistage flash evaporator, one of the important design parameter was what is the optimum operating top brine Temperature. The decision was governed by the type of feed pre-treatment chosen (Nada, 2000).

The top brine temperature is the highest saturation temperature of a thermal desalination plant. In MSF process, the main objective is to produce more distillate by using higher temperature economically over a justifiable temperature range. The feed is boiled above its saturated pressure at the brine heater. The highest temperature (TBT) is thus obtained. After the brine heater, the feed is throttled to flash chamber at a lower pressure corresponding to its saturation pressure. The choice of TBT depends upon a number of factors (Spiegler and Liard, 1980) as described below.

- Surface area of the condenser
- Scale formation and corrosion control
- Recycle ratio
- Performance ratio

Surface area of the condenser

Vapour release temperature of stages affects both performance and surface area. That is why, it is necessary to optimise the heating process and vapour release by flashing occurring in the expansion process. However, the increase of vapour release temperature reduces the heating area of the brineheater but increases the condensing area of stages. So, the condenser surface area will affect the selection of TBT and vice versa.

Scale formation and corrosion control

Scale formation and corrosion is one of the key factors in designing any process nowadays. Scale formation and corrosion are dependent on the top brine temperature and the chemicals, which are used to prevent scale formation and corrosion. The maximum brine temperature at which a desalting plant can be operated without the danger of depositing scales on the evaporator and the heater tubes depends on the type of process cycle and the method of scale control used. If seawater is heated much above ambient temperature some of the dissolve salts crystallize and precipitate out in the form of a scale crust on the evaporator. Therefore, it decreases the total heat transfer area and will reduce heat transfer co-efficient; consequently, it decreases the overall cycle efficiency.

Recycle ratio

The small recycle flow needs a high temperature operation of the plant. Also, possibility of degasifications minimises the corrosion of the evaporator material. However, the high brine concentration increases the top brine temperature.

Performance ratio

The performance ratio (the amount of fresh water produced per amount of steam used) can

be increased without increasing the plant size investment cost by increasing the flashing temperature (TBT).

The increase in top brine temperature (TBT) decreases the plant size (number of stages) consequently. However, the increasing TBT increases cost of material of construction, cost of scale control and corrosion control and recycle ratio. The magnitude of the boiling point elevation (TE) of the thermal desalination process depends on the nature of chemicals or additives used to control the scale and corrosion and the state of heating system. Therefore a reliable correlation of the top brine temperature (TBT) of desalination plants and process is essential for plant designers.

2.3 Process Modelling and Simulation

2.3.1 Process modelling

In a model, real process that is being investigated is represented using mathematical expression which predicts the real process behaviour. A typical chemical engineering model includes the mass and energy balance, physical property correlations, chemical kinetics, etc. and can be described by nonlinear sets of algebraic equations (for steady state process) and differential algebraic equations (for dynamic process) (Pantelides et al., 1988).

Due to the advancement of the microcomputers, the models are now directly connected to the plant operation to carry out the plant performance calculations, generate management information and also to perform limited alarm diagnostic. With the improvement of the microcomputers and availability of the cheaper microcomputers, process modelling using the microcomputers has become cost effective.

Two types of modelling are prominent in chemical engineering. A steady state model

ignores the changes in process variables with time whereas the dynamic model considers dynamic characteristics. The dynamic models are useful to understand the start-up and shutdown characteristics of the process (Ingham et al., 1999)..

The typical modelling approach (Figure 2.3) in recent years for simulation and optimisation uses numerical solvers. The numerical solvers may involve SQP based methods or any other non-gradient based optimiser such as GA, SA algorithm and in simulation the solver may involve Newton-Raphson method, etc.

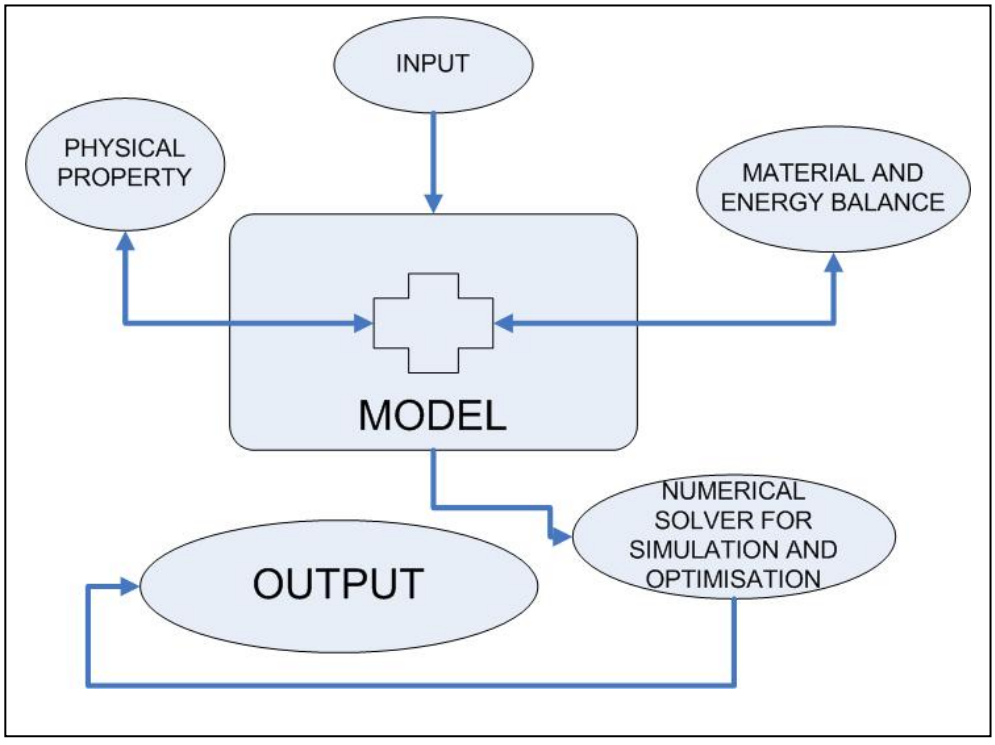

Figure 2.3 Typical Simulation and Optimisation Architecture

There are several approaches to develop hybrid model found in the literature (Mujtaba. and Hussain, 2001). In this work, a hybrid model (Figure 2.4) is developed by combining the first principle based model (e.g. mass and energy balance) with NN based correlation (e.g. physical property calculations).

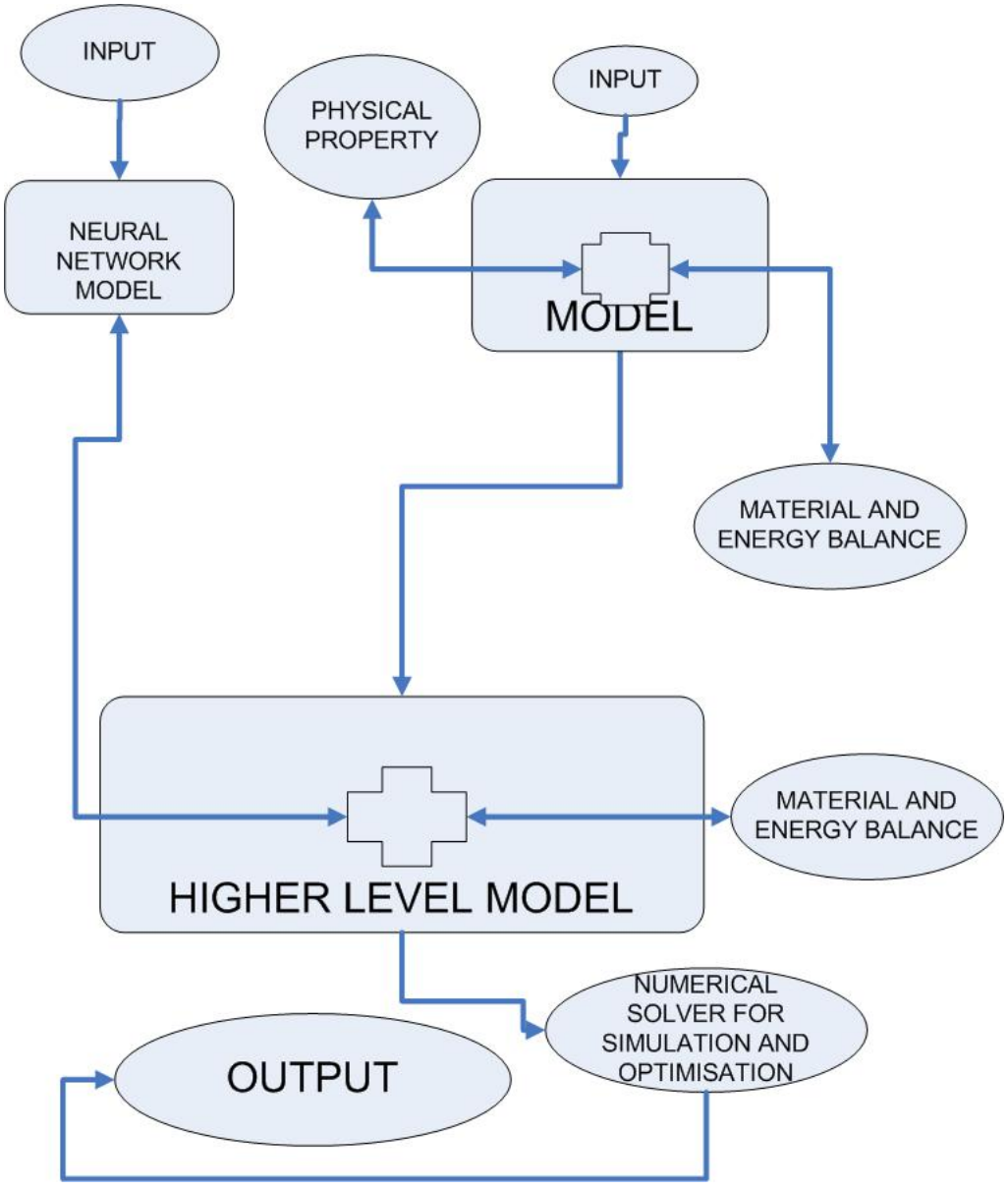

Figure 2.4 Hybrid model for Simulation and Optimisation Architecture

2.3.2 Simulation

Simulation is the technique for design validation; process integrity and operation study (Ingham et al., 1999). Any experimental work is expensive and the real plant operation is an expensive and time consuming. Computer aided modelling, simulation and optimisation saves the time and money by providing the fewer configuration of the experimental work. In addition, computer simulation, optimisation saves the money in design and operation.

The long-term performance and reliability of individual plant vary from plant to plant and day to day for various reasons such as operating conditions, scaling and fouling of heat transfer surfaces in boilers and different desalination units. Therefore, better operations of the existing plant depend on the better understanding of the different parameters of the plant. Simulation helps to visualise the ultimate picture and trends of various conditions of existing plant as well as those of a new situation of the plant (Maniar and Deshpande, 1996).

2.4 Process Optimisation

The chemical industries are facing challenges due to increase in cost of energy, environmental regulations and global completion in product quality and pricing. Moreover, for certain product, specialised quality product to meet the customer demand is a great challenge.

The most feasible technical and economical solution is achieved by optimisation technique. Optimisation techniques especially provide an efficient way to minimise the cost of operation or maximising the profit by better operation and management. Typical chemical engineering problem have many solutions. Optimisation technique and along with

computer software makes it efficient, feasible and cost effective to achieve better production, maximum profit and minimum cost and so on for an existing plant operation.

Optimisation technique has become a major quantitative tool to meet all these challenges in different fields of science, engineering and business. Different types of optimisation solvers are widely accepted tools to design new plant and its operation (Vassiliadis et al., 1994).

Some of the basic steps have been suggested to develop the optimisation model in the literature (Edgar, 2001) are:

- To optimise a process an objective function, equality constraints and inequality constraints mast be defined.
- The optimisation model represents the referred process which takes into account bounds on the variables, empirical relations and physical laws.

The most of the optimisation solvers are based on the NLP (Non linear Programming) algorithm. The basic steps that are suggested in the literature (Pardoe,1990) (www.psenterprise.com) to avoid the failure in the NLP optimisation solvers are:

- Parameter adjustments: In most of the solvers default tolerances are set. So according to the problem the parameters should be adjusted.
- Scaling: The performance of the most NLP solver greatly influenced by relative scale of the variables and functions.
- Model formulation: Discontinuities or undefined function arguments should be avoided.
- Starting points: The performance of the solvers strongly depends on the initial guess

of the variables. The starting points of physical systems should represent realistic operating conditions.

- Local and global optimum: The user should check that the results are feasible or not.

2.4.1 MILP and MINLP based optimisations

Mixed Integer Linear Programming (MILP) and Mixed Integer Nonlinear Programming (MINLP) refer to mathematical programming with continuous and discrete variables and linearities or nonlinearities in the objective function and constraints. MILP and MINLP have been widely used over the years in several industries including process industries (Kondili et al., 1993; Mussati et al., 2004). MINLP algorithms can handle large-scale, highly combinatorial and highly non-linear problems.

In general, MINLP based optimisation has been described mathematically as:

$$\text{minimise } z = f(x,y)$$

$$\text{subject to } g(x,y) \geq 0$$
$$x \in X$$
$$y \in Y \quad \text{(integer, binary or other)}$$

Where $f(x,y)$ is a nonlinear objective function which describes the model of the process and inequalities $g(x,y)$ is nonlinear constraint function or specification. The variables x, y are the decision variables, where y denotes integer, binary or enumerated variable and x is continuous variable.

Many process-engineering problems such as plant operation, design, location and scheduling problem often contain alternative solutions that are not continuous (Sharif et al., 1998). These decision variables are binary, integer and other kinds. In the past, these problems are treated as a continuous problem and round the real variables to nearest integer values that leads to a sub optimal (Mujtaba and Macchiettto, 1996). As a consequence, operation of these processes may lead to big economic penalty.

However, with the development of sophisticated computers and numerical methods mixed integer programming (MILP, MINLP) is more desirable to handle global optimisation system with discrete and continuous variables. Due to advancement in the optimisation algorithm and modelling software such as (GAMS, gPROMS), MINLP optimisation techniques have been used in several process engineering fields for process design and synthesis. An extensive literature survey can be found in the literature. Some of the prominent applications using the MILP, MINLP based technique are described below.

- Feasible product schedules (Shah et al., 1993)
- Multi period optimisation of dynamic systems (Sharif et al., 1998)
- Supply chain management (Papageorgiou et al., 2001)
- Synthesis of heat exchangers (Yee et al., 1990)

2.4.2 MINLP solution methods

Outer Approximation (OA), Branch-and-Bound (B&B), Extended Cutting Plane, and Generalized Bender's Decomposition (GBD) are some of the well known methods in the literature for solving MINLP problem.

Branch and Bound methods

It is the most popular approach (Floudas, 1995). It can handle both linear, nonlinear relations among continuous variables and binary variables or integer variables that appear linearly.

Mathematically, it can be written as:

$$\text{minimise} \qquad z = f(x, y) + c^T y$$

$$\text{subject to} \qquad h(x) = 0$$
$$g(x) + My \leq 0$$
$$x \in X$$
$$y \in Y \qquad \text{(integer, binary or other)}$$

where, x is the continuous variables, y is the integer variables, M is the matrix of the binary variables.

Outer approximation

Duran and Grossman (1986) and Floudas (1995) introduced the outer approximation (OA) algorithm for solving MINLP problems. In each major iteration, it solves two subproblems: a continuous variable nonlinear program (NLP) and a linear mixed-integer linear program (MILP).

- NLP sub-problem

$$\text{maximise} \qquad z = f(x) + c^T y^k$$

$$\text{subject to} \qquad h(x) = 0$$
$$g(x) + My^k \leq 0$$
$$x \in X$$

The optimal objective value of this problem is the lower bound on the MINLP optimal value. At iteration k, it is formed by linearization of all the nonlinear function about the optimal solutions.

- MILP sub-problem

$$\text{maximise} \qquad z + c^T y$$

$$\begin{aligned}\text{subject to} \qquad & z \geq f(x) + \nabla f^T(x)(x - x_i), \quad i = 1, \cdots k \\ & h(x^i) + \nabla h^T(x^i)(x - x^i) = 0, \quad i = 1, \cdots k \\ & g(x) + \nabla g^T(x^i)(x - x^i) + My^i \leq 0 \\ & x \in X, \qquad y \in Y\end{aligned}$$

Disjunctive programming

Occasionally, MINLP model formulation is difficult task, the logic base technique called disjunctive programming make possible to handle the nonlinearities by using the logic variables.

The general form of this technique can be expressed as:

$$\text{minimise} \qquad z = f(x) + \sum_{k \in K} c_k$$

$$\begin{aligned}\text{subject to} \qquad & g(x) \leq 0 \\ & h(x) = 0 \\ & x \in X \\ & y \in Y \quad (\text{true, false})^m\end{aligned}$$

Reviews of MINLP optimisation techniques can be found in the literature (Edgar, 2001). A

summary of the MINLP optimisation techniques is carried out by different researchers has been shown in the Table 2.1.

Table 2.1 Summary of the MINLP based optimisation techniques (Edgar et al., 2001)

Researchers (Year)	Fields
Guptaand Ravindran (1985) Borchers and Mitchell, 1994; Leyffer, 2001	Branch& Bound (BB)
Raman and Grossman (1994)	Disjunctive programming
Grossmann and Duran (1986)	Outer-Approximation
van Roy and Wolsey (1986)	LP/NLP based Branch & Bound

2.4.3 Modelling and simulation of MSF desalination process

The development of the thermal desalination process model is similar to other standard chemical process. The mass and energy balance and the operation of the equipment are determined by nonlinear equations. All the thermal stage (effect) and recycle stream are used for producing the required amount of product and packets of equations for flash stage (effect) are repeated number of times. The process performance depends on the heat transfer system.

Due to the increase of the fossil fuel price in recent years, energy optimisation and better control and operation of existing plant is necessary in desalination like other chemical process to utilise the energy efficiently. Simulation and optimisation would be able to provide valuable saving in the operation and deign by utilising the energy and chemicals more efficiently. The pioneering work on MSF desalination is due to (Husain, 2003). Numerous studies on modelling and simulation of MSF plants are available in the

literature. Among them are steady state modelling studies by Beamer and Wilde (1971), Hayakawa et al. (1973), Helal et al. (1986), and El-Dessouky and Ettouney (1997) and dynamic modelling studies by Glueck and Bradshaw (1970), Delene and Ball (1971), Rimawi et al. (1989) and Husain et al. (1994).

Several methods have been used for solving the MSF process model equations. Among them are: S*equential Iterative Method* (Glueck and Bradshaw, 1970; Beamer and Wilde, 1971; Hayakawa et al., 1973), *Tri diagonal Matrix* (TDM) (Helal et al., 1986;Husain et al., 1994) and *Equation Oriented Solvers* in Commercial Software (Husain et al. 1993, 1994) such as SPEEDUP. El-Dessouky and Bingulac (1996) applied an iterative method containing five loops that were implemented using iterative package Line Algebra and Systems (LAS).

2.4.4 Optimisation of MSF desalination process

Mussati et al. (2004a) considered formulation of two different types of optimisation problems where total entropy and total annualised cost were minimised while optimising the number of stages and the amount of heat supplied for a given water demand, total heat exchange area and for a single seawater temperature. A very simple model was considered in the work. However, the main purpose of the work was to develop optimisation algorithm to solve the problem where model reformulation was required.

Mussati et al. (2004b) considered minimisation of total annualised cost for dual purpose plant (desalination and electricity) while optimising the configuration of plant equipment (MSF with fixed number of stages, gas turbine, steam turbine, pre-heater, splitter, heat transfer area, etc) for a given water demand and for a single seawater temperature. Amount of electricity generated was an output of the solution of the optimisation problem. A

detailed model (Griffin and Keller, 1965; El-Dessouky et al., 1995) implemented in GAMS (General Algebraic Modelling System) (Brooke, 1992) was considered in the work. However, the main purpose of the work was to develop optimisation algorithm to solve the problem where model reformulation was required.

For a 20 stage MSF process and a given water demand for a single seawater temperature, Mussati et al. (2005) focuses on the minimization of total cost (Valero et al., 1993; Bejan et al., 1996) while optimization a superstructure of alternative configurations of a Dual Purpose Desalination Plants producing water and electricity. The superstructure of alternative configurations and the mathematical model proposed by Mussati et al. (2004b) have been modified in order to include other competitive and optional configurations air-preheater, additional heater in steam generator, condensing steam turbine, etc. They considered MINLP optimization problem formulation within GAMS.

2.5 Conclusions

This chapter highlights different desalination technologies that have been developed over the years and are being operated at different regions of the world. Special attention is given to MSF desalination process and the role of TBT on design and operation is highlighted.

General literature on process modelling and optimisation is presented together with those relevant to MSF process. Further literature on MSF process modelling, simulation and optimisation are provided in later chapters of this thesis.

Chapter 3

Neural Network based Correlations for Calculating Temperature Elevation

3.1 Introduction

The use of Neural Networks (NNs), in all aspects of process engineering activities, such as modelling, design, optimisation and control, has considerably increased in recent years (Mujtaba and Hussain, 2001). Different NN based techniques (architecture, training) have been adopted in different field of science to overcome the difficulties of first principle based modelling. The non-linear relationship between input and output of a system can be built up cost effectively by NNs.

In this chapter, NNs are used to develop correlations for estimating TE for given salinity (in terms of weight percent) and BPT (in terms of degree centigrade). The ultimate objective is to use these correlations within an MSF process modelling and optimisation framework (see next chapters).

In this chapter, three NN based correlations for three different sources of experimental data are developed and the results are compared with those obtained by the experiments. In addition, one of the NN based correlations is redeveloped by adding more experimental data from other data sources.

3.2 Neural Network Application in Chemical and Process Engineering

Realistic process model is very complicated and time consuming because it consists of a lot of non-linear relation. Even it is unachievable when the basic mechanism is not understood.

Neural networks can learn a non-linear relation from example (input output) and solve the problem easily.

NN has been widely used extensively in chemical engineering. NN has been used over the years such as in process modelling, adaptive control, model based control, hybrid process monitoring, fault detection, dynamic modelling, and parameter estimation process flow sheet simulations, on-line process optimisation and visualization, parameter estimation, fault diagnosis, error detection, data reconciliation, process analysis, oil and gas exploration, manufacturing, process control, product design and analysis, visual quality inspection system, machine analysis, project bidding, dynamics of chemical process systems (Aziz et al., 2001; Bhat and McAvoy, 1990; Bomberger et al., 2001; Eikens et al., 2001a; Eikens et al., 2001b; Hagan et al., 1996; Scheffer and Filho, 2001; Darwish et al., 2007).

In chemistry, neural network determines the molecular structure by comparing the data obtained by spectroscopic analysis. In process control, NN determine the complex relationship between the controlled and manipulated variable comparing the data obtained from the monitoring of the process and the fault detection (Zupan and Gasteiger, 1999; Mujtaba et al., 2006).

NN shows great promise over the recent years to solve problems that have proven to be difficult for the standard technique using digital computers. NN is inherently parallel in structure like human brain and has capabilities for storing knowledge from analysing information.

In the recent history NN has become very popular by different researchers from a wide range of disciplines i.e. aerospace, automotive, transportation; telecommunications,

electronics, robotics, speech; financial, insurance, securities, banking; manufacturing, oil and gas; medical and defence (Hagan et al., 1996).

3.2.1 NN architecture

NN provides a non-linear mapping between input and output variables and is useful in providing cross-correlation among these variables without modelling and simulating the system. The mapping is performed by the use of processing elements and connection weights (Aldrich and Slater, 2001).

The architecture of NN consists of a number of layers, a number of neurons; transfer functions and weights and biases and how layers are connected among themselves. With the increase of number of layers and neurons, the NN's capabilities of approximating complex functions increases (provided data are not over fitted).

In process engineering feed forward network whose signals flow in the forward direction from the input units to the output units and incorporates feedback in its operation are widely used because of its simplicity and available mathematical algorithms to perform its function. A typical NN architecture is shown in Figure 3.1.

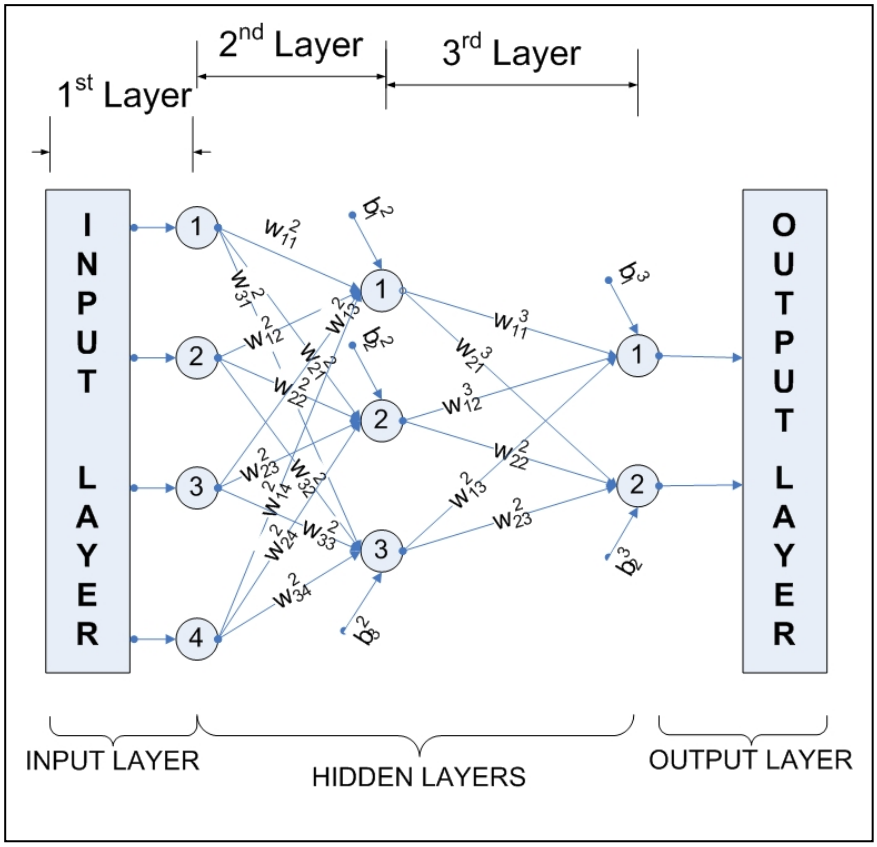

Figure 3.1: A Typical NN Architecture

Neuron

Neuron is a mathematical processing element of the Neural Network. The neurons in the input layer are called the input. Similarly, the neurons in the output layer are output. Input layer neuron receives information from either sensory inputs or signals from other systems outside the one being modelled. Hidden layer neurons have no direct connections to the outside world, they receive information from the input layer and process them in a hidden way. Output layer neurons receive processed information and sends output signals out of the system.

Weights and biases

The weight is positive if the associated connection is excitatory and negative if the connection is inhibitory. Each neuron connection is associated to a quantity, called weight factor, which act relative connection strength among the neurons to one another.

The bias input is connected to each of the hidden and output neurons in a network. Function of the bias is to act as an offset for the activation of neurons.

Transfer function

A transfer function is used to determine node's output using a mathematical operation on the total activation of the node. The transfer function can transform the node's activation in a linear or non-linear manner. Common types of transfer functions are shown in Table 3.1.

It is interesting to note that sigmoid transfer function shows the similar nonlinearity observed in human brains (Moris et al., 1994). Hyperbolic functions have negative response for negative value and vice versa, which helps to distinguish between the responses and it is more sensitive to the small changes because of its greater slope than sigmoid function.

Table 3.1. Commonly used transfer function (Hagan et al., 1996)

Name of the Transfer Function	Mathematical function	
Sigmoid transfer function	$f(x)=\frac{1}{1+e^{-x}}$ $[0 \le f(x) \le 1]$	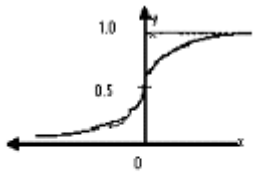 sigmoid
Hyperbolic transfer function	$f(x)=\tanh(x)=\frac{e^{x}+e^{-x}}{e^{x}+e^{-x}}$ $[-1 \le f(x) \le 1]$	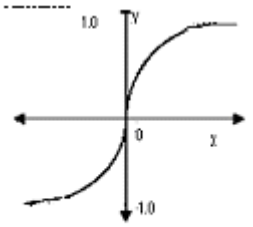 hyperbolic
Gaussian transfer function	$f(x)=\exp\left(\frac{-x^{2}}{2}\right)$ $[0 \le f(x) \le 1]$	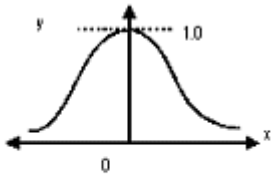 gaussian

3.2.2 Backpropagation training algorithm

All learning or training algorithm can be classified as supervised learning and unsupervised learning. In supervised learning, the network is provided with a training data set. The data set consists of inputs and targets (desired outputs). Whereas in unsupervised learning, there are no targets supplied to the network. The weights and biases are modified in response to the inputs alone.

Back propagation of errors is not the name of specific neural network architecture, but the supervised learning rule. Back propagation training algorithm is used in mainly three types of network: Elman back propagation network, cascade-forward back propagation network and feed-forward multi layer back propagation network. Among them multi layer back propagation network is used widely (Hagan, 1996). In subsequent chapters, feed-forward multi layer network using back propagation algorithm is named as NN.

Back propagation algorithm was introduced by Werbos and publicized by Rumelhart and co-worker (Hagen et al., 1996). Standard back propagation is a gradient descent algorithm, as is the Widrow-Hoff learning rule, in which the network weights are moved along the negative of the gradient of the performance function. In 1960 Widrow and his graduate student Hoff introduces Adaline (Adaptive Linear Neural Network) or the LMS (least mean square) algorithm. Widrow Hoff learning is an approximate steepest descent algorithm in which performance of the network determine by the mean square error (the difference between the output and target) (Hagan et al., 1996).

The steps of training performance optimisation

To increase the efficiency of neural network training the following steps have been taken in Matlab Neural network Toolbox (Math Works, 2006).

a. Generalization and processing of data

Neural networks interpolate data very well, but they are inefficient with extrapolation (Hagan et al., 1996). Smooth distribution of data should be chosen as training data.

Data over fitting is handled by early stopping and regularization. The data sets are divided into training, validation and test subsets. One fourth of the data is taken for the validation

set, one fourth is taken for the test set and one-half is taken for the training set. Data is taken the sets as equally spaced points throughout the original data.

Before training, it is often useful to scale the inputs and targets so that they always fall within a specified range. For an example, typical log sigmoid function and tan sigmoid / hyperbolic function is not good at dealing with/distinguish the value less than -1 and greater than the +1. This is a useful structure for function approximation (or regression) problems.

b. Optimum network architecture

There are several type of NN available in the literature such as multi-layer back propagation, competitive layer back propagation and Elman back propagation are available in literature. After processing the data, the next step is the selection of the architecture (the number of layer and nodes in each layer). Transfer function of each layer is then selected. Then the weights and biases are randomly initialised. Nevertheless, finding the optimum number of hidden layers and its corresponding nodes is not straightforward; it solely depends on the application of NN used for the development of the model and the required accuracy. To determine the optimal number of layer train the network using various configurations, select the one, which gives the optimum value. The desired number of neurons is an important factor due to fact that as the number of neurons increases the accuracy of the computation increases.

c. The training, validation and testing of neural network using Back propagation-training algorithm

Backpropagation training is chosen in most of the neural network application in process engineering. Various widely used training algorithms suitable for different field are

available in the toolbox. Among them are Levenberg-Marquardt algorithm, gradient based algorithm are widely used for process engineering in Back propagation training.

The back propagation converges slowly with the increase of no of hidden layer. It can produce the local minima report. Several modifications of the original back propagation are found in the literature to improve the performance of the algorithm. Among them, the LMS error converges to solution where learning rate is not large (such as quadratic function). Again, Hessian matrix of a quadratic function is not constant. So the curvature becomes elliptical. It makes the fluctuation of the network output from the target. Back propagation learning rate updates weights and biases by optimisation technique such as gradient descent algorithm. This training normally takes much time to minimise the square error.

To achieve the faster training variable learning rate can be applied that is available in Matlab Neural Network toolbox. Further detail of Back propagation is given in 3.3.4.

d. Visualisation and statistical analysis

Visualisation and statistical analysis help to understand network response easily. A learning curve characterizes the average error for both the recall of training data sets and the generalization of the testing sets as a function of the number of examples in the training data set. It helps to visualize how well a network performs recall and generalization.

To visualize the relationship between the neural net output and targets, a linear regression between the networks outputs will be performed and the network prediction for corresponding targets are plotted.

3.3 Neural Network Based Correlations for TE

Adequate knowledge of the total heat transfer area, the length of the flash chamber, control of the corrosion and scale formation are needed for modelling, design and scale up of MSF processes. These parameters are dependent on/ inter-related with the TBT (also known as the maximum attainable temperature) (Spiegler and Liard, 1980). The optimum TBT is controlled according to the types of pre-treatment in the process (Nada, 2002). The TBT is one of the important parameters needed for designing, modelling, simulation and optimisation of the process. In a typical MSF process model the TBT, which is the maximum attainable temperature of the MSF process, is the outlet temperature of brine heater or the feed entering into the first stage (Figure 3.2). This temperature is also the boiling point temperature (BPT) for seawater entering the first stage. According to the Dühring's rule (Foust et al., 1980), the seawater BPT is usually calculated by summing up the BPT of pure water at a given pressure and the TE due to salinity. Note the TE is a function of the dissolved solids concentration and BPT. The accurate measurement or estimation of seawater physical properties (density, heat capacity, BPT, TE, etc.) is of considerable importance in the development, design and operation of desalination plants. For example, if more than 20 stages are connected in an MSF plant, small error in calculating TE can lead to considerable errors in the calculation of heat transfer area, length of the flash chambers, etc. (Spiegler and Liard, 1980).

Top Brine Temperature (TBT) is one of the many important parameters that affect optimal design and operation of MSF processes. Within the MSF process model, calculation of TBT is therefore important (see Chapter 5, 6 and 7). For a given pressure, TBT is a function of Boiling Point Temperature (BPT) at zero salinity and Temperature Elevation (TE) due to salinity.

3.3.1 Empirical correlations for TE

Few correlations, developed in the past and commonly used to calculate TE are listed in Table 3.2.

Table 3.2 Different correlations for estimating TE

Correlation 1: Bromley et al. (1974)
Experimental Data Source: Bromley et al. (1974)

$$TE = 13832.0 \times x \times BPT^2 \times \left(\begin{array}{l} 1+0.001373\times BPT-0.00272\times BPT \times \sqrt{\frac{x}{100}}+\frac{17.86\times x}{100}- \\ \frac{0.0152\times x}{100\times BPT}\times\frac{(BPT-225.9)}{(BPT-236)}-\frac{2583\times x}{100\times BPT}\times\left(1-\frac{x}{100}\right) \end{array} \right)$$

where, BPT = boiling point of pure water at ^oK and x is in weight percent

Correlation 2: Helal et al. (1986)

$$TE = \left(\begin{array}{l} \left(\frac{565.757}{T} - 9.81559 +1.54739 \times \ln T\right) - (337.178/T -6.41981 +0.922753 \ln T)\times C \\ +\left(\frac{32.681}{T} -0.55368 +0.079022\times \ln T\right)\times C^2 \end{array} \right) \times \left(\frac{C}{\left(\frac{266919.6}{T^2}-\frac{379.669}{T}+0.3341+69\right)} \right)$$

Correlation 3: Fabuss (1980)
Data Source: Fabuss (1980)

$TE = \alpha_0 \times C + \beta_0 \times C^2$, where C is the technical concentration factor of seawater,

$\alpha_0 = \alpha_1 + \alpha_2 \times BPT + \alpha_3 \times BPT^2$ and $\beta_0 = \beta_1 + \beta_2 \times BPT + \beta_3 \times BPT^2$

where, α_1=0.2009, α_2 = 0.2867E-2 and α_3 =0.002E-4; β_1 = 0.0257, β_2=0.193E-2 and β_3 =0.0001E-4

BPT = boiling point of pure water at ^oC

Correlation 4: El-Dessouky and Ettouney (2000)

$TE = Ax + Bx^2 + Cx^3$

where $A=8.325\times10^{-2}+1.883\times10^{-4}\times T+4.02\times10^{-6}\times T^2$;

$B=-7.625\times10^{-4}+9.02\times10^{-5}\times T+5.2\times10^{-7}\times T^2$

$C=1.522\times10^{-4}-3\times10^{-6}\times T^{-3}\times10^{-8}\times T^2$; T = BPT in ^oC and x = salinity in weight percent

Here, TE = Temperature Elevation

3.3.2 Why NN based correlation for TE?

The seawater composition (Total Dissolved Solids (TDS), different salts such as Boron, Calcium and the acidity of the seawater) varies for different plants located over various regions. These empirical correlations cannot easily adapt the new data reliably for different seawater composition. As seawater compositions are subject to wide variations over a wide operating range and seawater condition for different plant, therefore, these correlations can lead to inaccurate predictions of TE. Good correlations, which act over a wide range of operation and composition of seawater and can be updated very easily, are therefore necessary for modelling, simulation, and design of MSF processes.

NN based correlations (models) can be updated in terms of new sets of weights and biases for the same architecture or for a new architecture reliably with new plant data.

For a given set of inputs, NNs are able to produce a corresponding set of outputs according to some mapping relationship. This relationship is encoded into the network structure during a period of training (also called learning), and is dependant upon the parameters of the network, i.e. weights and biases (Hagan et al., 1996).

This feature of NN based correlation makes it flexible in the process industries for development of correlation using computer software automatically without the help of expert knowledge.

3.3.3 NN architecture and development of correlation for TE

With reference to a typical neural network architecture shown in Figure 3.1 each neuron j in the i-th layer (except in the input layer) is connected with all the neurons of the $(i-1)$-

th layer with a bias (b_j^i) and through weights (w_{jk}^i), where k denotes the neuron of $(i-1)$-th layer. The total number of neurons in layer i is n_i and the transfer function for layer i and neuron j is f_j^i. In each layer, the value of the neuron j is calculated by:

$$a_j^i = f_j^i \left(\sum_{k=1}^{n_{i-1}} w_{jk}^i \times a_k^{i-1} + b_j^i \right) \tag{3.1}$$

The training, validation and testing of Neural Network using (Back propagation training algorithm)

Training, validation and testing of neural network

In this work, the Levenberg-Marquardt back propagation algorithm is chosen to train the network (Matlab Toolbox, Hagan et al., 1996). This algorithm needs more space and it does not converge quickly like other algorithm (BFGS), but it gives closest value to the target data (experimental data).

A suitably trained and validated network should be able to predict realistic output even when the network is presented with new inputs (test data). However, neural networks are able to interpolate data very well but are not quite efficient with extrapolation (Mujtaba and Hussain, 1996). The training of a neural network usually requires a large number of data sets. In this work, the training data sets are randomly selected covering the whole range of the data. When a set of input is fed in the network, it returns the output. The network calculates the error between the output and the target. This error is fed back to the network and weights and biases are adjusted according to Least Mean Square (LMS) error criteria. The process is continued until the network output is close to the target. This is known as

training by back propagation method (Figure 3.2). Testing the network is a way of checking the performance of a trained network i.e. how well the network can predict the output given an input that is not used in the training set.

In the proposed NN based correlations, an optimum network architecture (in terms of number of hidden layers and neurons in each layer) is chosen for each network and then the network is fed with the input data (salinity, BPT) to predict the output (TE).

A multi-layered feed forward network, trained using the back-propagation method mentioned above, is used to obtain the optimum NN architecture. All the input data has been scaled, so that they will have zero mean and standard deviation equal to 1, to find the most accurate neural network relationship for the input/output relationship.

A training graph (LMS error vs. time) is used to find how long it takes to get a good NN architecture and how many times the network needs to reinitialise the weights and biases (for a new architecture, according to Figure 3.3). The NN predicted output value is rescaled to its original units. The statistical regression between predicted value and output data is plotted to find the overall trends of the data.

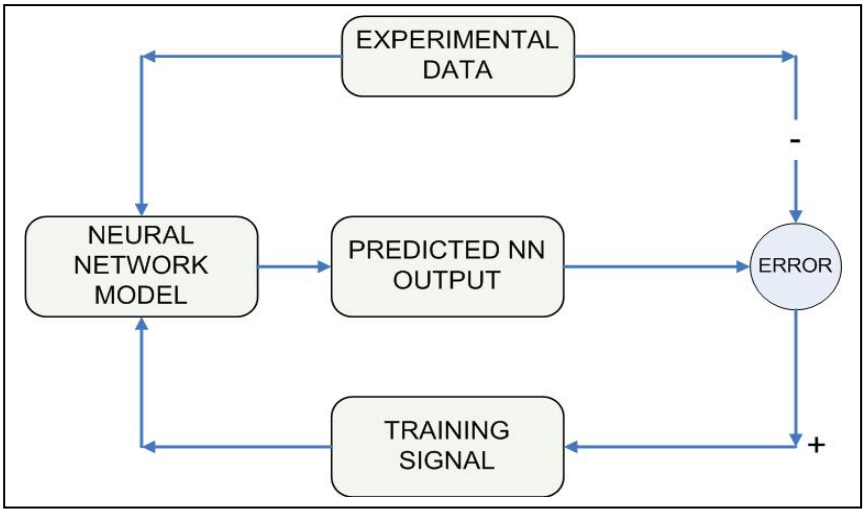

Figure 3.2 Neural Network Backpropagation Training Scheme

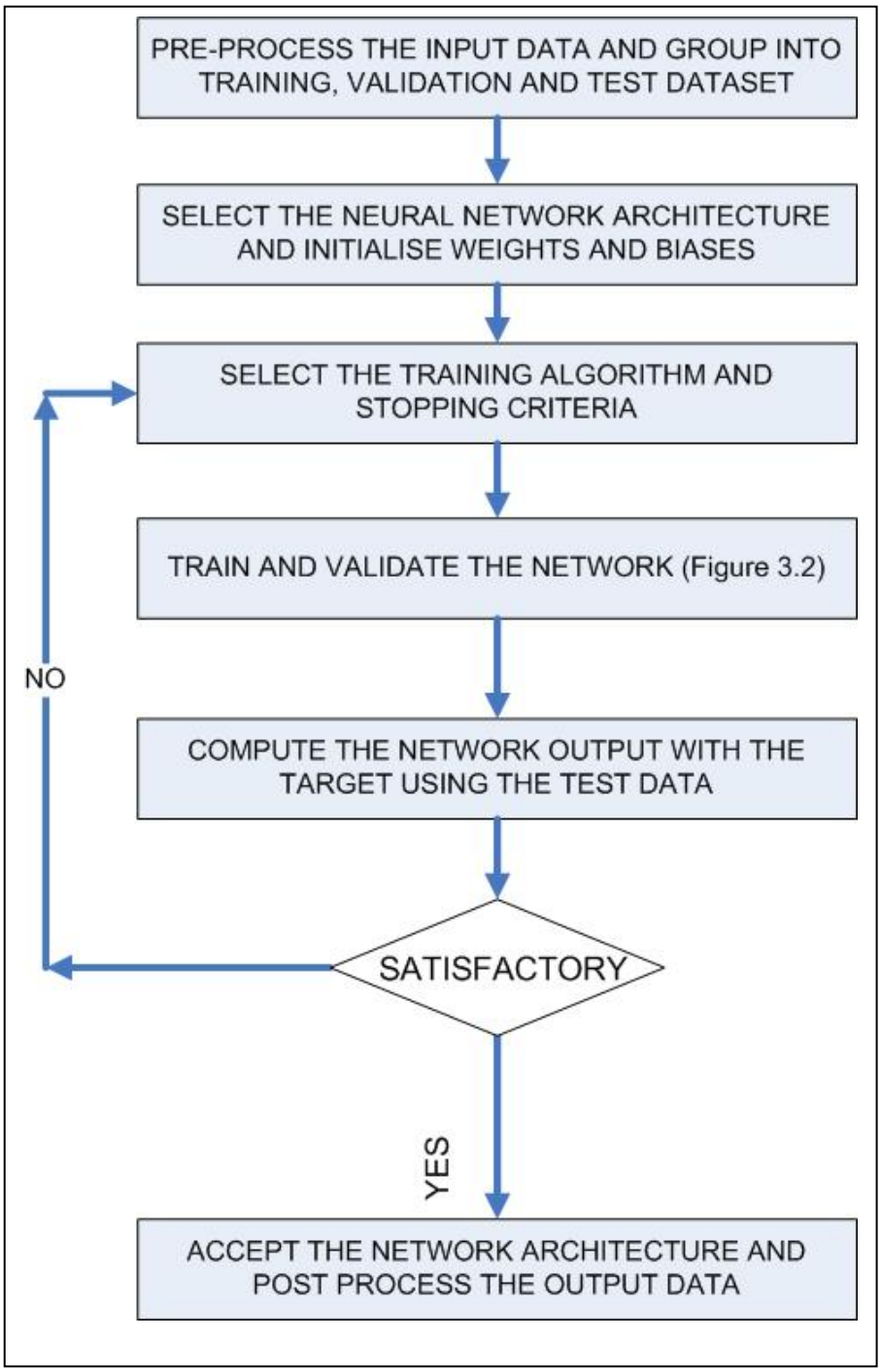

Figure 3.3 Determination of the Optimum Network Structure

Development of correlations

Once optimum network architecture is found, the weights and biases are used to develop the NN based correlations. This is explained bellow.

The correlation estimates TE in terms of salinity (x) and BPT. TE is expressed in ^{o}C, x is expressed in weight percent and BPT is expressed in ^{o}C.

The input data is scaled up with mean and its standard deviation as:

$$x_{scaleup} = \frac{(x - mean\_x)}{std\_x} \tag{3.2}$$

$$BPT_{scaleup} = \frac{(BPT - mean\_BPT)}{std\_BPT} \tag{3.3}$$

where $mean\_x$ is the average of x and $mean\_BPT$ is the average of BPT; std_x is standard deviation of x and std_BPT is standard deviation of BPT data used to develop the correlation.

There are two input neurons and one output neuron in the NN based correlations. The values are:

$a_1^1 = x_{scaleup}$ and $a_2^1 = BPT_{scaleup}$

$$a_j^l = TE_{scaleup} \tag{3.4}$$

where l is the output layer. The output value is rescaled to find the value in original units.

$$TE = TE_{scaleup} \times std\_TE + mean\_TE \tag{3.5}$$

where $mean\_TE$ and std_TE are average and standard deviation respectively of the TE data used for developing the correlation.

The NN based correlations developed in this work is explained with respect to 3-layered

NN architecture. In 3-layered NN architecture there is one input layer, one hidden layer and one output layer (Figure 3.4).

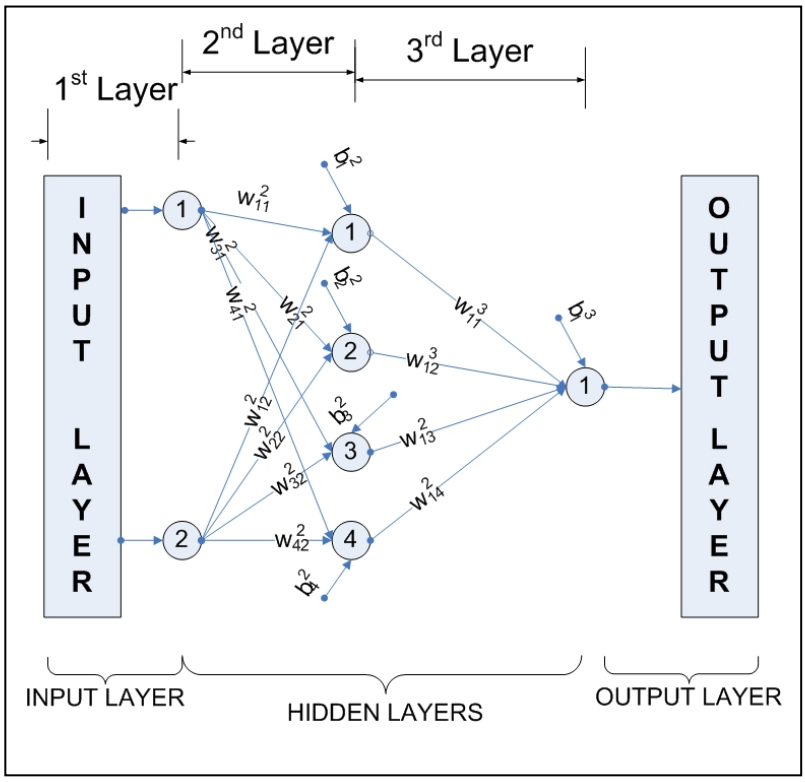

Figure 3.4 A Three-Layered Neural Network

The weights, biases and transfer functions are shown in Table 3.3. For 3-layered network, the correlation is given by:

$$a_1^3 = f_1^3\left(\sum_{k=1}^{4}(w_{1k}^3 a_k^2)+b_1^3\right) \tag{3.6}$$

where a_k^2 is given by:

$$a_k^2 = f_j^2\left(\sum_{k=1}^{2}(w_{jk}^2 a_k^1)+b_j^2\right) \tag{3.7}$$

for $j = 1$ in layer 2, the equation (3.7) can be expressed as:

$$a_1^2 = f_1^2\left(w_{11}^2 a_1^1 + w_{12}^2 a_2^1 + b_1^2\right) \tag{3.8}$$

In this work we used $f_j^2 = \tanh$ and $f_1^3 = 1$ Eq. (3.8) becomes:

$$a_1^2 = \tanh\left(w_{11}^2 x_{scaleup} + w_{12}^2 BPT_{scaleup} + b_1^2\right) \tag{3.9}$$

In general, for 2nd layer, the value of j -th neuron can be given by:

$$a_j^2 = \tanh\left(w_{j1}^2 \times x_{scaleup} + w_{j2}^2 \times BPT_{scaleup} + b_j^2\right) \tag{3.10}$$

Equation (3.6) can be written now for $TE_{scaleup}$

$$TE_{scaleup} = a_1^3 = w_{11}^3 \times a_1^2 + w_{12}^3 \times a_2^2 + w_{13}^3 \times a_3^2 + w_{14}^3 \times a_4^2 + b_1^3 \tag{3.11}$$

Table 3.3. Weights and biases and transfer functions for 3-layered network

2nd layer				3rd layer		
weights		bias	transfer function	weights	bias	transfer function
w_{11}^2	w_{12}^2	b_1^2	$f_1^2 = \tanh$	w_{11}^3	b_1^3	$f_1^3 = 1$
w_{21}^2	w_{22}^2	b_2^2	$f_2^2 = \tanh$	w_{12}^3		
w_{31}^2	w_{32}^2	b_3^2	$f_3^2 = \tanh$	w_{13}^3		
w_{41}^2	w_{42}^2	b_4^2	$f_4^2 = \tanh$	w_{14}^3		

Similarly, for 4-layered correlation (Figure 3.5), the value of the output neuron can be given by:

$$a_1^4 = f_1^4\left(\sum_{k=1}^{4} w_{1k}^4 \times a_k^3 + b_1^4\right) \tag{3.12}$$

The Equation 3.12 can be expanded using the procedure outlined for 3-layer correlation.

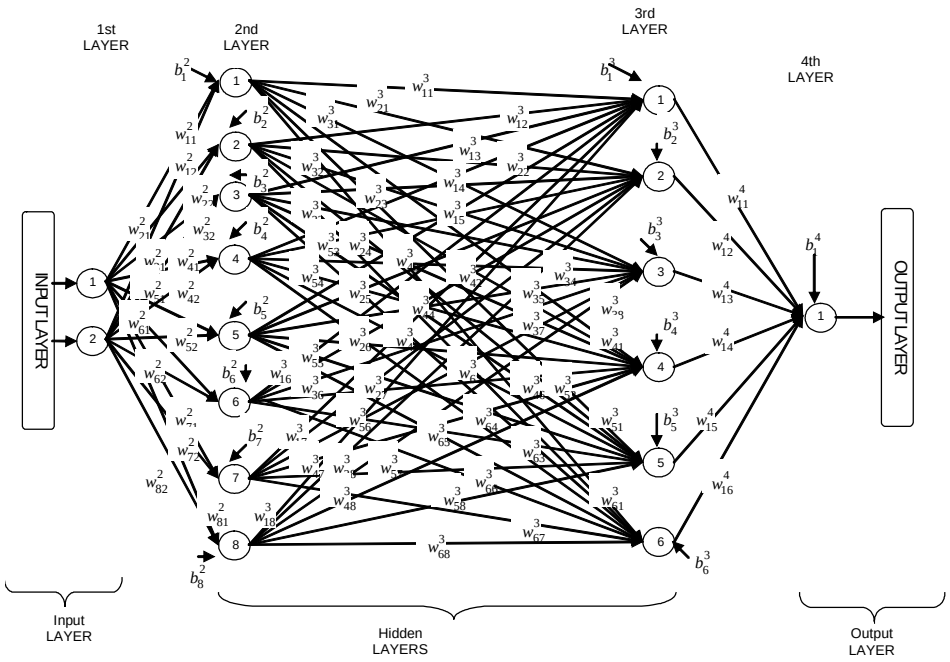

Figure 3.5 A Four Layer Neural Network

3.4 Experimental Data and Correlations

3.4.1 Experimental data

The input data for the NN based correlations are taken from three different experimental data sources (Bromley et al., 1974; M.W. Kellog, 1965; Badger et al., 1959 and Fabuss, 1980). The experimental data are different for different sources due to the variation in seawater constituents and experimental methods used. This makes the prediction of different correlation by different authors different (i.e. correlations shown in Table 3.2).

From Bromley Data (Bromley et al., 1974), 56 data points of (salinity, temperature, TE) were selected with salinity range from (0.19 to 7.135 wt%) and Temperature range (60 to 120 ^{O}C) (Table 3.4).

From Kellog data (M.W. Kellog Co., 1965) 92 data points were selected from published experimental data presented in graphical form with temperature range from (10 to 177.67 ^{O}C) for three different salinity (3.4446, 6.892 and 10.338 wt %) values.

From Badger Data (Badger et al., 1959), 68 data points were selected from published experimental data presented in graphical form with salinity range from (0.88 to 14.98 wt%) for four different temperature (37.78, 65.66, 93.33 and 121.11 ^{O}C) values (Table 3.5).

Fabuss (1980) published 24 data sets of (salinity, temperature, TE) with salinity range from (1.5 to 13 wt%) and Temperature range (20 to 150 ^{O}C). Each data set corresponds to one salinity (e.g.1.5 wt%) and 14 different temperature (20, 30, 40, 50, 60, 70, 80, 90, 100, 110, 120, 130, 140, 150 ^{O}C) values and 14 TE Values. There are total of 24*14 = 336 data points in Fabuss (1980) which were used for one of the NN based correlations (Table 3.6).

3.4.2 NN based correlations for different data sets

In this work, 4 different NN based correlations to estimate TE are developed. The correlations (NN_Cor_1, NN_Cor_2, NN_Cor_3) are based on the three different data sources mentioned earlier (Bromley, Badger, Fabuss data respectively). The last correlation NN_Cor_4 is based on the all the data from all the sources (Bromley, Badger, Fabuss and Kellog data).

In the first three NN based correlations, one hidden layer is used and the optimum numbers of neurons in the hidden layer was found to be four (Figure 3.4). Between the input and the hidden layer hyperbolic tangent function and between the hidden and output layers a linear function is used as transfer functions (as mentioned earlier).

For each of the NN based correlations, first 2 input data points are selected for training (bold), the next input data point for validation (italic) and the fourth one is selected for

testing (normal) the correlation (shown in Tables 3.4 – 3.6). This selection process continues sequentially until all the data points are exhausted. Thus, the total input data are divided into three sets: training (50%), validation (25%), and testing (25%) datasets.

For NN_Cor_4 two hidden layers are used and the optimum numbers of neurons in the first and the second layer are found to be eight and six respectively. Between the input and the first hidden layer and between the hidden layers a hyperbolic tangent function and between the last hidden and output layers a linear function is used as transfer functions.

Total of 552 data is selected from the four sources for NN_Cor_4. The first 6 data points are selected for training, the next data points for validation and the eighth one is selected for testing model. This selection process continues sequentially until all the data points are exhausted. Thus, the total data are divided into three sets: training (75%), validation (12.5%) and testing (12.5%) datasets.

Table 3.4 Bromley data (Bromley, 1974) used in NN_Cor_1

Salinity	BPT	TE	Salinity	BPT	TE
0.6186	**60**	**0.071**	**0.7981**	**100**	**0.118**
0.6369	**60**	**0.072**	**1.001**	**100**	**0.147**
1.1263	*60*	*0.128*	*1.2566*	*100*	*0.185*
1.1735	60	0.134	1.683	100	0.248
1.5707	**60**	**0.178**	**1.7117**	**100**	**0.251**
1.6867	**60**	**0.192**	**2.151**	**100**	**0.318**
2.2542	*60*	*0.258*	*3.03*	*100*	*0.454*
3.0542	60	0.356	3.3541	100	0.505
3.735	**60**	**0.440**	**3.473**	**100**	**0.524**
4.5285	**60**	**0.542**	**3.618**	**100**	**0.547**
5.178	*60*	*0.629*	*4.281*	*100*	*0.657*
5.7635	60	0.709	4.876	100	0.756
6.4212	**60**	**0.803**	**5.0555**	**100**	**0.789**
7.1354	**60**	**0.907**	**5.0648**	**100**	**0.790**
0.6239	*80*	*0.081*	*0.19101*	*120*	*0.033*
1.253	80	0.163	0.6887	120	0.116
1.8504	**80**	**0.241**	**1.2813**	**120**	**0.213**
2.5375	**80**	**0.332**	**1.9457**	**120**	**0.324**
2.643	*80*	*0.347*	*2.5357*	*120*	*0.425*
3.467	80	0.461	2.6012	120	0.437
3.469	**80**	**0.461**	**3.0582**	**120**	**0.516**
4.0254	**80**	**0.542**	**3.3534**	**120**	**0.567**
4.779	*80*	*0.654*	*3.9086*	*120*	*0.670*
5.3929	80	0.749	4.4208	120	0.764
5.8352	**80**	**0.816**	**4.911**	**120**	**0.856**
5.9126	**80**	**0.830**	**5.4038**	**120**	**0.951**
6.3231	*80*	*0.894*	*5.9291*	*120*	*1.056*
6.4064	80	0.910	6.4108	120	1.154

Note: Training data in bold, Validation data in italic, Test data in plain

Table 3.5. Badger data (Badger et al., 1959) used in NN_Cor_2

Salinity	BPT	TE	Salinity	BPT	TE
0.88	**37.8**	**0.070**	**2.64**	**93.3**	**0.280**
1.76	**37.8**	**0.140**	**3.53**	**93.3**	**0.450**
2.64	*37.8*	*0.170*	*4.41*	*93.3*	*0.560*
3.53	37.8	0.280	5.29	93.3	0.760
4.41	**37.8**	**0.380**	**6.17**	**93.3**	**0.900**
5.29	**37.8**	**0.520**	**7.05**	**93.3**	**1.080**
6.17	*37.8*	*0.630*	*7.93*	*93.3*	*1.250*
7.05	37.8	0.760	8.81	93.3	1.460
7.93	**37.8**	**0.900**	**9.69**	**93.3**	**1.630**
8.81	**37.8**	**1.010**	**10.58**	**93.3**	**1.810**
9.69	*37.8*	*1.110*	*11.46*	*93.3*	*1.880*
10.58	37.8	1.250	12.37	93.3	2.150
11.46	**37.8**	**1.350**	**13.21**	**93.3**	**2.360**
12.37	**37.8**	**1.530**	**14.1**	**93.3**	**2.500**
13.21	*37.8*	*1.670*	*14.98*	*93.3*	*2.780*
14.1	37.8	1.810	0.88	121.1	0.070
14.98	**37.8**	**1.940**	**1.76**	**121.1**	**0.240**
0.88	**65.56**	**0.070**	**2.64**	**121.1**	**0.350**
1.76	*65.56*	*0.170*	*3.53*	*121.1*	*0.560*
2.64	65.56	0.210	4.41	121.1	0.690
3.53	**65.56**	**0.350**	**5.29**	**121.1**	**0.940**
4.41	**65.56**	**0.490**	**6.17**	**121.1**	**1.040**
5.29	*65.56*	*0.660*	*7.05*	*121.1*	*1.250*
6.17	65.56	0.760	7.93	121.1	1.530
7.05	**65.56**	**0.940**	**8.81**	**121.1**	**1.740**
7.93	**65.56**	**1.040**	**9.69**	**121.1**	**1.940**
8.81	*65.56*	*1.220*	*10.58*	*121.1*	*2.150*
9.69	65.56	1.390	11.46	121.1	2.360
10.58	**65.56**	**1.530**	**12.37**	**121.1**	**2.640**
11.46	**65.56**	**1.600**	**13.21**	**121.1**	**2.810**
12.37	*65.56*	*1.880*	*14.1*	*121.1*	*2.990*
13.21	65.56	1.940	14.98	121.1	3.330
14.1	**65.56**	**2.220**			
14.98	**65.56**	**2.360**			
0.88	*93.3*	*0.070*			
1.76	93.3	0.210			

Note: Training data in bold, Validation data in italic, Test data in plain

Table 3.6. Fabuss Data (Fabuss, 1980) used in NN_Cor_3

Salinity	BPT	TE	Salinity	BPT	TE	Salinity	BPT	TE
1.5	**20**	**0.118**	**3**	**80**	**0.407**	**4.5**	**140**	**0.882**
1.5	**30**	**0.131**	**3**	**90**	**0.434**	**4.5**	**150**	**0.923**
1.5	*40*	*0.144*	*3*	*100*	*0.460*	*5*	*20*	*0.437*
1.5	50	0.157	3	110	0.487	5	30	0.483
1.5	**60**	**0.170**	**3**	**120**	**0.514**	**5**	**40**	**0.529**
1.5	**70**	**0.183**	**3**	**130**	**0.541**	**5**	**50**	**0.575**
1.5	*80*	*0.196*	*3*	*140*	*0.568*	*5*	*60*	*0.621*
1.5	90	0.209	3	150	0.595	5	70	0.667
1.5	**100**	**0.222**	**3.5**	**20**	**0.293**	**5**	**80**	**0.713**
1.5	**110**	**0.235**	**3.5**	**30**	**0.324**	**5**	**90**	**0.759**
1.5	*120*	*0.248*	*3.5*	*40*	*0.355*	*5*	*100*	*0.805*
1.5	130	0.261	3.5	50	0.387	5	110	0.852
1.5	**140**	**0.274**	**3.5**	**60**	**0.418**	**5**	**120**	**0.898**
1.5	**150**	**0.287**	**3.5**	**70**	**0.449**	**5**	**130**	**0.945**
2	*20*	*0.160*	*3.5*	*80*	*0.481*	*5*	*140*	*0.991*
2	30	0.177	3.5	90	0.512	5	150	1.038
2	**40**	**0.195**	**3.5**	**100**	**0.544**	**5.5**	**20**	**0.488**
2	**50**	**0.212**	**3.5**	**110**	**0.575**	**5.5**	**30**	**0.538**
2	*60*	*0.229*	*3.5*	*120*	*0.607*	*5.5*	*40*	*0.589*
2	70	0.247	3.5	130	0.639	5.5	50	0.640
2	**80**	**0.264**	**3.5**	**140**	**0.670**	**5.5**	**60**	**0.691**
2	**90**	**0.282**	**3.5**	**150**	**0.702**	**5.5**	**70**	**0.743**
2	*100*	*0.299*	*4*	*20*	*0.340*	*5.5*	*80*	*0.794*
2	110	0.317	4	30	0.376	5.5	90	0.845
2	**120**	**0.334**	**4**	**40**	**0.412**	**5.5**	**100**	**0.896**
2	**130**	**0.352**	**4**	**50**	**0.448**	**5.5**	**110**	**0.948**
2	*140*	*0.370*	*4*	*60*	*0.484*	*5.5*	*120*	*0.999*
2	150	0.387	4	70	0.520	5.5	130	1.051
2.5	**20**	**0.203**	**4**	**80**	**0.556**	**5.5**	**140**	**1.102**
2.5	**30**	**0.225**	**4**	**90**	**0.593**	**5.5**	**150**	**1.154**
2.5	*40*	*0.247*	*4*	*100*	*0.629*	*6*	*20*	*0.539*
2.5	50	0.269	4	110	0.666	6	30	0.595
2.5	**60**	**0.291**	**4**	**120**	**0.702**	**6**	**40**	**0.651**
2.5	**70**	**0.313**	**4**	**130**	**0.738**	**6**	**50**	**0.708**
2.5	*80*	*0.335*	*4*	*140*	*0.775*	*6*	*60*	*0.764*
2.5	90	0.357	4	150	0.812	6	70	0.820
2.5	**100**	**0.379**	**4.5**	**20**	**0.388**	**6**	**80**	**0.876**
2.5	**110**	**0.401**	**4.5**	**30**	**0.429**	**6**	**90**	**0.933**
2.5	*120*	*0.423*	*4.5*	*40*	*0.470*	*6*	*100*	*0.989*
2.5	130	0.445	4.5	50	0.511	6	110	1.046
2.5	**140**	**0.468**	**4.5**	**60**	**0.552**	**6**	**120**	**1.103**
2.5	**150**	**0.490**	**4.5**	**70**	**0.593**	**6**	**130**	**1.159**
3	*20*	*0.247*	*4.5*	*80*	*0.634*	*6*	*140*	*1.216*
3	30	0.274	4.5	90	0.675	6	150	1.273
3	**40**	**0.300**	**4.5**	**100**	**0.716**	**6.5**	**20**	**0.592**
3	**50**	**0.327**	**4.5**	**110**	**0.758**	**6.5**	**30**	**0.654**
3	*60*	*0.354*	*4.5*	*120*	*0.790*	*6.5*	*40*	*0.715*
3	70	0.380	4.5	130	0.840	6.5	50	0.776

Note: Training data in bold, Validation data in italic, Test data in plain

Table 3.6. Fabuss Data (Fabuss, 1980) used in NN_Cor_3 (cont'd)

Salinity	BPT	TE	Salinity	BPT	TE	Salinity	BPT	TE	Salinity	BPT	TE
6.5	**60**	**0.838**	**8**	**120**	**1.536**	**10**	**40**	**1.198**	**11.5**	**100**	**2.137**
6.5	**70**	**0.899**	**8**	**130**	**1.614**	**10**	**50**	**1.298**	**11.5**	**110**	**2.255**
6.5	*80*	*0.961*	*8*	*140*	*1.693*	*10*	*60*	*1.399*	*11.5*	*120*	*2.374*
6.5	90	1.022	8	150	1.771	10	70	1.499	11.5	130	2.493
6.5	**100**	**1.084**	**8.5**	**20**	**0.817**	**10**	**80**	**1.599**	**11.5**	**140**	**2.613**
6.5	**110**	**1.146**	**8.5**	**30**	**0.900**	**10**	**90**	**1.700**	**11.5**	**150**	**2.732**
6.5	*120*	*1.208*	*8.5*	*40*	*0.983*	*10*	*100*	*1.801*	*12*	*20*	*1.258*
6.5	130	1.270	8.5	50	1.066	10	110	1.902	12	30	1.382
6.5	**140**	**1.332**	**8.5**	**60**	**1.149**	**10**	**120**	**2.003**	**12**	**40**	**1.506**
6.5	**150**	**1.394**	**8.5**	**70**	**1.232**	**10**	**130**	**2.104**	**12**	**50**	**1.630**
7	*20*	*0.647*	*8.5*	*80*	*1.315*	*10*	*140*	*2.205*	*12*	*60*	*1.754*
7	30	0.713	8.5	90	1.399	10	150	2.307	12	70	1.878
7	**40**	**0.780**	**8.5**	**100**	**1.482**	**10.5**	**20**	**1.062**	**12**	**80**	**2.003**
7	**50**	**0.846**	**8.5**	**110**	**1.566**	**10.5**	**30**	**1.167**	**12**	**90**	**2.127**
7	*60*	*0.913*	*8.5*	*120*	*1.650*	*10.5*	*40*	*1.273*	*12*	*100*	*2.252*
7	70	0.980	8.5	130	1.734	10.5	50	1.379	12	110	2.377
7	**80**	**1.047**	**8.5**	**140**	**1.817**	**10.5**	**60**	**1.485**	**12**	**120**	**2.502**
7	**90**	**1.114**	**8.5**	**150**	**1.902**	**10.5**	**70**	**1.591**	**12**	**130**	**2.628**
7	*100*	*1.181*	*9*	*20*	*0.876*	*10.5*	*80*	*1.698*	*12*	*140*	*2.753*
7	110	1.248	9	30	0.965	10.5	90	1.804	12	150	2.879
7	**120**	**1.315**	**9**	**40**	**1.053**	**10.5**	**100**	**1.911**	**12.5**	**20**	**1.326**
7	**130**	**1.382**	**9**	**50**	**1.142**	**10.5**	**110**	**2.018**	**12.5**	**30**	**1.456**
7	*140*	*1.450*	*9*	*60*	*1.231*	*10.5*	*120*	*2.125*	*12.5*	*40*	*1.586*
7	150	1.517	9	70	1.319	10.5	130	2.232	12.5	50	1.716
7.5	**20**	**0.702**	**9**	**80**	**1.408**	**10.5**	**140**	**2.339**	**12.5**	**60**	**1.847**
7.5	**30**	**0.774**	**9**	**90**	**1.497**	**10.5**	**150**	**2.446**	**12.5**	**70**	**1.977**
7.5	*40*	*0.846*	*9*	*100*	*1.587*	*11*	*20*	*1.126*	*12.5*	*80*	*2.108*
7.5	50	0.918	9	110	1.676	11	30	1.237	12.5	90	2.239
7.5	**60**	**0.990**	**9**	**120**	**1.765**	**11**	**40**	**1.349**	**12.5**	**100**	**2.370**
7.5	**70**	**1.062**	**9**	**130**	**1.855**	**11**	**50**	**1.461**	**12.5**	**110**	**2.501**
7.5	*80*	*1.135*	*9*	*140*	*1.944*	*11*	*60*	*1.573*	*12.5*	*120*	*2.632*
7.5	90	1.207	9	150	2.034	11	70	1.685	12.5	130	2.764
7.5	**100**	**1.279**	**9.5**	**20**	**0.937**	**11**	**80**	**1.798**	**12.5**	**140**	**2.896**
7.5	**110**	**1.352**	**9.5**	**30**	**1.031**	**11**	**90**	**1.910**	**12.5**	**150**	**3.028**
7.5	*120*	*1.425*	*9.5*	*40*	*1.125*	*11*	*100*	*2.023*	*13*	*20*	*1.395*
7.5	130	1.497	9.5	50	1.219	11	110	2.135	13	30	1.531
7.5	**140**	**1.570**	**9.5**	**60**	**1.314**	**11**	**120**	**2.248**	**13**	**40**	**1.668**
7.5	**150**	**1.643**	**9.5**	**70**	**1.408**	**11**	**130**	**2.361**	**13**	**50**	**1.804**
8	*20*	*0.759*	*9.5*	*80*	*1.503*	*11*	*140*	*2.475*	*13*	*60*	*1.941*
8	30	0.836	9.5	90	1.598	11	150	2.588	13	70	2.078
8	**40**	**0.914**	**9.5**	**100**	**1.693**	**11.5**	**20**	**1.191**	**13**	**80**	**2.215**
8	**50**	**0.991**	**9.5**	**110**	**1.788**	**11.5**	**30**	**1.309**	**13**	**90**	**2.352**
8	*60*	*1.069*	*9.5*	*120*	*1.883*	*11.5*	*40*	*1.427*	*13*	*100*	*2.489*
8	70	1.146	9.5	130	1.978	11.5	50	1.545	13	110	2.627
8	**80**	**1.224**	**9.5**	**140**	**2.074**	**11.5**	**60**	**1.663**	**13**	**120**	**2.765**
8	**90**	**1.302**	**9.5**	**150**	**2.169**	**11.5**	**70**	**1.781**	**13**	**130**	**2.902**
8	*100*	*1.380*	*10*	*20*	*0.999*	*11.5*	*80*	*1.899*	*13*	*140*	*3.041*
8	110	1.458	10	30	1.098	11.5	90	2.018	13	150	3.179

Note: Training data in bold, Validation data in italic, Test data in plain

3.5 The Correlations

With reference to Figure 3.4, the NN based correlations (NN_Cor_1, NN_Cor_2 and NN_Cor_3) can be expressed as follows:

The values of hidden layer neurons are:

$$a_1^2=\tanh\left(w_{11}^2 \times x_{scaleup} + w_{12}^2 \times BPT_{scaleup} + b_1^2\right) \quad (3.13)$$

$$a_2^2=\tanh\left(w_{21}^2 \times x_{scaleup} + w_{22}^2 \times BPT_{scaleup} + b_2^2\right) \quad (3.14)$$

$$a_3^2=\tanh\left(w_{31}^2 \times x_{scaleup} + w_{32}^2 \times BPT_{scaleup} + b_3^2\right) \quad (3.15)$$

$$a_4^2=\tanh\left(w_{41}^2 \times x_{scaleup} + w_{42}^2 \times BPT_{scaleup} + b_4^2\right) \quad (3.16)$$

and $$TE_{scaleup} = a_1^3 = w_{11}^3 \times a_1^2 + w_{12}^3 \times a_2^2 + w_{13}^3 \times a_3^2 + w_{14}^3 \times a_4^2 + b_1^3 \quad (3.17)$$

Table 3.7 shows the scaled up parameters for different correlations. The different weights and biases for the different NN based correlations are shown in Tables 3.8-3.10.

Table 3.7. Scaled up parameters for NN based correlations

	NN_Cor_1	NN_Cor_2	NN_Cor_3	NN_Cor_4
std _x	2.169	4.606	3.466	3.574
std _BPT	21.02	31.274	40.371	39.738
std _TE	0.352	0.864	0.717	0.738
mean _x	4.037	7.492	7.25	6.872
mean _BPT	91.549	79.444	85	86.060
mean _TE	0.606	1.154	1.185	1.128

Table 3.8. Weights and biases of the NN_Cor_1

2nd layer			3rd layer	
weights		bias	weights	Bias
w_{11}^2 = 0. 917	w_{12}^2 = 1. 396	b_1^2 = 2 .448	w_{11}^3 = 0.005	b_1^3 = 2. 312
w_{21}^2 = 0. 213	w_{22}^2 = 0.087	b_2^2 = - 0.829	w_{12}^3 = 6 .364	
w_{31}^2 = 0.514	w_{32}^2 = - 0.174	b_3^2 = 0.409	w_{13}^3 = 0.466	
w_{41}^2 = - 0.580	w_{42}^2 = 0. 225	b_4^2 = -.2. 398	w_{14}^3 = - 1.797	

Table 3.9. Weights and biases of the NN_Cor_2

2nd layer			3rd layer	
weights		bias	weights	Bias
w_{11}^2 = -2 .087	w_{12}^2 = 1.502	b_1^2 = 2.828	w_{11}^3 = 0.008	b_1^3 = 2 .145
w_{21}^2 = -1.405	w_{22}^2 = 0.321	b_2^2 = - 0.115	w_{12}^3 = - 0. 216	
w_{31}^2 = - 0. 315	w_{32}^2 = - 0.148	b_3^2 = 0.785	w_{13}^3 = - 3. 923	
w_{41}^2 = - 0. 879	w_{42}^2 = 0.510	b_4^2 = -1.723	w_{14}^3 = - 0. 322	

Table 3.10. Weights and biases of the NN_Cor_3

2nd layer			3rd layer	
weights		bias	weights	bias
w_{11}^2 = - 0.701	w_{12}^2 = -7.97E-5	b_1^2 = - 1.517	w_{11}^3 =- 103.250	b_1^3 = 36.133
w_{21}^2 = - 4.52	w_{22}^2 = 0.111	b_2^2 = 3.117	w_{12}^3 = 0.285	
w_{31}^2 = 0.559	w_{32}^2 = 0.006	b_3^2 =- 1.398	w_{13}^3 = 148.050	
w_{41}^2 = 0.718	w_{42}^2 = - 0.038	b_4^2 = - 0.127	w_{14}^3 =- 5.976	

With reference to Figure 3.5, the NN_Cor_4can be expressed as follows:

The values of 2nd layer neurons are:

$$a_1^2 = \tanh\left(w_{11}^2 \times x_{scaleup} + w_{12}^2 \times BPT_{scaleup} + b_1^2\right) \quad (3.18)$$

$$a_2^2 = \tanh\left(w_{21}^2 \times x_{scaleup} + w_{22}^2 \times BPT_{scaleup} + b_2^2\right) \quad (3.19)$$

$$a_3^2 = \tanh\left(w_{31}^2 \times x_{scaleup} + w_{32}^2 \times BPT_{scaleup} + b_3^2\right) \quad (3.20)$$

$$a_4^2 = \tanh\left(w_{41}^2 \times x_{scaleup} + w_{42}^2 \times BPT_{scaleup} + b_4^2\right) \quad (3.21)$$

$$a_5^2 = \tanh\left(w_{51}^2 \times x_{scaleup} + w_{52}^2 \times BPT_{scaleup} + b_5^2\right) \quad (3.22)$$

$$a_6^2 = \tanh\left(w_{61}^2 \times x_{scaleup} + w_{62}^2 \times BPT_{scaleup} + b_6^2\right) \quad (3.23)$$

$$a_7^2 = \tanh\left(w_{71}^2 \times x_{scaleup} + w_{72}^2 \times BPT_{scaleup} + b_7^2\right) \quad (3.24)$$

$$a_8^2 = \tanh\left(w_{81}^2 \times x_{scaleup} + w_{82}^2 \times BPT_{scaleup} + b_8^2\right) \quad (3.25)$$

The weights and biases of the 2nd, 3rd and 4th layers are shown in Tables 3.11 – 3.13 respectively.

Table 3.11. Weights and biases of the NN_Cor_4 (2nd layer)

weights		Bias
$w_{11}^2 =$ 0.46	$w_{12}^2 =$ 0.52	$b_1^2 =$ -1.84
$w_{12}^2 =$ 0.23	$w_{22}^2 =$ 0.33	$b_2^2 =$ - 0 .20
$w_{13}^2 =$ 5.77	$w_{23}^2 =$ - 0.39	$b_3^2 =$ - 4.91
$w_{14}^2 =$ 2.98	$w_{24}^2 =$ 0.33	$b_4^2 =$ 1.96
$w_{15}^2 =$ 10.87	$w_{25}^2 =$ - 0.16	$b_5^2 =$ 1.04
$w_{16}^2 =$ 0.18	$w_{26}^2 =$ - 0.07	$b_6^2 =$ 0.55
$w_{17}^2 =$ - 0.09	$w_{27}^2 =$ 0.5	$b_7^2 =$ - 0.80
$w_{18}^2 =$ - 0.50	$w_{28}^2 =$ 0. 28	$b_8^2 =$ - 4.18

The values of 3rd layer neurons are:

$$a_1^3 = \tanh\left(\begin{array}{l} w_{11}^3 \times a_1^2 + w_{12}^3 \times a_2^2 + w_{13}^3 \times a_3^2 + w_{14}^3 \times a_4^2 \\ + w_{15}^3 \times a_5^2 + w_{16}^3 \times a_6^2 + w_{17}^3 \times a_7^2 + w_{18}^3 \times a_8^2 + b_1^3 \end{array}\right) \quad (3.26)$$

$$a_2^3=\tanh\left(\begin{matrix}w_{21}^3\times a_1^2+w_{22}^3\times a_2^2+w_{23}^3\times a_3^2+w_{24}^3\times a_4^2\\+w_{25}^3\times a_5^2+w_{26}^3\times a_6^2+w_{27}^3\times a_7^2+w_{28}^3\times a_8^2+b_2^3\end{matrix}\right) \quad (3.27)$$

$$a_3^3=\tanh\left(\begin{matrix}w_{31}^3\times a_1^2+w_{32}^3\times a_2^2+w_{33}^3\times a_3^2+w_{34}^3\times a_4^2\\+w_{35}^3\times a_5^2+w_{36}^3\times a_6^2+w_{37}^3\times a_7^2+w_{38}^3\times a_8^2+b_3^3\end{matrix}\right) \quad (3.28)$$

$$a_4^3=\tanh\left(\begin{matrix}w_{41}^3\times a_1^2+w_{42}^3\times a_2^2+w_{43}^3\times a_3^2+w_{44}^3\times a_4^2\\+w_{45}^3\times a_5^2+w_{46}^3\times a_6^2+w_{47}^3\times a_7^2+w_{48}^3\times a_8^2+b_4^3\end{matrix}\right) \quad (3.29)$$

$$a_5^3=\tanh\left(\begin{matrix}w_{51}^3\times a_1^2+w_{52}^3\times a_2^2+w_{53}^3\times a_3^2+w_{54}^3\times a_4^2\\+w_{55}^3\times a_5^2+w_{56}^3\times a_6^2+w_{57}^3\times a_7^2+w_{58}^3\times a_8^2+b_5^3\end{matrix}\right) \quad (3.30)$$

$$a_6^3=\tanh\left(\begin{matrix}w_{61}^3\times a_1^2+w_{62}^3\times a_2^2+w_{63}^3\times a_3^2+w_{64}^3\times a_4^2\\+w_{65}^3\times a_5^2+w_{66}^3\times a_6^2+w_{67}^3\times a_8^2+w_{68}^3\times a_8^2+b_6^3\end{matrix}\right) \quad (3.31)$$

Table 3.12 Weights and biases of 3rd layer of NN_Cor_4 (3rd layer)

weights				Bias
w_{11}^3 = 0.91	w_{12}^3 = 2 .11	w_{13}^3 = 4.78	w_{14}^3 = 0.15	b_1^3 = -1.21
w_{15}^3 = - 0.11	w_{16}^3 = 1.69	w_{17}^3 = 1.85	w_{18}^3 = 0.03	
w_{21}^3 = -1. 93	w_{22}^3 = - 1.42	w_{23}^3 = 0.02	w_{24}^3 = -1. 27	b_2^3 = -0.54
w_{25}^3 = 1.58	w_{26}^3 = -1.97	w_{27}^3 = - 1.02	w_{28}^3 = - 0.19	
w_{31}^3 = 1. 06	w_{32}^3 = 1.57	w_{33}^3 = 0.33	w_{34}^3 = 1.46	b_3^3 = -1.55
w_{35}^3 = - 0.76	w_{36}^3 = - 0.51	w_{37}^3 = - 0.98	w_{38}^3 = - 0.48	
w_{41}^3 = 3.29	w_{42}^3 = 1.90	w_{43}^3 = 5.22	w_{44}^3 = - 0. 30	b_4^3 = 0.38
w_{45}^3 = 1.45	w_{46}^3 = 0.21	w_{47}^3 = 1.53	w_{48}^3 = 0.03	
w_{51}^3 = 1.50	w_{52}^3 = -1.00	w_{53}^3 = -0.05	w_{54}^3 = -1.43	b_5^3 = 2.31
w_{55}^3 = - 1.65	w_{56}^3 = 0.34	w_{57}^3 = -0.42	w_{58}^3 = - 0.20	
w_{61}^3 = - 0.51	w_{62}^3 = - 0.82	w_{63}^3 = -1.10	w_{64}^3 = -1.31	b_6^3 = -1.86
w_{65}^3 = - 0.98	w_{66}^3 = 1.44	w_{67}^3 = - 0.42	w_{68}^3 = - 0.13	

The values of 4th layer neurons are:

and $TE_{scaleup}$ =

$$a_1^4 = w_{11}^4 \times a_1^3 + w_{12}^4 \times a_2^3 + w_{13}^4 \times a_3^3 + w_{14}^4 \times a_4^3 + w_{15}^4 \times a_5^3 + w_{16}^4 \times a_6^3 + b_1^4 \quad (3.31)$$

Table 3.13 Weights and biases of 4th layer of NN_Cor_4

weights		bias
w_{11}^4 = - 2.16	w_{14}^4 = 2.10	b_1^4 = 0.76
w_{12}^4 = - 1.25	w_{15}^4 = 1.35	
w_{13}^4 = 2.25	w_{16}^4 = 0.22	

The statistical regression between predicted (A) value of TE by NN correlations and experimental data (T) is plotted to find the overall trends of the predicted data (example, Figure 3.6). The regression analysis plot is used to determine the optimum network. The network architecture is updated (according to Figure 3.3) until the regression value (R) is close to 1.

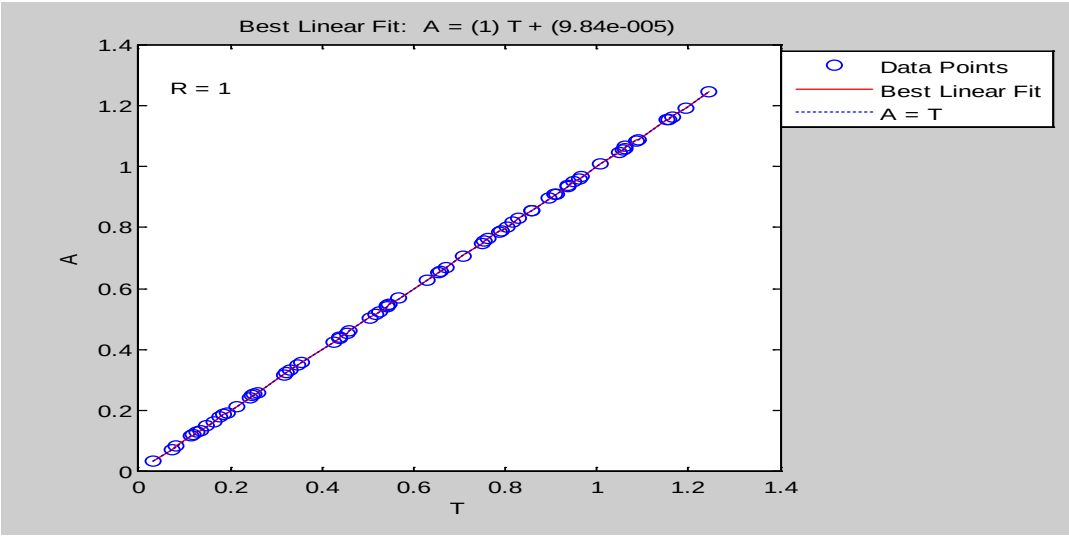

Figure 3.6 Regression of NN_Cor_1 Predicted Data with Experimental TE (Source: Bromley Data)

3.6 Results and Discussions

The input data range for the first 3 NN based correlations are shown in Table 3.14. Sample experimental data from different sources and predictions by different NN based correlations are shown in Figures 3.7-3.9. For each data source, the corresponding NN based correlation predicts the TE values close to the experimental data.

Table 3.14 The salinity and temperature data range for different NN based correlations

NN based Correlation	x range (wt %)	BPT range (^{o}C)	Number of data used
NN_Cor_1	0.19-7.136	60-120	56
NN_Cor_2	0.88-14.98	37-121.11	68
NN_Cor_3	1.5-13	20-150	336

Each correlation was also used to predict TE values based on (salinity, BPT) which were never used for training, validation or testing the correlation. For example, NN_Cor_1 is used to predict TE at BPT = 75 ^{O}C at different salinity values (Figure 3.7); NN_Cor_2 is used to predict TE at BPT = 90 ^{O}C at different salinity values (Figure 3.8); and NN_Cor_3 is used to predict TE at BPT = 116 ^{O}C at different salinity values (Figure 3.9). The results clearly show that the predictions by the correlations follow the expected trends.

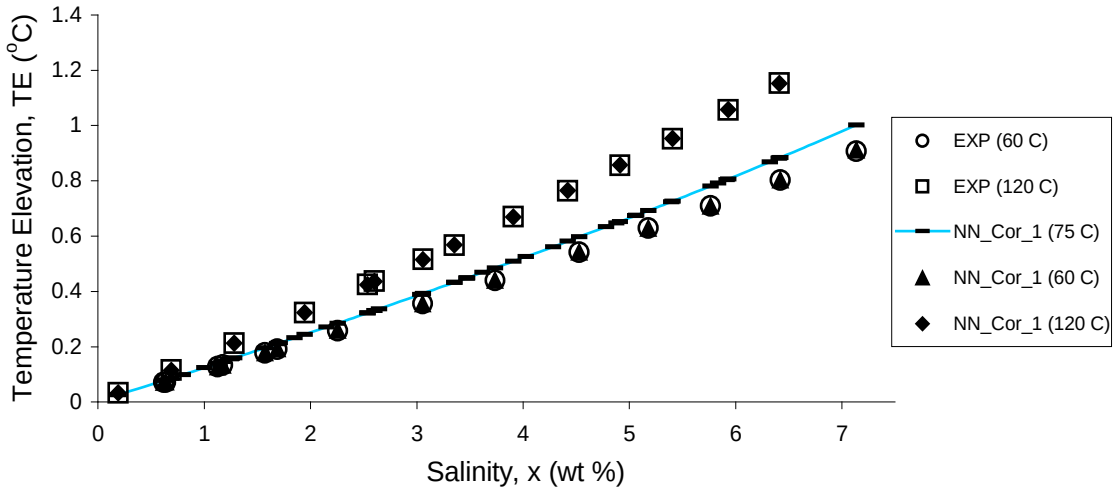

Figure 3.7. Experimental Temperature Elevation by Bromley et al. and Prediction by NN_Cor_1

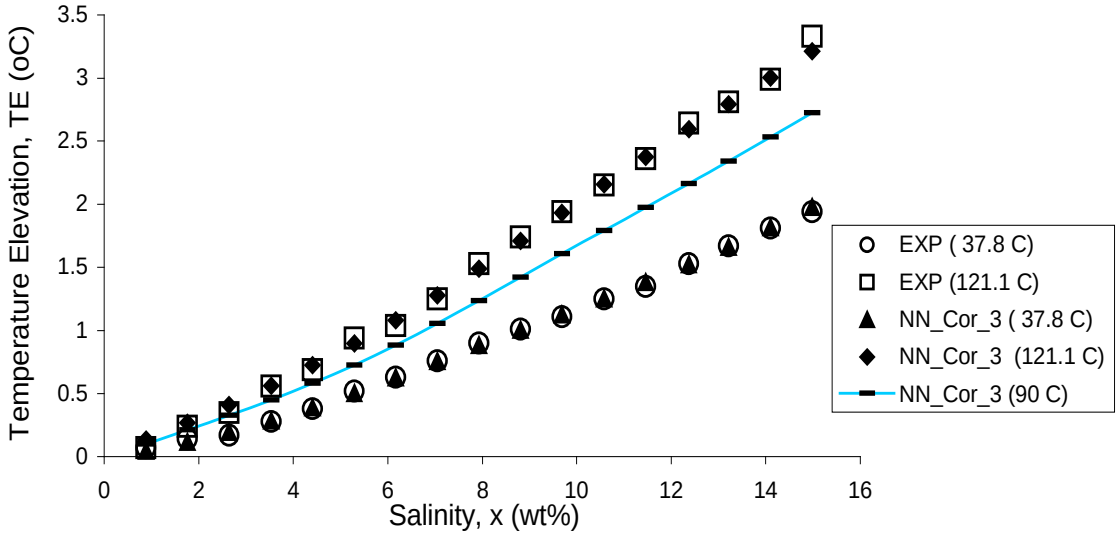

Figure 3.8. Experimental Temperature Elevation by Badger et. al. and Prediction NN_Cor_2

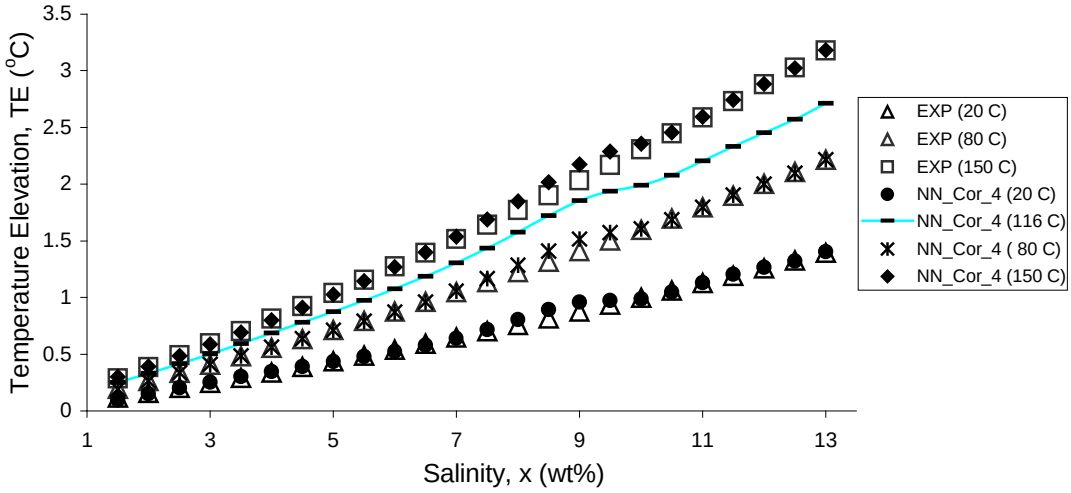

Figure 3.9. Experimental Temperature Elevation by Fabuss. and Prediction NN_Cor_3

It would be interesting at this point to investigate how different NN based correlations predict TE values using the (salinity, BPT) data from sources other than the source used to develop the correlation using the same range. For example NN_Cor_1 was developed using the salinity range (x) = <0.19, 7.136> and BPT range =<60,120 C> (Table 3.14). NN_Cor_1 is now used to predict TE values using Badger data within the range of x =<0.88, 7.136> and BPT <60,120 C>. The results are shown in Table 3.15. Similarly prediction of TE by NN_Cor_1 using Fabuss' data within the range of x = <1.5, 7.136> and BPT = <60,120> are shown in Table 3.16. Predictions by NN_Cor_2 for Bromley and Fabuss data within a given range of salinity and BPT are shown in Tables 3.17 and 3.18. Predictions by NN_Cor_3 for Bromley and Badger data are shown in Tables 3.19 and 3.20.

In each of the Tables 3.15-3.20, the predicted TE is compared with the experimental TE. It is interesting to note that predictions of TE by NN_Cor_1 are close to Fabuss's data (compare TEs in Table 3.16). Also predictions of TE by NN_Cor_3 are close to Bromley data (Table 3.19).

However, predictions of TE by NN_Cor_1 and NN_Cor_3 were not as close as expected to the experimental TE by Badger data (Table 3.15, Table 3.20). Also predictions of TE by NN_Cor_2 were not close to experimental TE by Bromley and Fabuss data (Table 3.17 and 3.18).

Table 3.15. Comparison of prediction by NN_Cor_1 and experimental data from Badger data

Range: x = <0.88 - 7.136> BPT = <60 - 120>

Salinity	BPT	TE_{EXP}	TE_{NN}	Salinity	BPT	TE_{EXP}	TE_{NN}
0.88	65.56	0.069	0.103	0.88	93.33	0.069	0.125
1.76	65.56	0.174	0.208	1.76	93.33	0.208	0.248
2.64	65.56	0.208	0.317	2.64	93.33	0.278	0.376
3.53	65.56	0.347	0.430	3.53	93.33	0.451	0.512
4.41	65.56	0.486	0.546	4.41	93.33	0.556	0.650
5.29	65.56	0.660	0.667	5.29	93.33	0.764	0.795
6.17	65.56	0.764	0.794	6.17	93.33	0.903	0.945
7.05	65.56	0.938	0.930	7.05	93.33	1.076	1.103
Maximum deviation				0.1083			

Table 3.16. Comparison of prediction by NN_Cor_1 and experimental data from Fabuss data

Range: x = <1.5 - 7.136> BPT = <60 - 120>

Salinity	BPT	TE_{EXP}	TE_{NN}	Salinity	BPT	TE_{EXP}	TE_{NN}	Salinity	BPT	TE_{EXP}	TE_{NN}
1.5	60	0.170	0.171	3.5	60	0.418	0.411	5.5	60	0.691	0.671
1.5	70	0.183	0.182	3.5	70	0.449	0.438	5.5	70	0.743	0.717
1.5	80	0.196	0.194	3.5	80	0.481	0.467	5.5	80	0.794	0.764
1.5	90	0.209	0.207	3.5	90	0.512	0.497	5.5	90	0.845	0.813
1.5	100	0.222	0.220	3.5	100	0.544	0.528	5.5	100	0.896	0.864
1.5	110	0.235	0.235	3.5	110	0.575	0.560	5.5	110	0.948	0.917
1.5	120	0.248	0.250	3.5	120	0.607	0.595	5.5	120	0.999	0.972
2	60	0.229	0.229	4	60	0.484	0.473	6	60	0.764	0.741
2	70	0.247	0.244	4	70	0.520	0.506	6	70	0.820	0.791
2	80	0.264	0.260	4	80	0.556	0.539	6	80	0.876	0.843
2	90	0.282	0.277	4	90	0.593	0.573	6	90	0.933	0.897
2	100	0.299	0.295	4	100	0.629	0.609	6	100	0.989	0.953
2	110	0.317	0.313	4	110	0.666	0.647	6	110	1.046	1.011
2	120	0.334	0.333	4	120	0.702	0.686	6	120	1.103	1.071
2.5	60	0.291	0.289	4.5	60	0.552	0.538	6.5	60	0.838	0.814
2.5	70	0.313	0.308	4.5	70	0.593	0.574	6.5	70	0.899	0.868
2.5	80	0.335	0.328	4.5	80	0.634	0.612	6.5	80	0.961	0.925
2.5	90	0.357	0.348	4.5	90	0.675	0.651	6.5	90	1.022	0.984
2.5	100	0.379	0.370	4.5	100	0.716	0.692	6.5	100	1.084	1.044
2.5	110	0.401	0.394	4.5	110	0.758	0.735	6.5	110	1.146	1.107
2.5	120	0.423	0.418	4.5	120	0.790	0.779	6.5	120	1.208	1.171
3	60	0.354	0.349	5	60	0.621	0.603	7	60	0.913	0.890
3	70	0.380	0.372	5	70	0.667	0.645	7	70	0.980	0.948
3	80	0.407	0.397	5	80	0.713	0.687	7	80	1.047	1.009
3	90	0.434	0.422	5	90	0.759	0.731	7	90	1.114	1.072
3	100	0.460	0.448	5	100	0.805	0.777	7	100	1.181	1.138
3	110	0.487	0.476	5	110	0.852	0.825	7	110	1.248	1.205
3	120	0.514	0.505	5	120	0.898	0.875	7	120	1.315	1.274
Maximum deviation								0.0434			

Table 3.17. Comparison of prediction by NN_Cor_2 and experimental data form Bromley data

Range: x = <0.88 - 7.136> BPT = <60 - 120>

Salinity	BPT	TE_{EXP}	TE_{NN}	Salinity	BPT	TE_{EXP}	TE_{NN}
1.13	60	0.128	0.098	1.25	80	0.163	0.135
1.17	60	0.134	0.102	1.85	80	0.241	0.206
1.57	60	0.178	0.140	2.54	80	0.331	0.289
1.69	60	0.192	0.152	2.64	80	0.347	0.302
2.25	60	0.258	0.209	3.47	80	0.461	0.408
3.05	60	0.356	0.294	3.47	80	0.461	0.408
3.74	60	0.440	0.374	4.03	80	0.542	0.484
4.53	60	0.542	0.476	4.78	80	0.654	0.595
5.18	60	0.629	0.569	5.39	80	0.749	0.693
5.76	60	0.709	0.660	5.84	80	0.816	0.768
6.42	60	0.803	0.767	5.91	80	0.830	0.782
7.14	60	0.907	0.888	6.32	80	0.894	0.855
1.00	100	0.147	0.123	6.41	80	0.910	0.870
1.26	100	0.185	0.158	6.57	80	0.937	0.901
1.68	100	0.248	0.217	6.58	80	0.936	0.902
1.71	100	0.251	0.221	6.75	80	0.964	0.934
2.15	100	0.318	0.283	6.99	80	1.008	0.980
3.03	100	0.454	0.411	1.28	120	0.213	0.191
3.35	100	0.505	0.460	1.95	120	0.324	0.294
3.47	100	0.524	0.479	2.54	120	0.425	0.389
3.62	100	0.547	0.501	2.60	120	0.437	0.400
4.28	100	0.657	0.607	3.06	120	0.516	0.478
4.88	100	0.756	0.707	3.35	120	0.567	0.529
5.06	100	0.789	0.738	3.91	120	0.670	0.628
5.06	100	0.790	0.739	4.42	120	0.764	0.723
5.45	100	0.857	0.808	4.91	120	0.856	0.817
6.03	100	0.960	0.918	5.40	120	0.951	0.914
6.52	100	1.049	1.015	5.93	120	1.056	1.023
6.59	100	1.061	1.028	6.41	120	1.154	1.127
6.62	100	1.062	1.035	6.59	120	1.193	1.167
6.72	100	1.088	1.055	6.87	120	1.246	1.228
6.74	100	1.090	1.059				
7.10	100	1.157	1.134				
7.14	100	1.167	1.143				
Maximum deviation				0.06635			

Table 3.18. Comparison of prediction by NN_Cor_2 and experimental data from Fabuss data

Range: x = <1.5 - 13> BPT = <37 - 121.11>

Salinity	BPT	TE_{EXP}	TE_{NN}	Salinity	BPT	TE_{EXP}	TE_{NN}	Salinity	BPT	TE_{EXP}	TE_{NN}
1.5	40	0.144	0.099	4	40	0.412	0.344	6	40	0.651	0.613
1.5	50	0.157	0.116	4	50	0.448	0.374	6	50	0.708	0.654
1.5	60	0.170	0.133	4	60	0.484	0.407	6	60	0.764	0.698
1.5	70	0.183	0.150	4	70	0.520	0.443	6	70	0.820	0.745
1.5	80	0.196	0.164	4	80	0.556	0.481	6	80	0.876	0.797
1.5	90	0.209	0.178	4	90	0.593	0.520	6	90	0.933	0.853
1.5	100	0.222	0.191	4	100	0.629	0.561	6	100	0.989	0.912
1.5	110	0.235	0.206	4	110	0.666	0.603	6	110	1.046	0.974
1.5	120	0.248	0.224	4	120	0.702	0.645	6	120	1.103	1.038
2	40	0.195	0.141	4.5	40	0.470	0.405	6.5	40	0.715	0.687
2	50	0.212	0.162	4.5	50	0.511	0.437	6.5	50	0.776	0.732
2	60	0.229	0.183	4.5	60	0.552	0.473	6.5	60	0.838	0.780
2	70	0.247	0.204	4.5	70	0.593	0.511	6.5	70	0.899	0.832
2	80	0.264	0.224	4.5	80	0.634	0.553	6.5	80	0.961	0.888
2	90	0.282	0.243	4.5	90	0.675	0.597	6.5	90	1.022	0.947
2	100	0.299	0.261	4.5	100	0.716	0.643	6.5	100	1.084	1.011
2	110	0.317	0.280	4.5	110	0.758	0.690	6.5	110	1.146	1.077
2	120	0.334	0.302	4.5	120	0.790	0.738	6.5	120	1.208	1.146
2.5	40	0.247	0.186	5	40	0.529	0.471	7	40	0.780	0.761
2.5	50	0.269	0.209	5	50	0.575	0.505	7	50	0.846	0.811
2.5	60	0.291	0.234	5	60	0.621	0.543	7	60	0.913	0.865
2.5	70	0.313	0.259	5	70	0.667	0.585	7	70	0.980	0.921
2.5	80	0.335	0.284	5	80	0.713	0.630	7	80	1.047	0.982
2.5	90	0.357	0.309	5	90	0.759	0.678	7	90	1.114	1.046
2.5	100	0.379	0.333	5	100	0.805	0.728	7	100	1.181	1.114
2.5	110	0.401	0.357	5	110	0.852	0.780	7	110	1.248	1.185
2.5	120	0.423	0.384	5	120	0.898	0.834	7	120	1.315	1.259
3.5	40	0.355	0.287	5.5	40	0.589	0.541	7.5	40	0.846	0.834
3.5	50	0.387	0.315	5.5	50	0.640	0.578	7.5	50	0.918	0.891
3.5	60	0.418	0.345	5.5	60	0.691	0.618	7.5	60	0.990	0.950
3.5	70	0.449	0.378	5.5	70	0.743	0.663	7.5	70	1.062	1.013
3.5	80	0.481	0.412	5.5	80	0.794	0.711	7.5	80	1.135	1.079
3.5	90	0.512	0.447	5.5	90	0.845	0.763	7.5	90	1.207	1.148
3.5	100	0.544	0.483	5.5	100	0.896	0.818	7.5	100	1.279	1.221
3.5	110	0.575	0.518	5.5	110	0.948	0.875	7.5	110	1.352	1.297
3.5	120	0.607	0.555	5.5	120	0.999	0.934	7.5	120	1.425	1.377
Maximum deviation								0.1531			

Table 3.19. Comparison of prediction by NN_Cor_3 and experimental data from Bromley data

Range: x = <1.5 - 7.136> BPT = <60 - 120>

Salinity	BPT	TE_{EXP}	TE_{NN}	Salinity	BPT	TE_{EXP}	TE_{NN}
1.57	60	0.178	0.172	1.85	80	0.241	0.243
1.69	60	0.192	0.187	2.54	80	0.331	0.343
2.25	60	0.258	0.261	2.64	80	0.347	0.359
3.05	60	0.356	0.367	3.47	80	0.461	0.481
3.74	60	0.440	0.457	3.47	80	0.461	0.482
4.53	60	0.542	0.560	4.03	80	0.542	0.565
5.18	60	0.629	0.644	4.78	80	0.654	0.679
5.76	60	0.709	0.723	5.39	80	0.749	0.773
6.42	60	0.803	0.820	5.84	80	0.816	0.844
7.14	60	0.907	0.943	5.91	80	0.830	0.856
1.68	100	0.248	0.253	6.32	80	0.894	0.927
1.71	100	0.251	0.257	6.41	80	0.910	0.942
2.15	100	0.318	0.325	6.57	80	0.937	0.972
3.03	100	0.454	0.468	6.58	80	0.936	0.973
3.35	100	0.505	0.521	6.75	80	0.964	1.005
3.47	100	0.524	0.541	6.99	80	1.008	1.054
3.62	100	0.547	0.566	1.95	120	0.324	0.329
4.28	100	0.657	0.678	2.54	120	0.425	0.430
4.88	100	0.756	0.781	2.60	120	0.437	0.441
5.06	100	0.789	0.813	3.06	120	0.516	0.523
5.06	100	0.790	0.814	3.35	120	0.567	0.577
5.45	100	0.857	0.883	3.91	120	0.670	0.681
6.03	100	0.960	0.992	4.42	120	0.764	0.779
6.52	100	1.049	1.089	4.91	120	0.856	0.875
6.59	100	1.061	1.104	5.40	120	0.951	0.974
6.62	100	1.062	1.111	5.93	120	1.056	1.083
6.72	100	1.088	1.131	6.41	120	1.154	1.190
6.74	100	1.090	1.135	6.59	120	1.193	1.233
7.10	100	1.157	1.216	6.87	120	1.246	1.298
7.14	100	1.167	1.225				
Maximum deviation				0.0588			

Table 3.20. Comparison of prediction by NN_Cor_3 and experimental data Badger data

Range: x = <01.5 - 10.38> BPT = <37 - 121.1>

Salinity	BPT	TE_{EXP}	TE_{NN}	Salinity	BPT	TE_{EXP}	TE_{NN}
1.76	37.78	0.139	0.157	1.76	65.56	0.174	0.206
2.64	37.78	0.174	0.260	2.64	65.56	0.208	0.325
3.53	37.78	0.278	0.361	3.53	65.56	0.347	0.447
4.41	37.78	0.382	0.456	4.41	65.56	0.486	0.566
5.29	37.78	0.521	0.549	5.29	65.56	0.660	0.686
6.17	37.78	0.625	0.648	6.17	65.56	0.764	0.814
7.05	37.78	0.764	0.772	7.05	65.56	0.938	0.965
7.93	37.78	0.903	0.932	7.93	65.56	1.042	1.152
8.81	37.78	1.007	1.099	8.81	65.56	1.215	1.349
9.69	37.78	1.111	1.153	9.69	65.56	1.389	1.436
10.58	37.78	1.250	1.249	10.58	65.56	1.528	1.546
11.46	37.78	1.354	1.404	11.46	65.56	1.597	1.727
12.37	37.78	1.528	1.531	12.37	65.56	1.875	1.886
1.76	93.33	0.208	0.253	1.76	121.11	0.243	0.300
2.64	93.33	0.278	0.389	2.64	121.11	0.347	0.451
3.53	93.33	0.451	0.531	3.53	121.11	0.556	0.613
4.41	93.33	0.556	0.675	4.41	121.11	0.694	0.781
5.29	93.33	0.764	0.822	5.29	121.11	0.938	0.956
6.17	93.33	0.903	0.979	6.17	121.11	1.042	1.142
7.05	93.33	1.076	1.159	7.05	121.11	1.250	1.352
7.93	93.33	1.250	1.374	7.93	121.11	1.528	1.596
8.81	93.33	1.458	1.601	8.81	121.11	1.736	1.854
9.69	93.33	1.632	1.722	9.69	121.11	1.944	2.011
10.58	93.33	1.806	1.848	10.58	121.11	2.153	2.153
11.46	93.33	1.875	2.053	11.46	121.11	2.361	2.383
12.37	93.33	2.153	2.244	12.37	121.11	2.639	2.606
Maximum deviation				0.1783			

Sample experimental data from different sources and predictions by different NN_Cor_4 are shown in Tables 3.21. For each data source, the corresponding NN based correlation predicts the TE values close to experimental data (maximum deviations). NN_Cor_4 is based on wide range of salinity and temperature.

Table 3.21. Comparison of prediction by NN_Cor_4 and experimental data sources

. Sample Bromley data				Sample Badger data			
x	T	TE	TE_{NN}	x	T	TE	TE_{NN}
0.619	60.00	0.071	0.062	3.4446	50.00	0.500	0.377
0.637	60.00	0.072	0.064	3.4446	60.00	0.575	0.408
1.126	60.00	0.128	0.116	3.4446	70.00	0.600	0.441
1.174	60.00	0.134	0.121	3.4446	80.00	0.620	0.474
1.571	60.00	0.178	0.167	3.4446	90.00	0.650	0.508
1.687	60.00	0.192	0.182	3.4446	100.00	0.680	0.542
2.254	60.00	0.258	0.254	3.4446	110.00	0.700	0.579
3.054	60.00	0.356	0.358	3.4446	120.00	0.725	0.621
3.735	60.00	0.440	0.445	3.4446	130.00	0.760	0.670
4.529	60.00	0.542	0.525	3.4446	140.00	0.800	0.729
5.178	60.00	0.629	0.618	3.4446	150.00	0.820	0.798
5.764	60.00	0.709	0.731	3.4446	160.00	0.860	0.875
6.421	60.00	0.803	0.767	3.4446	170.00	0.900	0.960
7.135	60.00	0.907	0.922	3.4446	180.00	0.930	1.051
0.624	80.00	0.081	0.070	3.4446	190.00	0.970	1.148
1.253	80.00	0.163	0.148	3.4446	200.00	1.000	1.254
Max. Dev.			0.0492	Max. Dev.			0.1606
. Sample Fabuss data							
x	T	TE	TE_{NN}	x	T	TE	TE_{NN}
3	100.00	0.460	0.452	3.5	40.00	0.355	0.354
3	110.00	0.487	0.478	3.5	50.00	0.387	0.384
3	120.00	0.514	0.508	3.5	60.00	0.418	0.416
3	130.00	0.541	0.545	3.5	70.00	0.449	0.449
3	140.00	0.568	0.596	3.5	80.00	0.481	0.483
3	150.00	0.595	0.664	3.5	90.00	0.512	0.518
3.5	20.00	0.293	0.304	3.5	100.00	0.544	0.554
3.5	30.00	0.324	0.327	3.5	110.00	0.575	0.592
Max. Dev.		Max. Dev.					0.1780

Even though the predictions by NN_Cor_4 within the range of each data source are not as close to experimental TE as expected (compare Table 3.21), they were very good and are within acceptable engineering accuracy. In an MSF process, the salinity and temperature range can be very wide between 1st and last stage and in that circumstances use of NN_Cor_4 would be desirable.

Comparison of predictions (in terms of maximum, minimum, and average deviation) by Correlation 2 (of Table 3.2) and all NN based correlations are shown in Table 3.22. Note none of the data from Correlation 2 was used for training, validation and testing of NN based correlations. It can be noted that predictions by NN correlations were very good (low average deviation) where enough data is used to train the NN model within the (salinity, temperature) range.

Table 3.22. Comparison of prediction by NN_Cor_4 and experimental data sources

Correlations	Max. Dev	Min. Dev.	Avg. Dev.
Correlation2: Salinity range=<2, 28> and BPT range =<20, 280>			
Salinity range=<2, 14.9> and BPT range =<10, 170> Tested with 990 data points			
NN_Cor_4	0.8114	0.0000	0.0440
Salinity range=<2, 7> and BPT range =<60, 120> Tested with 175 data points			
NN_Cor_1	0.0133	0.0001	0.0025
Salinity range=<2, 14.9> and BPT range =<40, 120> Tested with 599 data points			
NN_Cor_2	0.2620	0.0000	0.0368
Salinity range=<2, 13> and BPT range =<20, 150> Tested with 715 data points			
NN_Cor_3	0.1581	0.0000	0.0375

It is anticipated from these observations that the seawater constituents for Bromley and Fabuss are similar while that for Badger is different.

It is important to note that if the seawater constituents change, development of traditional correlations such as those listed in Table 3.2 will require much effort. Updating the constant coefficients of the correlations may not be sufficient and structure of the correlation may be altered altogether.

However, due to advancement of the microcomputer, plant automation becomes reliable means of plant maintenance. NN based correlation can be updated in terms of new sets of weights and biases for the same architecture (same no. of hidden layers and no. of neurons) reliably with new plant data by training, validation and testing according to Figure 3.3 using the plant automation software. The NN based correlation can be updated in two situations.

Situation 1 where there are two NN based correlations for two plants and there is a need for a correlation for predicting TE for a third plant. The seawater constituents of the third plant are close to and between those of the existing plants experimental data. However, the experimental data from the third plant are not enough to develop the NN based correlation from its source. In this particular situation, one can develop a temporary correlation for the new plant with the existing NN architecture (no of nodes and hidden layers are fixed) using the algorithm outlined in Figure 3.3.

Situation 2 is where rapid industrialisation or natural disaster may lead to environmental change of the seabed. In such situation, seawater constituents of plant intake may change over the time. Plant automation technique (Tarifa et al., 2003) can detect the discrepancy between the experimental TE and predicted TE by NN based correlation. In this situation,

plant automation software can update an existing NN based correlation with the existing NN architecture or with a new architecture using the algorithm outlined in Figure 3.3.

For example, here the existing NN architecture (of NN_Cor_1) is updated using Fabuss data in addition to Bromley data. Let the new correlation be called as NN_Cor_5. The scaled parameters are shown in Table 3.23. The weights and biases of Table 3.8 are updated. The new values are shown in Table 3.24. Table 3.16 is now updated and the results are in Table 3.25. TE values are now more close to TE values obtained by Fabuss (Comparison of Table 3.16 and 3.25). Similarly, the existing NN model architecture (of NN_Cor_1) is updated using Badger data (for salinity 2, 3.5, 5.5, 6, 7) in addition to Bromley data to develop the new correlation NN_Cor_6. The weights and biases of Table 3.8 are updated. The new values are shown in Table 3.26. Table 3.15 is now updated and the results are in Table 3.27. TE values are now close to TE values obtained by Badger (Comparison of Table 3.15 and 3.27). However, change in architecture would definitely provide more close TE values.

Table 3.23. Scaled up parameter for NN based correlations

	NN_Cor_5	NN_Cor_6
std _ x	2.027	4.004
std _ BPT	32.393	27.477
std _ TE	0.355	0.717
mean _ x	4.397	5.714
mean _ BPT	88.429	85.436
mean _ TE	0.658	0.872

Table 3.24. Weights and biases of the NN_Cor_5

2nd layer			3rd layer	
weights		bias	weights	bias
$w_{11}^2 = -0.011$	$w_{12}^2 = 0.231$	$b_1^2 = 0.873$	$w_{11}^3 = 2.126$	$b_1^3 = 0.309$
$w_{21}^2 = -0.307$	$w_{22}^2 = -0.236$	$b_2^2 = 1.137$	$w_{12}^3 = -3.264$	
$w_{31}^2 = 0.182$	$w_{32}^2 = -0.042$	$b_3^2 = 0.631$	$w_{13}^3 = 4.849$	
$w_{41}^2 = -0.488$	$w_{42}^2 = -0.293$	$b_4^2 = -2.404$	$w_{14}^3 = 1.944$	

Table 3.25. Comparison of prediction by NN_Cor_5 and experimental data from Fabuss & Bromley

Salinity	BPT	TE_{EXP}	TE_{NN}	Salinity	BPT	TE_{EXP}	TE_{NN}
Bromley data Range: x = <0.19 - 7.136> BPT = <60 - 120>							
4.529	60	0.542	0.549	0.798	100	0.118	0.116
5.178	60	0.629	0.637	1.001	100	0.147	0.146
6.421	60	0.803	0.811	1.257	100	0.185	0.183
1.253	80	0.163	0.162	1.946	120	0.324	0.322
2.643	80	0.347	0.351	3.353	120	0.567	0.571
Maximum deviation				0.0231			
Fabuss data Range: x = <1.5 - 7> BPT = <20 - 150>							
3.5	120	0.607	0.598	5.5	110	0.948	0.929
3.5	130	0.639	0.632	5.5	120	0.999	0.983
5.5	20	0.488	0.493	7	50	0.846	0.834
5.5	100	0.896	0.876	7	60	0.913	0.895
Maximum deviation				0.0254			
Fabuss and Bromley data Range: x = <0.19 - 7> BPT = <20 - 150>							
Maximum deviation				0.0254			

Table 3.26. Weights and biases of the NN_Cor_6

2nd layer			3rd layer	
weights		bias	weights	bias
$w_{11}^2 = 0.097$	$w_{12}^2 = 0.130$	$b_1^2 = -0.652$	$w_{11}^3 = 14.681$	$b_1^3 = -0.11$
$w_{21}^2 = -2.466$	$w_{22}^2 = -5.557$	$b_2^2 = 9.422$	$w_{12}^3 = -0.113$	
$w_{31}^2 = -0.002$	$w_{32}^2 = -0.178$	$b_3^2 = 0.509$	$w_{13}^3 = 7.813$	
$w_{41}^2 = -3.688$	$w_{42}^2 = -0.168$	$b_4^2 = -3.825$	$w_{14}^3 = 0.048$	

Table 3.27. Comparison of prediction by NN_Cor_6 and experimental data from Badger & Bromley

Salinity	BPT	TE_{EXP}	TE_{NN}	Salinity	BPT	TE_{EXP}	TE_{NN}
Badger Data Range: x = <0.88 - 7.136> BPT = <60 - 120>							
0.88	65.56	0.069	0.101	0.88	93.33	0.069	0.117
1.76	65.56	0.174	0.192	1.76	93.33	0.208	0.227
2.64	65.56	0.208	0.288	2.64	93.33	0.278	0.348
3.53	65.56	0.347	0.404	3.53	93.33	0.451	0.488
4.41	65.56	0.486	0.528	4.41	93.33	0.556	0.635
5.29	65.56	0.660	0.657	5.29	93.33	0.764	0.786
6.17	65.56	0.764	0.789	6.17	93.33	0.903	0.941
7.05	65.56	0.938	0.927	7.05	93.33	1.076	1.101
Maximum deviation				0.0799			
Bromley data Range: x = <0.19 - 7.136> BPT =<60 - 120>							
0.62	60.00	0.071	0.069	4.28	100.00	0.657	0.639
0.64	60.00	0.072	0.071	4.88	100.00	0.756	0.744
1.13	60.00	0.128	0.122	5.06	100.00	0.789	0.776
1.17	60.00	0.134	0.127	5.06	100.00	0.790	0.778
1.57	60.00	0.178	0.166	5.45	100.00	0.857	0.847
1.25	80.00	0.163	0.153	1.95	120.00	0.324	0.302
1.85	80.00	0.241	0.221	2.54	120.00	0.425	0.401
2.64	80.00	0.347	0.320	5.93	120.00	1.056	1.052
Maximum deviation				0.0303			
Badger and Bromley data Range: x = <0 - 14.98> BPT = <37.78 - 121.11>							
Maximum deviation				0.0828			

3.7 Conclusions

In this work, several NN based correlations for predicting TE of seawater are developed. For each correlation, a multi-layered feed forward network trained with back propagation method is used. The NN based correlations can predict the experimental TE and TE obtained using correlations form literature very closely.

The proposed NN model structure (with one hidden layer and four neurons in hidden layer) is capable of predicting the experimental TE very closely (low maximum deviation). For a given architecture, any correlation can be updated with additional data from other sources or a new correlation can be developed for the new source data. Predictions by different NN

based correlations (for different salinity and BPT) within the training range follow the expected trends and it is within the engineering accuracy.

It is found that redevelopment of an NN based correlation form an existing one with new data is very easy. However, the prediction of TE by the new correlation solely depends on the source of data (i.e., the seawater constituents and conditions and above all, accuracy of the data).

Out of all the NN based correlations presented in this chapter the NNCor_1 is implemented within the MSF process model presented in later chapters of this work. If desired, similar correlations can be developed for other seawater properties such as density, viscosity, etc. in future.

Chapter 4

Modelling Simulation and Optimisation Features of gPROMS

4.1 . gPROMS: the Modelling Software

4.1.1 Introduction

Process Systems Enterprise (PSE) is one of the world's leading software package providers for the process manufacturing industries. gPROMS (**g**eneral **P**rocess **M**odelling **S**ystem) Model builder commonly known as gPROMS is one of the modelling platform of PSE for steady state and dynamic simulation, optimisation, experiment design and parameter estimation of any process (Oh and Pantelides, 1996; Georgiadis et al., 2005; Gosling, 2005). gPROMS allows user to model the transient behaviour of individual unit operations to be described in terms of mixed systems of integral, partial differential and algebraic equations (IPDAEs). The gPROMS is a robust and open structure software (CAPE-OPEN, 2007; Gosling, 2005).

The major products of PSE are:

- gPROMS®
- ModelEnterprise®
- ModelCare®

4.1.2 The gPROMS model builder family of products

gPROMS Model Builder software package has the following components:

- gPROMS Model Builder
- gO: CFD

- go: Run
- go: Cape Open
- go: Simulink and
- go: Matlab

gO: CFD, go: Cape Open, go: Simulink, go: Matlab enable control engineers to deploy complex gPROMS process models within other software environment. gPROMS model can be exported to most of the modelling and solution engine in packages such as FLUENT, Aspen Plus, Hysys, Matlab, Simulink, or various automation systems using the above mention package component. It has the capability of automatic generation of CAPE-OPEN Unit Operation models can be exported as a CAPE -OPEN Unit Operation Model (Gosling, 2005).

4.1.3 Features of gPROMS

gPROMS has a standard Process Model Library to develop the process flowsheet. It uses high-level language to describe complex physics based on the equation-oriented technology. It has built in numerical solver for process simulation and optimisation problem.

A single gPROMS model of a process can perform many activities. Such as:

- Laboratory experiment design and optimisation
- Detailed design of the complex unit
- Process flowsheeting
- Simultaneous optimisation
- Detailed design and optimisation
- Design of optimal procedure

gPROMS has been chosen by model developers because of the following advantages.

- Reversible-irreversible, symmetric-asymmetric, continuities-discontinuities and discrete system are handled by gPROMS simulators. These capabilities of gPROMS for solution of process makes more robust and faster. It analyses the processes by physical and chemical relationships.
- Equations of physical systems can be written as they appear in technical papers or books i.e. without reformulation.
- It is an equation-based system. It can handle a large number of differential and algebraic equations. Dynamic models with over 100,000 differential and algebraic equations have been simulated using their software (gPROMS, 2004). In addition, it can also handle PDE equations.
- Single or multi-dimensional arrays of both variables and equations can be described either implicitly or explicitly. All variables, other than those that are functions of time only, can be featured as distributions over one or more continuous and/or discrete domains.
- gPROMS allows using a single equipment model (described by several equations) for multiple operating procedures (process) and single process can be used for several optimisation tasks. It provides greater flexibility and model development time is reduced.
- It allows simultaneous optimisation of equipment sizes and operating procedures that saves capital and operational cost in long run.
- gPROMS analyses the mathematical model in identifying structural problems and errors in the modelling and/or the problem specification. The degrees of freedom of equations, index of given DAE system, boundary condition and initial conditions

are checked by gPROMS.

All of the above features of gPROMS reduce both time and numerical expertise to perform model-based activities and assist the user. It can easily link to external components, for example, physical properties packages or control system software, MS office.

In this work, gPROMS (Version 2.3.4) Model Builder is used to develop model for simulation and optimisation of MSF desalination process.

4.2 Model Development using gPROMS

In gPROMS model builder, the project-tree (Figure 4.1) shows all the currently opened projects and cases.

The Project (Figure 4.2) has several sub sections, among them the important sections are

- Variables types
- Models
- Tasks
- Process
- Optimisation
- Parameter estimation
- Experimental design

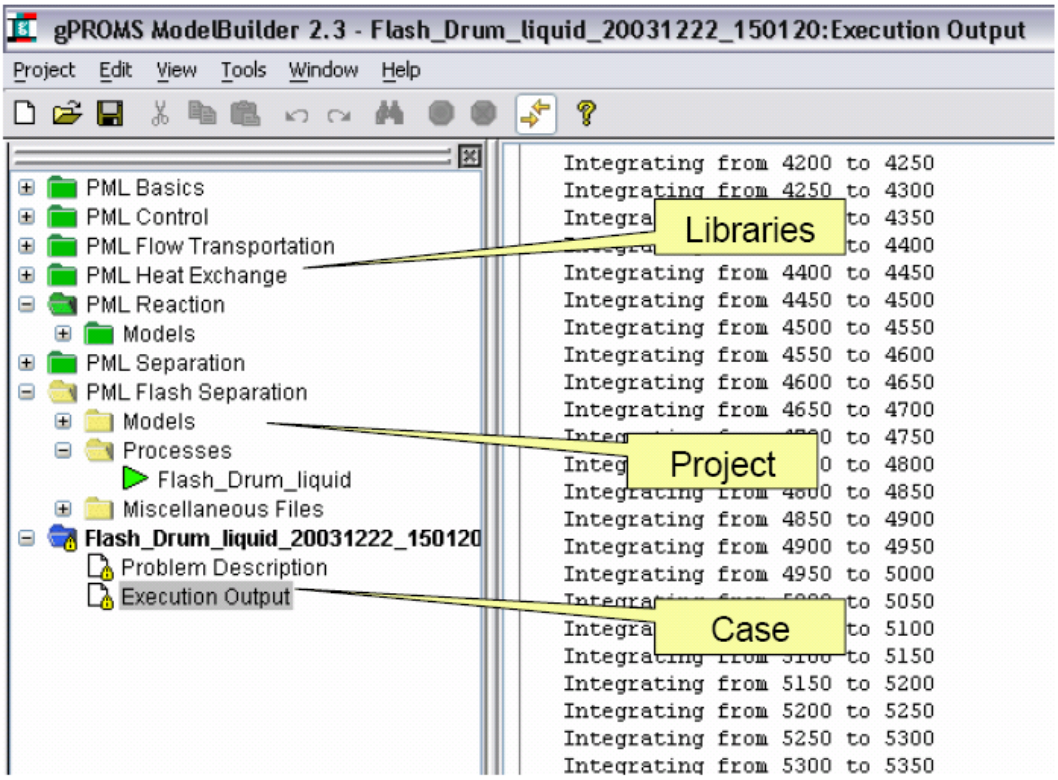

Figure 4.1 gPROMS Model Builder Project Tree

In VARIABLES TYPES section, the types and range of the variables are specified for different MODEL, PROCESS. Equipment Unit equations, physical properties equations and flowsheet equations are written in MODEL section. PROCESS section contains specifications for simulating the process. Optimising the operation of the process is written in OPTIMISATION section. MODEL and TASK can be constructed in a hierarchy of arbitrary depth. TASKS and MODEL can be constructed hierarchically.

At higher level, TASK/PROCESS is composed of several elementary operations of lower level TASKs. All variables may be defined as distribution of one or more continuous and discrete systems.

4.2.1 Defining a model

MODEL is defined as the modelling of physical, chemical and biological plant behaviour.

The model consists of the following sections:

- PARAMETER
- VARIABLE
- UNIT
- STREAM and PORT
- EQUATION

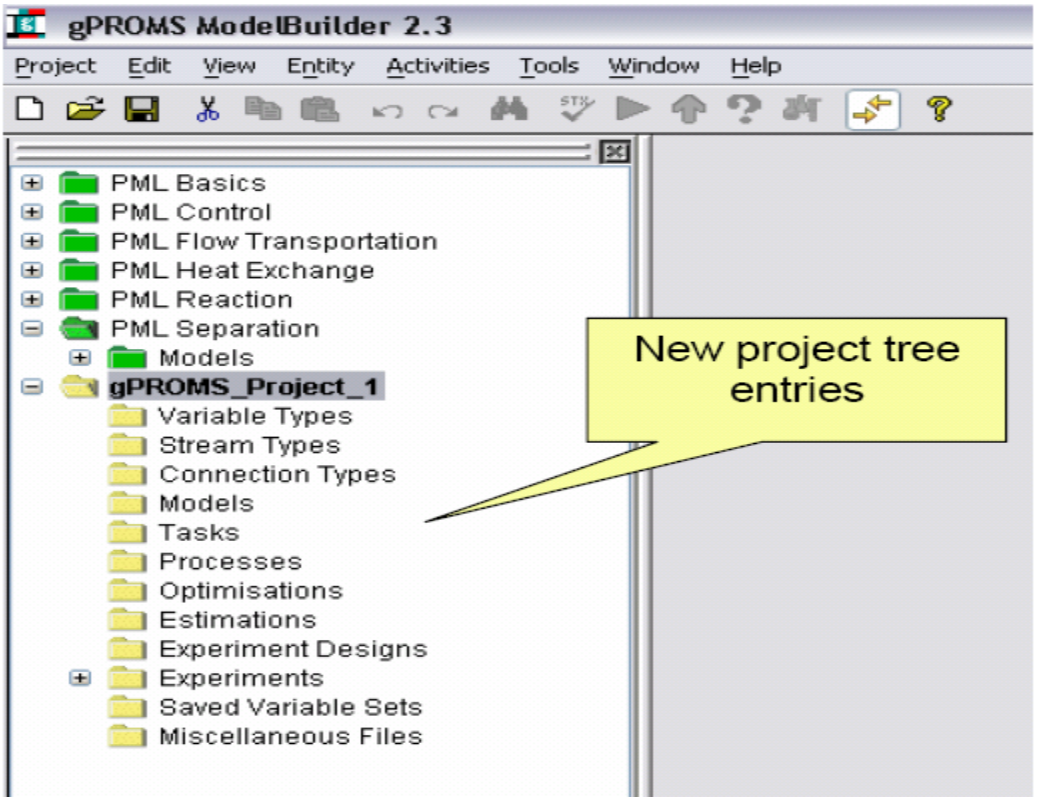

Figure 4.2 Subsection of a Project Tree

Three types of constants (REAL, INTEGER, LOGICAL) are declared in PARAMETER section. Parameters are the constant and values must be provided before simulation starts. In VARIABLE section, variables and corresponding variable type of the model are declared. Variables may or may not vary with time. Values of the variables may be

assigned or calculated by simulation. Variables type can be defined such as temperature, enthalpy, length, etc.

The specific piece of equipment of the process is referred in the Unit section. In EQUATION and BOUNDARY sections, equipment equations are specified. Equations are differential (differential operator $ is the derivative sign in gPROMS) or algebraic operators. It has some built in functions for partial equations and integral functions by using the PARTIAL and INTEGRAL operator respectively. Conditional equations (for reversible & systematic discontinuities, reversible & asymmetric discontinuities, irreversible discontinuities) in MODEL and PROCESS is handled by the deferent operator such as WHEN…END, CASE.... END.

Model Palette (Figure 4.3) is used to graphically display in a project and graphically connect the model in a flowsheet model. gPROMS model builder allows the user to develop the composite model and flow sheet graphically. It will help developing flow sheet quickly for model based activities such as simulation, optimisation etc. User defines the icon/ how the model will appear in the model palette or top level model such as flow sheet.

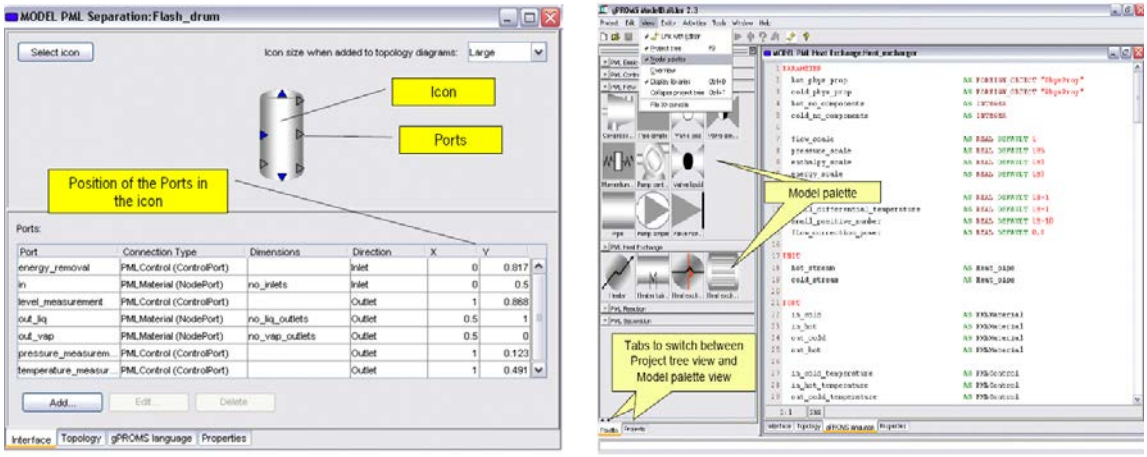

Figure 4.3 Model Palette and ICON

4.2.2 Development of graphical interface for process flowsheet in gPROMS

Like most of the modern simulator package gPROMS also provide an interface to develop a complex system from several subsystems. The physical system in such case is developed as a number of subsystems MODELs and TASKs. These subsystems are merged by connection equations known as STREAM or PORTs in the high level MODEL (Master Model).

Master MODEL interface requires sub-model icons and definition of the model ports and the characteristics of the connection between the ports. The Master MODEL (flowsheet of the process) is analysed by the composition of different level of Models in hierarchical order (Figure 4.4). Equations are used to connect the different model variables. PORTS and TOPOLOGY can be used for the development of flow sheet models. Lower level models can consist of another composite model. The cross-referenced libraries or projects connect lower level models if it is not in the same library or it may be in the same project.

In chapter 5, Master MODEL *Flowsheet* model consists of recovery section, rejection section and brine heater model. Each *recovery section* and *rejection section* model consists of number of *stage* models (sub-models). Differential and algebraic relations such as feed condition, the physical properties of the saline water describe each model and its corresponding sub-models.

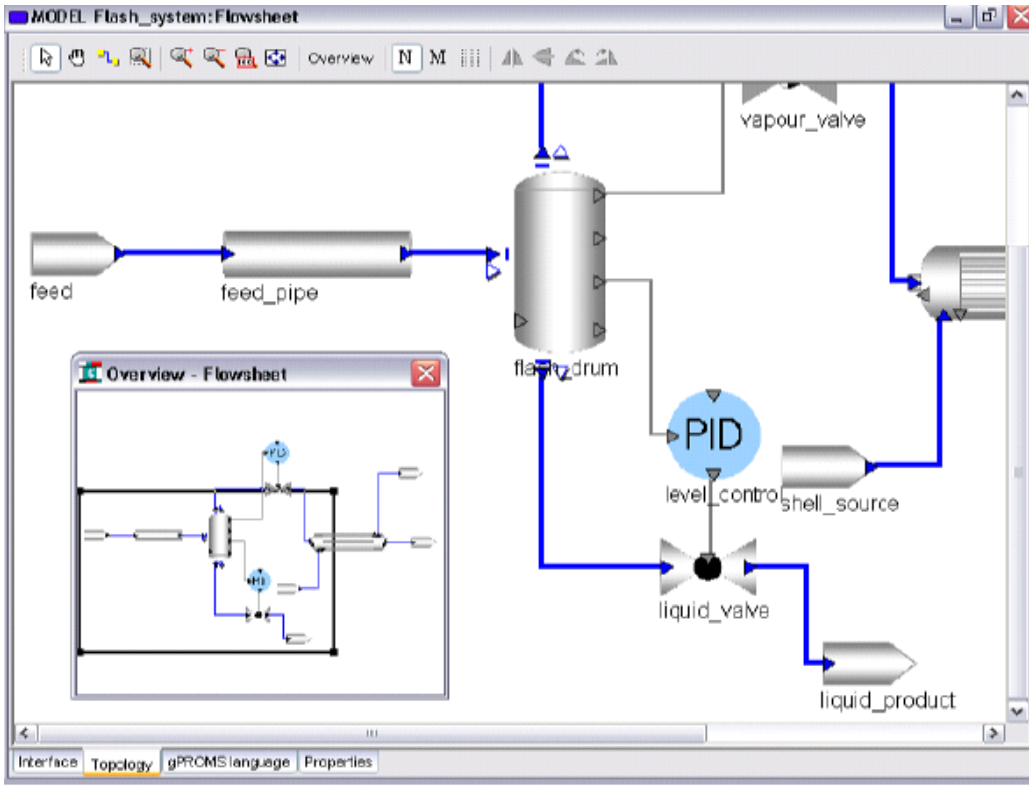

Figure 4.4 The graphical process flowsheet development using gPROMS model Libraries

4.2.3 Defining a task/process

TASK and PROCESS are defined as the modelling of operating procedures and control strategies. The PROCESS is analysed by the composition of different levels of Models in hierarchical order. gPROMS support the elementary TASKs as well as complex TASKs.

The Tasks/PROCESS are:

- What to do?
- How to do it?
- When to do it?

The TASKS are used in PROCESS to define individual operating procedures

The process consists of the following sections:

- PARAMETER

- VARIABLE
- UNIT
- EQUATION
- SET
- ASSIGN
- INITIAL
- SOLUTIONPARAMETERS and
- SCHEDULE

PARAMETER, VARIABLE, UNIT and EQUATION are described similarly to those in MODEL section (section 1.2.1).

In SET section PARAMETER values are defined. In ASSIGN section, degrees of freedom are specified. Operator called INITIAL inserts initial condition (for example for differential equations). Initial condition may be provided in the form of general equation. It has not only built in array of variables but also as arrays of equations. These equations may be defined explicitly or implicitly.

The operator called SWITCH, CONTINUE and SEQUENCE is used to defined the parallel, concurrent and sequential operation or tasks. The operator called RESET, REPLACE and REINITIALIZE is used to reinitialise different variables, parameters of the model.

The user (model developer) defines mathematical solvers and output specifications for the process output. Different solvers and sub solvers are available for simulation, optimisation, parameter estimation and experimental design (Tijl, 2005). Output specifications are used for display results in EXCEL and gRMS using the keyword gExcelOutput and gRMS

respectively. Main mathematical solvers for simulation, optimisation and parameter estimation are DASOLV, DOSOLV and PESOLV respectively. Operating schedule is specified in SCHEDULE subsection. A gPROMS project may contain different process of the same model for different simulation activity.

4.2.4 Optimisation

gPROMS provides an intelligent editor for formulation of optimisation problems. The optimisation entry has three additional tabs to formulate the optimisation problem quickly.

- General
- Controls and
- Constraints

In general tab, the user defines the process name, time horizon, control interval and whether the optimisation is steady state or dynamic. In this tab, whether the objective function is minimised or maximised, is specified. In the control tab user defines the types of control variables such as: Time invariant, Piecewise constant control, Piecewise linear control and the types of control variables such as continuous binary and integer. In constants tab, the end point constraints and their values of the intervals are defined. Three types of control variables can be defined:

- Equality constraints
- Inequality constraints
- Interior-point constraints

4.2.5 Foreign objects and foreign process, physical property packages

Foreign objects are a new type of variables, which may have zero or more inputs. The inputs may be scalar - vector or even the algebraic equations. The property packages are

typical example of foreign objects of the models.

Foreign Process is a mechanism to exchange the information between executing gPROMS simulations and external software. It can be easily interfaced with other programs. It has built in property package, which is useful for chemical engineering work. Built in model can be used as foreign process of the system.

Foreign object and foreign process are used to access data from the MS Excel, Matlab, Simulink, Aspen Plus and other Cape-Open software. A common physical properties package is provided within the gPROMS model builder. However, external physical property packages can also be connected to gPROMS via Physical Property Interface (PPI).

4.3 Simulation in gPROMS

gPROMS provides a range of the mathematical solvers for simulation, optimisation and parameter estimation. gPROMS supports an open software architecture regarding the mathematical solvers for simulation, optimisation and parameter estimation (Gosling, 2005).

The SOLUTIONPARAMETERS section of the PROCESS in a project allows the specification of parameters of the results and the mathematical solvers for each type of activity (simulation, optimisation and parameter optimisation). Built-in solvers solution parameters take the defaults values unless user specify any parameters.

There are three standard mathematical solvers for the solution of sets of nonlinear algebraic equations in gPROMS, namely BDNLSOL, NLSOL and SPARSE: BDNLSOL (Block Decomposition Non Linear Solver) solves the nonlinear algebraic equations with reversible symmetric discontinuities and rearranged to block triangular form. NLSOL is nonlinear solver, with and without block decomposition. SPARSE is sophisticated implementation of a Newton-type method without block decomposition.

Two mathematical solvers, namely DASOLV and SRADAU, solve mixed sets of differential and algebraic equations in gPROMS. These solvers are able to handle large, sparse systems of equations in which the variable values are restricted within specified lower and upper bounds. Moreover, it can also handle the partial derivatives. DASOLV implements variable time step/variable order Backward Differentiation Formulae (BDF) whereas SRADAU is based on a variable time step, fully-implicit Runge-Kutta method.

Mathematical solvers of the simulation are specified in PROCESS entry SOLUTION PARAMETER subsection as:

DASolver=”DASOLV”;

DASolver =” BDNLSOL”;

4.4 Optimisation in gPROMS

gPROMS provides a general numerical solver manager for the steady state and dynamic optimisation problem called DOSOLV.

Mathematical solvers for optimisation are specified in PROCESS entry SOLUTION PARAMETER subsection as:

DOSolver =”CVP_SS”;

DOSolver =” CVP_MS”;

PIECEWISE CONSTANT, PIECEWISE LINEAR and TIME INVARIANT must be ASSIGNed in the gPROMS PROCESS entity. The limits of the control variables by default are the values specified in VARIABLE TYPE entities or in the PRESET section of the PROCESS entity unless user specifies the limits of those variables in the optimisation entry. Other important parameters specified in the optimisation section are:

- Time horizon and its limits and different control interval
- Limits of the other variables and their limits called endpoint equality constraints and inequality constraints
- Interior point constraints variables and their limits in different control interval

4.4.1 MINLP optimisation using gPROMS

MINLP problems (Linear programming, Integer programming, Nonlinear programming problem) are solved by a single MINLP solver called "OAERP" and is a object of the common optimisation solver manager "DOSOLV".

gPROMS solver manager can integrate with any CAPE OPEN compliant solver (Gosling, 2005). Both time-invariant and piecewise constant time-varying controls can be discrete variables. The different keyword: BINARY, INTEGER, ENUM and SOS1 is used to specify the four types of discrete control variables binary, integer, enumerated and special order sets 1 types variables respectively.

4.5 Connecting to MS Excel Software

gPROMS provides built in feature to plot different variables in MS Excel. However, Microsoft Excel Foreign Object and Foreign Process interfaces provide better flexibility to send and receive data form the MS Excel. They are designed to allow gPROMS to interact dynamically with calculations performed in Microsoft Excel. The Microsoft Excel Foreign Object interface can be used to provide values for PARAMETERs and VARIABLEs in a gPROMS simulation. Different commands like SENT, RECEIVE are used to connect both software. Like other foreign objects and foreign process interface, this feature makes the gPROMS more users friendly.

4.6 Conclusions

The gPROMS is a robust and open structure software. gPROMS model builder has built in numerical solvers and common equipment which is very useful for process simulation and optimisation. Further information can be found in developers websites (www.psenterprise.com) and gPROMS user guide (gPROMS, 2004). Due to robustness and flexibility of this software as mentioned in detail in this chapter, gPROMS has been chosen to use for modelling, simulation and optimisation in this work.

Chapter 5

Hybrid Modelling and Simulation of MSF Process for Fixed Water Demand

5.1 Introduction

Modelling played an important role in simulation, optimisation and control of Multi-Stage Flash (MSF) desalination processes. The steady state MSF process model includes mass and energy balances, the geometry of the stages and physical properties which are functions of temperature and salinity which results in a set of non-linear algebraic equations (Helal et al., 1986; Husain et al., 1993; Husain et al., 1994; El-Dessouky and Bingulac, 1996).

Fresh water demand in arid regions is met mainly by Multi Stage Flash (MSF) desalination processes (El-Dessouky and Ettouney, 2002; Hussain, 2003). Seawater is the main source of raw material for these processes and is subject to seasonal temperature variation. For a given salinity, this seawater temperature variation will affect the rate of production of fresh water in an already built MSF process operating at the same conditions through out the year. The sensitivity of the temperature can be studied either in a real plant (which will be very expensive) or with a reliable process model.

In the absence of a real MSF process, these investigations are carried out using a model. As discussed in the previous chapter, gPROMS is a reliable and flexible tool for simulation, optimisation, and parameter estimation of highly complex processes. In this chapter, a hybrid MSF process model involving mass balance, energy balance and physical property correlations is developed using gPROMS modelling tool.

Accurate estimation of Temperature Elevation (TE) due to salinity is important in developing a reliable process model. Here, instead of using empirical correlations from literature, a Neural Network based correlation developed in Chapter 3 is used to determine the TE. This correlation is embedded in the gPROMS with rest of the model equation resulting a hybrid steady state process model.

The model is first validated against published literature (Rosso et al., 1996) and then is used to investigate how the design and operation parameters are to be adjusted to maintain a fixed demand of fresh water through out the year for changing seawater temperature.

5.2 MSF Process Description

As described in Chapter 1 and 2, an MSF process consists of three main sections: brine heater, recovery section with NR stages and a rejection section with NJ stages (Figure 5.1). Seawater enters into the last stage of the rejection stages (W_s) and passes through a series of tubes to remove heat from the stages. After the rejection section, seawater is partly discharged back to the sea (C_W) to balance the heat. The other part (F) is mixed with recycle brine (R) form the last stage of the rejection section and fed (W_R) before the last stage of the recovery section. Seawater (W_R) is flowing through the tubes in different stages to recover heat from the stages and the brine heater raises the seawater temperature to the maximum attainable temperature (also known as Top Brine Temperature, TBT). After that,

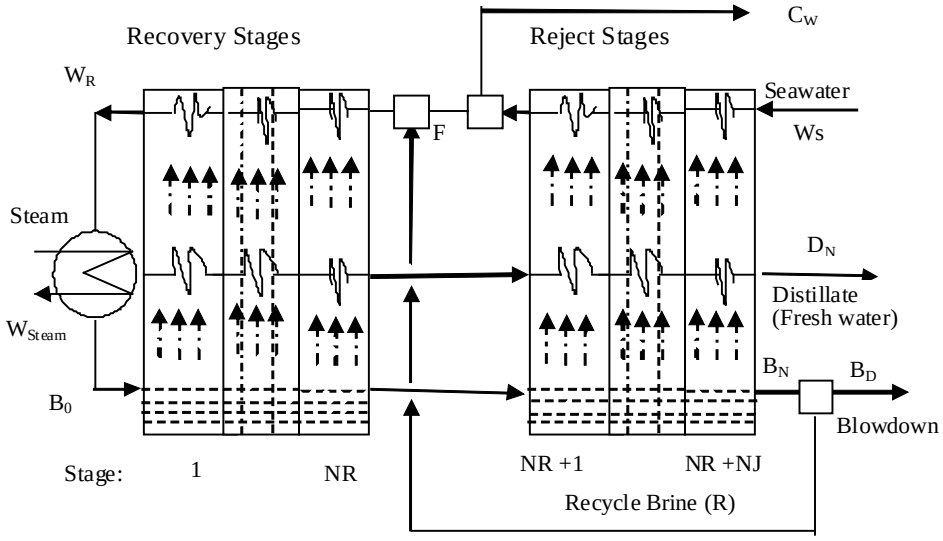

Figure 5.1. (a) A Typical MSF Process

it (B_o) enters into the first flashing stage and produce flashing vapour. This process continues until the last stage of the rejection section. The concentrated brine (B_N) from last stage is partly discharged to the sea (B_D) and the remaining (R) is recycled as mentioned before. The vapour from each stage is collected in a distillate tray to finally produce the fresh water (D_N).

5.3 Steady State MSF Process Model

The following assumptions are made in the model:

- the distillate from any stage is salt free
- heats of mixing are negligible
- no sub cooling of condensate leaving the brine heater
- there are no heat losses and

- there is no entrainment of mist by the flashed vapour.

In addition, the effect of CO_2 gas (usually present in thermal desalination process) solubility on scale formation in MSF process has not been modelled. However, further information on this can be found in Al-Anezi and Hilal (2007).

5.3.1 Model equations

The model equations for stage number j (Figure 5.2) are given in the following (all symbols are defined in the Nomenclature). The mathematical model equations and physical properties correlations presented here are reported by Helal et al. (1986), Rosso et al. (1996) and Husain et al. (2003).

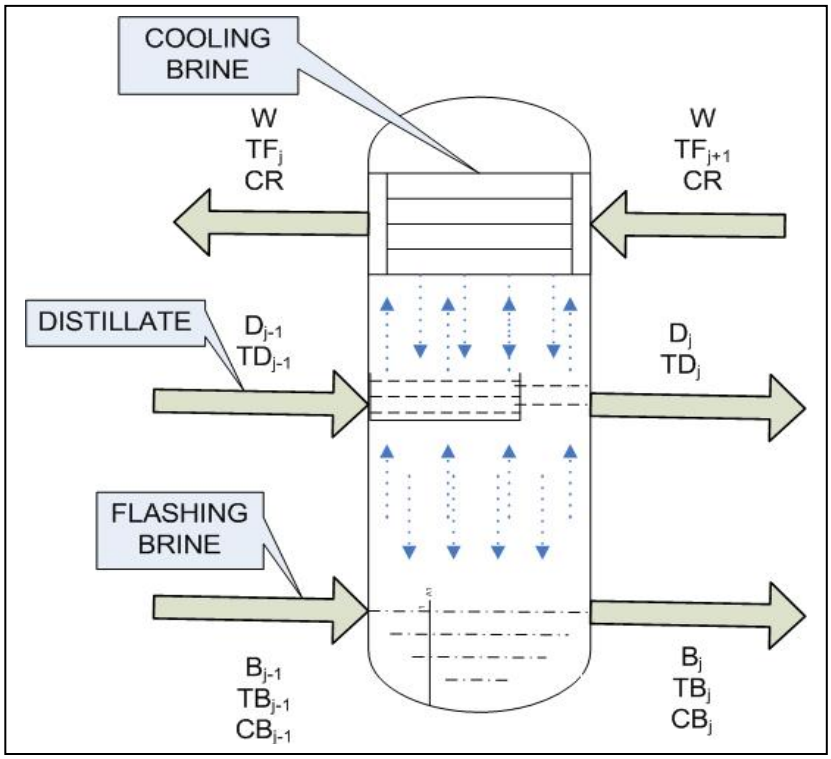

Figure 5.2 A Typical MSF Stage

(a) Stage model

Mass balance in the flash chamber:

$$B_{j-1} = B_j - V_j \tag{5.1}$$

Salt balance:

$$B_{j-1} \times CB_{j-1} = B_j \times CB_j \tag{5.2}$$

Mass balance for the distillate tray:

$$D_j = D_{j-1} - V_j \tag{5.3}$$

Enthalpy balance on flash brine:

$$B_j = (h_{Bj-1} - h_{vj}) / (h_{Bj} - h_{vj}) \times B_{j-1} \tag{5.4}$$

$$h_{vj} = f(T_{Sj}) \tag{5.5}$$

$$h_{Bj} = f(C_{Bj}, T_{Bj}) \tag{5.6}$$

Overall enthalpy balance

$$W_R \times S_{Rj} \times (T_{Fj} - T_{Fj+1}) = D_{j-1} S_{Dj-1} \times (T_{Dj-1} - T^*) + B_{j-1} S_{Bj-1} \times (T_{Bj-1} - T^*) - D_j S_{Dj} \times (T_{Dj} - T^*) - B_j S_{Bj} \times (T_{Bj} - T^*) \quad \text{(Recovery stage)} \tag{5.7}$$

$$W_s \times S_{Rj} \times (T_{Fj} - T_{Fj+1}) = D_{j-1} S_{Dj-1} \times (T_{Dj-1} - T^*) + B_{j-1} S_{Bj-1} \times (T_{Bj-1} - T^*) - D_j S_{Dj} \times (T_{Dj} - T^*) - B_j S_{Bj} \times (T_{Bj} - T^*) \quad \text{(Rejection stage)} \tag{5.8}$$

$$S_{Rj} = f(T_{Fj+1}, T_{Fj}, C_R) \quad \text{(Recovery stages)} \tag{5.9}$$

$$S_{Rj} = f(T_{Fj+1}, T_{Fj}, C_R) \quad \text{(Rejection stages)} \tag{5.10}$$

$$S_{Dj} = f(T_{Dj}) \tag{5.11}$$

$$S_{Bj} = f(T_{Bj}, C_{Bj}) \tag{5.12}$$

Heat transfer equation

$$W_R \times S_{Rj} \times (T_{Fj} - T_{Fj+1}) = \frac{U_j \times A_j \times (T_{Fj} - T_{Fj+1})}{\ln \frac{(T_{Dj} - T_{Fj+1})}{(T_{Dj} - T_{Fj})}} \quad \text{(Recovery stage)} \tag{5.13}$$

$$W_s \times S_{Rj} \times (T_{Fj} - T_{Fj+1}) = \frac{U_j \times A_j \times (T_{Fj} - T_{Fj+1})}{\ln \frac{(T_{Dj} - T_{Fj+1})}{(T_{Dj} - T_{Fj})}} \quad \text{(Recovery stage)} \tag{5.14}$$

Overall heat transfer coefficient:

$$U_j = f\left(W_R, T_{Fj}, T_{Fj+1}, T_{Dj}, D_j^i, D_j^o, L_j^i, f_j^i\right) \quad \text{(Recovery stage)} \tag{5.15}$$

$$U_j = f\left(W_s, T_{Fj}, T_{Fj+1}, T_{Dj}, D_j^i, D_j^o, L_j^i, f_j^i\right) \quad \text{(Recovery stage)} \tag{5.16}$$

Distillate and flashing brine temperature correlation:

$$T_{Bj} = T_{Dj} + TE_j + EX_j + \Delta_j \tag{5.17}$$

Distillate and flashed steam temperatures correlation:

$$TS_j = T_{Dj} + \Delta_j \tag{5.18}$$

$$TE_j = f(T_{Dj}, C_{Bj}) \tag{5.19}$$

$$\Delta_j = f(T_{Dj}) \tag{5.20}$$

$$EX_j = f(H_j, w_j, T_{Bj}) \tag{5.21}$$

(b) Brine Heater Model

$$B_0 = W_R \tag{5.22}$$

$$C_{B0} = C_R \tag{5.23}$$

Overall Enthalpy Balance:

$$B_0 \times S_{RH} \times (T_{B0} - T_{F1}) = W_{steam} \times \lambda_S \tag{5.24}$$

$$\lambda_S = f(T_{steam}) \tag{5.25}$$

Heat transfer equation:

$$W_R \times S_{RH} \times (T_{B0} - T_{F1}) = \frac{U_H \times A_H \times (T_{B0} - T_{F1})}{\ln \frac{(T_{steam} - T_{F1})}{(T_{steam} - T_{B0})}} \tag{5.26}$$

$$U_H = f\ (W_R, T_{B0}, T_{F1}, T_{steam}, D_H^i, D_H^o, f_H^i) \tag{5.27}$$

$$S_{RH} = f(T_{BO}, T_{F1}) \tag{5.28}$$

(c) Splitters Model

Blowdown splitter: $B_D = B_{NS} - R$ (5.29)

Reject seawater splitter: $C_W = W_S - F$ (5.30)

(d) Makeup Mixers Model

Mass balance: $W_R = R + F$ (5.31)

Salt Balance $R \times C_{BNS} + F \times C_S = W_R \times C_R$ (5.32)

Overall enthalpy balance: $W_R \times h_W = R \times h_R + F \times h_F$ (5.33)

$h_W = f(T_{Fm}, C_R)$ (5.34)

$h_F = f(T_{FNR+1}, C_F)$ (5.35)

$h_R = f(T_{BNS}, C_{BNS})$ (5.36)

where T^* is reference temperature = 0^oC, Note simulation results any vary slightly if the reference temperature is different.

5.3.2 Physical and chemical properties equations

The correlations for physical and chemical properties (except the calculation of TE) are taken from (Helal et al., 1986; Rosso et al., 1996 and Husain et al., 2003) are shown in Table 5.1.

5.4.2.1 Neural network based correlation for TE

The NN based correlation (NN_Cor_1) for the estimation of TE is described earlier in Chapter 3, which was developed based on Bromley (Bromley et al., 1974) data. This was based on 3-layer NN architecture with 4 neurons in the hidden layer and 1 neuron (TE) in the output layer. The correlation with the weights and biases for different layers is also presented in Chapter 3.

Table 5.1 Physical and Chemical properties Equations

Specific enthalpy of vapour:	Specific enthalpy of saturated water:
$h_{vj} = 596.912 + 0.46694 \times T_s - 0.000460256 \times T_s^2$, For brine heater, $h_v = h_{vj}$, $T_s = T_{steam}$ in °F Latent heat of vapour : $\lambda_s = h_v - h_D$	h_D =1.8 ×(-31.92 + 1.0011833 T_{steam} – 3 0833326 X 10^{-5} × T_{steam}^2 +4.666663 x 10^{-8} × T_{steam}^3 +3.1333334 x 10^{-10} × T_{steam}^4)
Specific heat capacity of pure water	
S_{Dj} = 1.0011833 - 6.1666652 × 10^{-5} T_D +1.3999989 × 10^{7} × T_D^2 +1.3333336 × 10^{-9} × T_D^3; For Brine, Seawater $S_{RH} = S_{Dj}, T_D = T_{Bj}$ in °F	
Specific heat capacity of seawater/brine	
S_{Bj} = [1- $C_B \times (0.011311 - 1.146 \times 10^{-5} T_B)] \times S_d$ For $S_{Rj} = S_{Bj}$, $C_B = C_S$ in wt%, $C_B = C_R$ in wt%, $T_B = T_{Fj+1}$ in °F, For Brine heater, $S_{RH} = S_{Bj}$, $C_B = C_R$ in wt%, $T_B = T_{F0}$ in °F	
Specific enthalpy of seawater/brine	
$h_{Bj} = 4.186 * ((4.185 - 5.381 \times 10^{-3} \times C_j + 6.26 \times 10^{-6} \times C_j^2) \times T_{Bj} - (3.055 \times 10^{-5} + 2.774 \times 10^{-6} \times C_j - 4.318 \times 10^{-8} \times C_j^2) \times T_{Bj}^2 / 2 + (8.844 \times 10^{-7} + 6.527 \times 10^{-8} \times C_j - 4.003 \times 10^{-10} * C_j^2) / T_{Bj}^3 / 3)$ For Mixer, $h_W = h_{Bj}, T_{Bj} = T_{Fm}, C_{Bj} = C_R$, $h_F = h_{Bj}, T_{Bj} = T_{FNR}, C_{Bj} = C_R$, $h_R = h_{Bj}, T_{Bj} = T_{BN}, C_{Bj} = C_{BNS}$, Density of Brine ρ_j = 16.01846× (62.707172 + 49.364088 × C_{Bj} – 0.43955304 × 10^{-2} × T_B –0.032554667 × $C_{Bj} \times T_B$ – 0.46076921 × 10^{-4} × T_B^2 + 0.63240299 × 10^{-4} × $C_B \times T_B^2$)	
Temperature loss due to demister and Nonequilibrium	
Δ_j = exp(1.885 - 0.02063× T_D) /1.8, EX_j = $\left(195.556 \times H_j^{1.1} (\varpi_j \times 10^{-3})^{0.5}\right) / \left(\Delta T_{Bj}^{2.5}\right) \times T_{Sj}^{2.5}\right)$ $\omega_j = W / w, \Delta T_{Bj} = (T_{Bj} - T_{Bj-1})$ in °F, where ,$W = W_R$ (recovery stage) in lb/h, $W = W_S$ (reject stage) in lb/h=(kg/h)	
Overall heat transfer coefficient	
$U_j = \frac{4.8857}{(y + z + 4.8857 \times f_j^i)}$ where, y = $[(v \times D^i]^{0.2}$ × [(160 + 1.92 × T_F) × v], $v = f(L_j, W_R / W_S, \rho, D^i, D_j^o,)$, z = 0.1024768 × 10^{-2} - 0.7473939× 10^{-5} × T_D +0.999077 × 10^{-7} × T_D^2 – 0.430046×10^{-9} × T_D^3 + 0.6206744 × 10^{-12} × T_{Dj}^4 For Brine heater U_H = U_j, $T_F = T_{B0}$ in °F, $T_{steam} = T_D$ in °F, $f_j^i = f_H^i, D_j^i = D_H^i$, $L_j = L_H, D^i = D_H^i, D_j^o = D_H^o$,	

Models for each unit operation (such as flash chamber, brine heater, splitter and mixer) are developed separately and connected via a high level modelling language of gPROMS.

5.3.3 Degrees of freedom analysis

For a total number of stages NS=NR+NJ (NR=number of stages in the recovery section, NJ = number of stages in the rejection section), the total number of equations (TNE) is: 25NS+27. The total number of variables (TNV) is: 18NS+16. Therefore, the Degrees of Freedom (D.F. = TNV-TNE) is: 7NS + 11. This means 7NS+11 variables must be specified before the model equations could be solved.

The variables in the model section 5.4.1 and 5.4.2 are

$$V_j,\ C_{Bj},\ D_j,\ B_j,\ T_{Dj},\ T_{Fj},\ T_{Bj},\ f_j^i,\ D_j^i,\ D_j^o, w_j,\ H_j, L_j,\ S_{Rj},\ S_{Dj},\ S_{Bj},\ U_j,\ T_{Sj},$$
$$DEL_j,\ TE_j,\ EX_j,\ h_{vj},\ h_{Bj},\ A_j,\ W_R,\ W_S,\ C_R,\ C_S,\ T_{FNS+1},\ B_0,\ C_{B0},\ W_{steam},\ \lambda_S,\ T_{steam},$$
$$T_{B0}, S_{RH},\ U_H,\ A_H,\ D_H^i,\ D_H^o,\ f_H^i, L_H, B_D,\ R,\ C_W,\ h_F,\ h_W,\ h_R,\ T_{Fm}$$

with $j = 1, 2, \ldots\ldots\ldots\ldots\ldots\ldots\ldots\ldots\ldots\ldots(Ns),\ NS = NR + NJ$

Total Number of variables (TNV) = 24NS+26

and Total Number of equations (TE) = 17NS+15.

So the Degrees of Freedom (D.F) = TNV-TE = 7NS+11

Specifications to satisfy D.F. are:

$$A_H,\ D_H^i,\ D_H^o,\ f_H^i,\ L_H,\ A_j,\ f_j^i,\ D_j^i,\ D_j^o, w_j,\ H_j,\ L_j,\ W_s,\ T_{steam},\ T_{FNS+1},\ C_S,\ R,\ C_W$$
$$= 7NS + 11$$

5.4 Interactive Flowsheet Model Development in gPROMS

An overview of the gPROMS MSF process model (in section 5.4) developed in gPROMS

flowsheet is shown in Figures 5.3 and 5.4. On the left hand panel of Figure 5.3 are a number of gPROMS entries corresponding to MSF process model such as (Variable Types, Connection Types, Models, Processes and Optimisation etc.). On the right hand panel, flowsheet level connections are shown. All the stages in the recovery or rejection sections are lumped as one unit here. Figure 5.4 shows the internal connections between the stages of the recovery or rejection section.

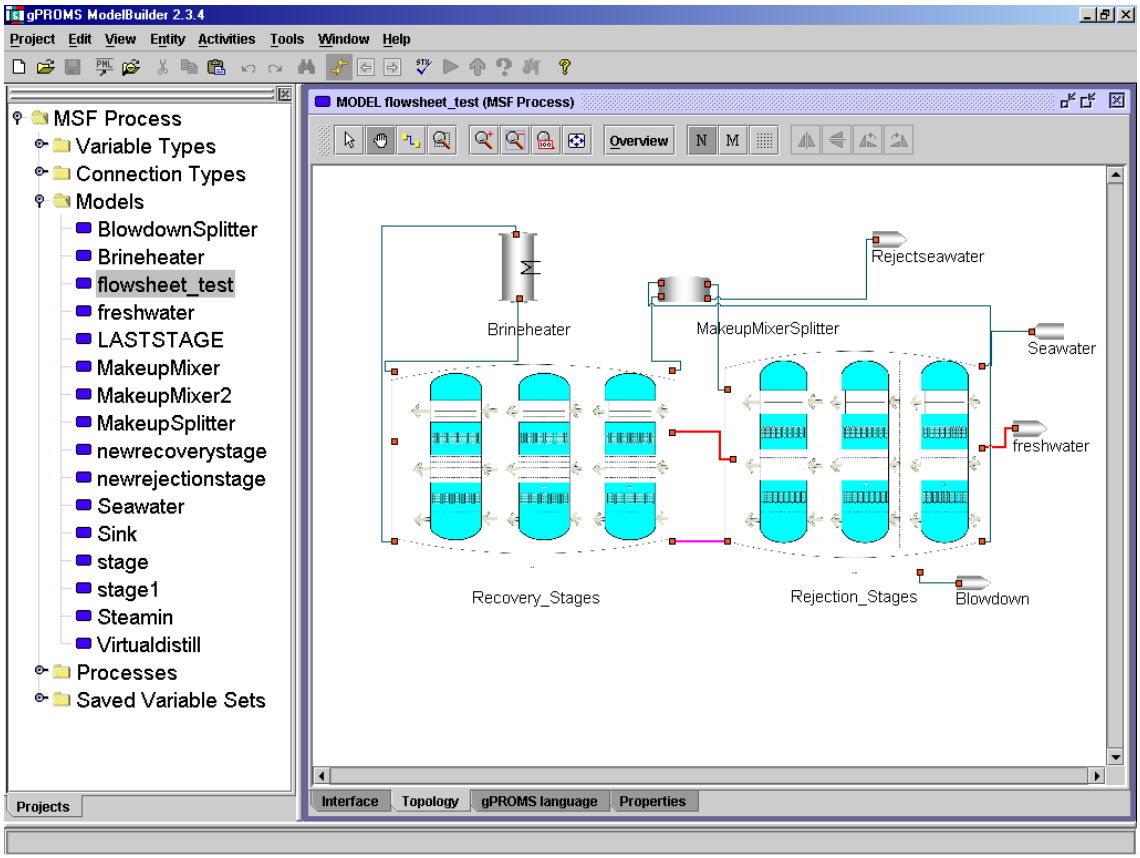

Figure 5.3 Flowsheet Level Connections of MSF Process within gPROMS

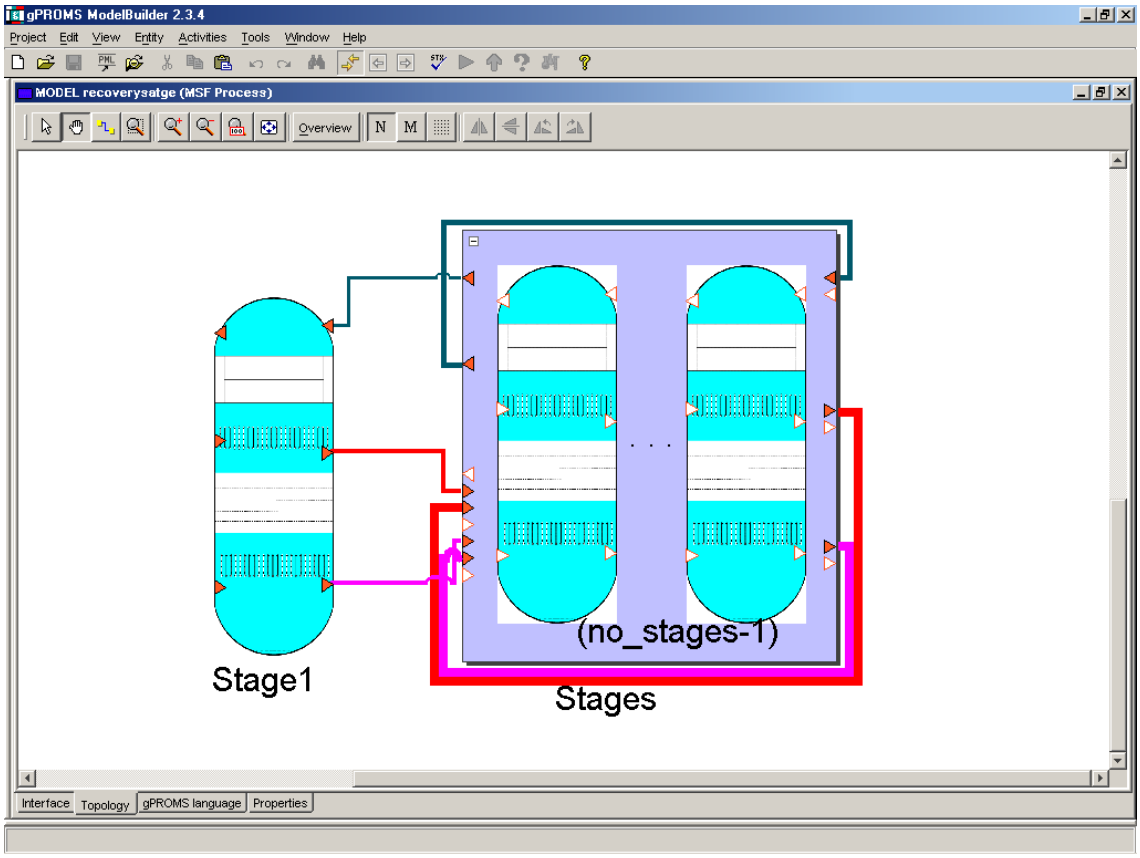

Figure 5.4 Internal Connection of Stages in Recovery Section

5.4.1 Different entry in model section of gPROMS

In gPROMS, in each UNIT (of the process flowsheet shown in Figure 5.3) a set of constant parameters that characterise the system are declared in the PARAMETER section. A set of variables that describe the time-dependent/independent behaviour of the system are declared in the VARIABLE section and a set of equations involving the declared variables and parameters are written in the EQUATION section of the MODEL.

5.4.2 Different entry in process section of gPROMS

A PROCESS (shown in the left panel of Figure 5.3) is partitioned into sections (UNIT, SET, ASSIGN, INITIAL, SOLUTION PARAMETERS and SCHEDULE). The UNIT

section here refers to the process flowsheet. Constant parameters are declared in the SET section. ASSIGN section includes variable specifications satisfying the degrees of freedom. INITIAL refers to initial conditions at time zero for dynamic simulation. The SOLUTIONPARAMETERS section is used to control the settings of the mathematical solvers and output specifications for the process, optimisation.

5.5 Model Validation

In this work, the case study reported by Rosso et al. (1996) is considered for model validation. There are total of 16 stages with NR = 13 recovery and NJ = 3 rejection stages. The specifications (satisfying the degrees of freedom) used by Rosso et al. (1996) and their simulation results are shown in Table 5.2 and 5.3 respectively.

Using the same specification as in Table 5.2, the simulation results obtained by the model developed in this chapter are presented in Table 5.4. Comparison of the results shown in Tables 5.3 and 5.4 clearly shows that they are in good agreement. The salinity and brine temperature ranges in this work are 6.29-6.82 wt% and 40-90^{o}C. Note the NN based correlation for estimating TE was developed with salinity range 0.19-7.23 wt% and 60-120 ^{o}C. Despite the temperature range of this work being slightly outside the 60-120^{o}C range, the simulation results are quite close to those reported by Rosso et al. (1996) even in the temperature range 35-60^{o}C (compare the results of stages 10-16 in Table 5.3 and 5.4). This clearly shows the good capability of NN based estimator.

Table 5.2. Constant Parameters and Input Data (Rosso et al., 1996)

	A_j / A_H	D_j^i / D_H^i	D_j^o / D_H^o	f_j^i / f_H^i	w_j / L_j / L_H	H_j
Brine heater	3530	0.022	0.0244	$1.86*10^{-4}$	12.2	
Recovery stage	3995	0.022	0.0244	$1.40*10^{-4}$	12.2	0.457
Rejection stage	3530	0.024	0.0254	$2.33*10^{-5}$	10.7	0.457

W_S	T_{steam}	$T_{seawater}$	C_S	R	C_W
$1.131x10^8$ kg/h	97°C	35 °C	5.7 wt%	$6.35x10^6$ kg/h	$5.62x10^6$ kg/h

Table 5.3. Summary of the Simulation Results by Rosso et al. (1996)

F	B_D	W_R	W_{steam}	C_R
$5.68x10^6$ kg/h	$4.75x10^6$ kg/h	$1.203x10^7$ kg/h	$1.189x10^5$ kg/h	$6.29x10^{-2}$ wt/wt

Stage Profiles (Brine heater stage j =0; TBT = T_{B0})						
Stage	B_j kg/h	D_j kg/h	C_{Bj} wt/wt	T_{Fj} °C	T_{Dj} °C	T_{Bj} °C
0	1.203E+07		*0.0629*			*89.74*
1	*1.197E+07*	*5.940E+04*	*0.0632*	*83.33*	*85.75*	*86.89*
2	*1.191E+07*	*1.187E+05*	*0.0635*	*80.41*	*82.87*	*84.01*
3	*1.185E+07*	*1.784E+05*	*0.0639*	*77.44*	*79.95*	*81.08*
4	*1.179E+07*	*2.385E+05*	*0.0642*	*74.43*	*76.97*	*78.11*
5	*1.173E+07*	*2.989E+05*	*0.0645*	*71.37*	*73.94*	*75.09*
6	*1.167E+07*	*3.595E+05*	*0.0649*	*68.28*	*70.88*	*72.04*
7	*1.161E+07*	*4.201E+05*	*0.0652*	*65.16*	*67.78*	*68.95*
8	*1.155E+07*	*4.806E+05*	*0.0655*	*62.01*	*64.65*	*65.84*
9	*1.149E+07*	*5.410E+05*	*0.0659*	*58.84*	*61.49*	*62.70*
10	*1.143E+07*	*6.010E+05*	*0.0662*	*55.65*	*58.32*	*59.55*
11	*1.137E+07*	*6.606E+05*	*0.0666*	*52.46*	*55.13*	*56.39*
12	*1.131E+07*	*7.197E+05*	*0.0669*	*49.27*	*51.93*	*53.24*
13	*1.125E+07*	*7.780E+05*	*0.0673*	*46.09*	*48.74*	*50.09*
14	*1.120E+07*	*8.296E+05*	*0.0676*	*44.06*	*45.87*	*47.28*
15	*1.115E+07*	*8.816E+05*	*0.0679*	*41.10*	*42.95*	*44.42*
16	*1.110E+07*	*9.341E+05*	*0.0682*	*38.07*	*39.98*	*41.51*

Table 5.4. Summary of the Simulation Results using the hybrid model in gPROMS

F	B_D	W_R	W_{steam}	C_R
$5.68x10^6$ kg/h	$4.76x10^6$ kg/h	$1.203x10^7$ kg/h	$1.189x10^5$ kg/h	$6.29x10^{-2}$ wt/wt

Stage Profiles (Brine heater stage j =0; TBT = T_{B0})						
Stage	B_j kg/h	D_j kg/h	C_{Bj} wt/wt	T_{Fj} °C	T_{Dj} °C	T_{Bj} °C
0	1.203E+07		0.0629			89.96
1	1.197E+07	5.738E+04	0.0632	83.68	86.04	87.14
2	1.191E+07	1.155E+05	0.0635	80.76	83.17	84.27
3	1.186E+07	1.741E+05	0.0638	77.78	80.24	81.35
4	1.180E+07	2.333E+05	0.0641	74.76	77.25	78.37
5	1.174E+07	2.930E+05	0.0644	71.69	74.21	75.34
6	1.168E+07	3.529E+05	0.0648	68.58	71.13	72.27
7	1.162E+07	4.130E+05	0.0651	65.43	68.00	69.16
8	1.156E+07	4.732E+05	0.0654	62.25	64.84	66.02
9	1.150E+07	5.334E+05	0.0658	59.04	61.64	62.85
10	1.144E+07	5.935E+05	0.0661	55.80	58.42	59.66
11	1.138E+07	6.533E+05	0.0665	52.55	55.18	56.45
12	1.132E+07	7.127E+05	0.0668	49.29	51.91	53.23
13	1.126E+07	7.716E+05	0.0672	46.02	48.64	50.01
14	1.121E+07	8.223E+05	0.0675	44.25	45.79	47.24
15	1.116E+07	8.741E+05	0.0678	41.25	42.84	44.36
16	1.110E+07	9.269E+05	0.0681	38.17	39.80	41.40

5.6 Sensitivity of Design and Operating Parameters

5.6.1 Effect of seawater temperature and steam temperature on freshwater production (fixed design)

Further simulation is carried out to study the sensitivity of seawater temperature ($T_{seawater}$) and steam temperature (T_{steam}) on the total amount of fresh water produced (D_{NS}), GOR (Gained output ratio/ Performance ratio), TBT and final bottom brine temperature (BBT). The results are summarised in Table 5.5.

With the increase of $T_{seawater}$ both TBT and BBT increase for a given T_{steam} = 97 °C (Cases 1-3). As the terminal temperature difference decreases, for a given design of the plant (heat transfer area, etc.) the amount of heat removal decreases. This consequently reduces the

amount of distillate produced per stage, thus reducing the total amount of freshwater. The corresponding reduction of the steam flow rate (W_{steam}) keeps the GOR almost constant. This simulation clearly shows that due to seasonal variation, more freshwater will be produced during winter (Case 1) than in summer (Case 3).

For a given seawater temperature, $T_{seawater}$ = 45 ^{o}C (although this temperature might seem a bit high, in future this might be a reality due to global warming), with the increase of T_{steam}, the terminal temperature difference increases. For a given design of the plant (heat transfer area, etc.) the amount of heat removal therefore increases. This consequently increases the amount of distillate produced per stage and the total amount of freshwater (Cases 4-6). A corresponding increase of GOR is thus noticed. Note, to maintain the supply of freshwater in summer at the winter level, there has to be an increase in T_{steam} from 97^{o}C to 116.5^{o}C (compare Case 1 and Case 5). To sustain the high temperature operation this might have knock-on effect on the capital investment.

Table5.5. Effect of $T_{seawater}$ and T_{steam} on D_{NS}, *GOR*, *TBT*, *BBT*

Case	$T_{seawater}$	D_{NS}	W_{steam}	*GOR*	*TBT*	*BBT*
1	23	1.09E+06	1.41E+05	7.73	88.6	30.3
2	35	9.31E+05	1.19E+05	7.82	90.1	41.2
3	45	7.88E+05	1.02E+05	7.72	91.0	50.2
	T_{steam}					
4	111.0	1.01E+06	1.21E+05	8.29	103.8	51.5
5	116.5	1.09E+06	1.29E+05	8.48	108.8	52.0
6	121.0	1.16E+06	1.35E+05	8.64	112.9	52.5

Gained output Ratio (*GOR*)=Total Fresh water produced/Amount of Steam Needed = D_{NS} / W_{steam}

5.6.2 Effects of number of stages and seawater temperature for fixed water demand

With the model presented in section 5.4, a series of simulation is carried out to study the sensitivity of seawater temperature ($T_{seawater}$) on the design and operating parameters of the

MSF process for a fixed water demand (D_{NS}) of 10^6 kg/hr. The seawater temperature is assumed to vary between 20 and 35 ^oC. The input data which are fixed for all cases are shown in Table 5.6. The total number of stages (*NS*) is varied from 16 to 20 (16, 17, 18 and 20). In all cases, the recovery section is composed of 3 stages and the number of stages in the recovery section is only varied.

Table 5.6. Constant Parameters and Input Data (Fixed Product Demand Cases)

	A_j / A_H	D_j^i / D_H^i	D_j^o / D_H^o	f_j^i / f_H^i	$w_j / L_j / L_H$	H_j
Brine heater	3530	0.022	0.0244	$1.86*10^{-4}$	12.2	
Recovery stage	3995	0.022	0.0244	$1.4*10^{-4}$	12.2	0.457
Rejection stage	3530	0. 024	0. 0254	$2.33*10^{-5}$	10.7	0.457

W_S	*TBT*	$T_{seawater}$	C_S	D_{NS}	C_W
$1.13*10^8$ kg/h	90 ^oC	<20 – 35> ^oC	5.7 wt%	$1.0*10^6$ kg/h	$5.62*10^6$ kg/h

The sensitivity of seawater temperature ($T_{seawater}$) on the steam flowrate (W_{steam}), steam temperature (T_s), bottom brine temperature (*BBT*) and recycled brine flowrate (*R*) for different number of stages are shown in Figures 5.5-5.8 respectively.

Figure 5.5-5.8 show that for a given design (*NS*), as the season changes from winter to summer, the plant has to be operated at higher steam flowrate, higher steam temperature and with higher rate of brine recycle. In addition, the consequence of this will be increased brine discharge temperature (*BBT*). The effect of these changes will be manifold. Higher steam flowrate (13% increase at $T_{seawater}$ = 35 ^oC compared to that at $T_{seawater}$ = 20 ^oC) and temperature for a fixed size of the brine heater will incur further capital cost due to different

materials of construction capable of withstanding high temperature. Higher amount of brine recycle (70% increase at $T_{seawater}$ = 35 ^{o}C compared to that at $T_{seawater}$ = 20 ^{o}C) will increase operating cost. These will therefore increase the cost of unit production of fresh water. On top of all these, higher discharge temperature (almost 8-10 ^{o}C above the seawater temperature) of the brine into the sea will affect the marine life.

Figures 5.5 and 5.6 also show that for a fixed seawater temperature (say, 25 ^{o}C), the higher the number of stages, the lower the steam flowrate and temperature are. This means that the operating cost can be lowered at the expense of capital cost. Qualitatively, it can be said that unit price for the water may not change. Note, no significant changes are noticed in the amount of brine recycle and brine discharge temperature (Figures 5.7 and 5.8) when number of stages are changed.

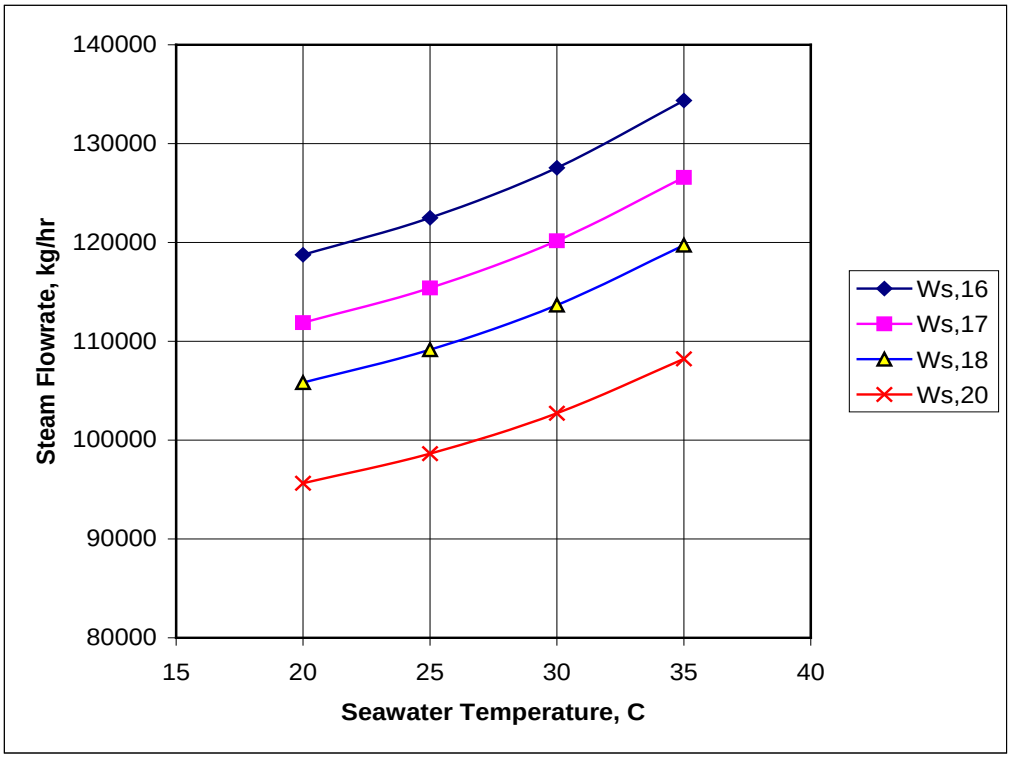

Figure 5.5. Effect of Seawater Temperature on Steam Flowrate for Different NS

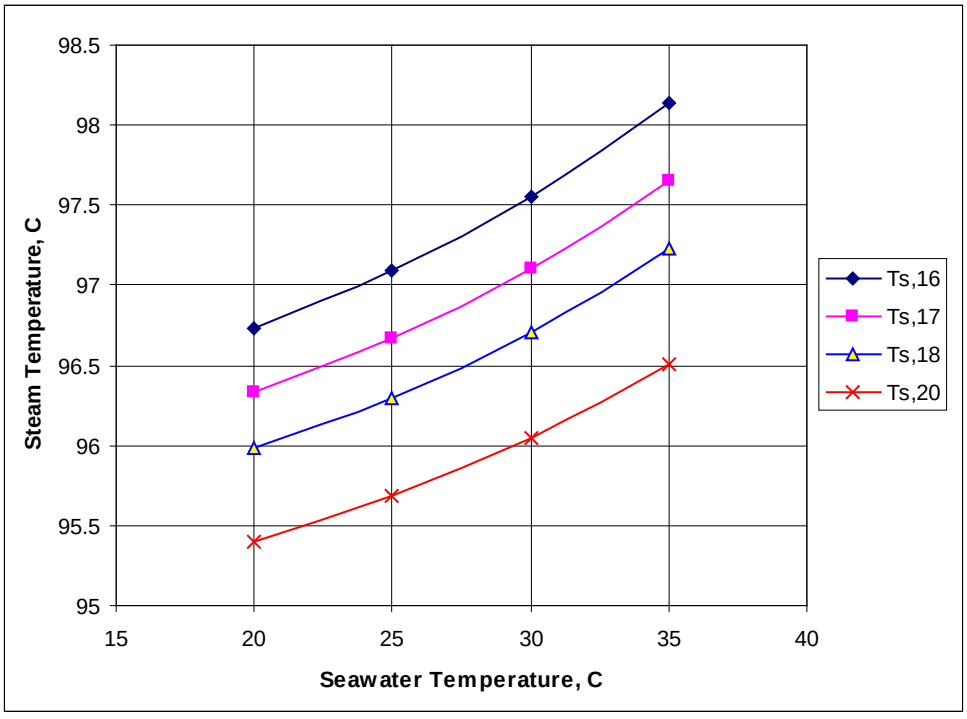

Figure 5.6. Effect of Seawater Temperature on Steam Temperature for Different NS

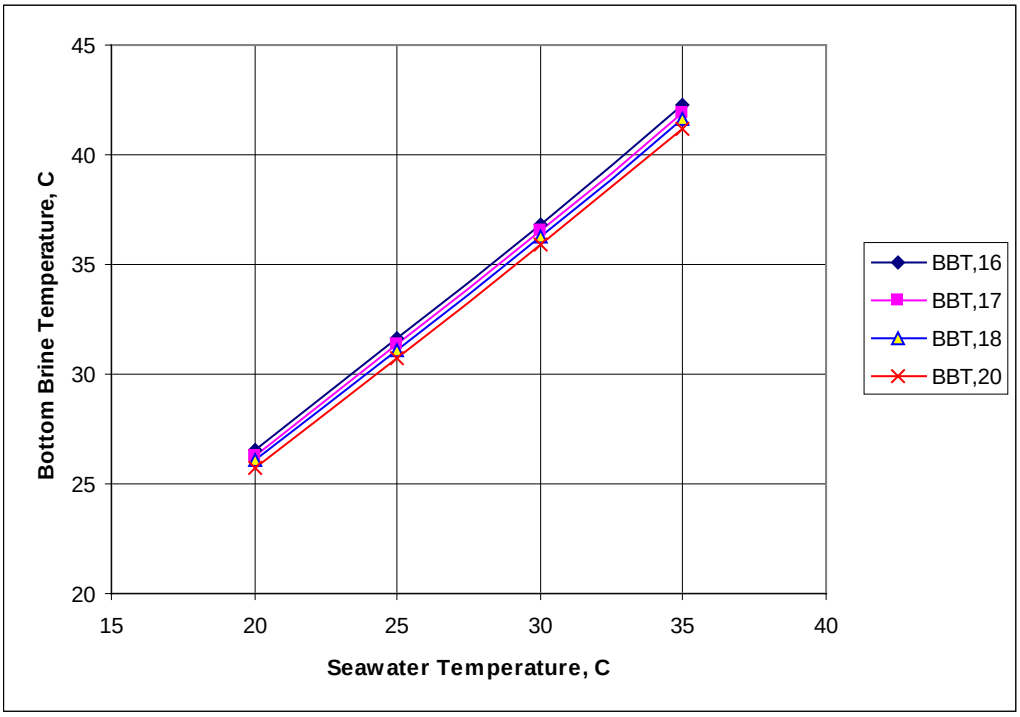

Fig. 5.7 Effect of Seawater Temperature on BBT for Different Number of Stages

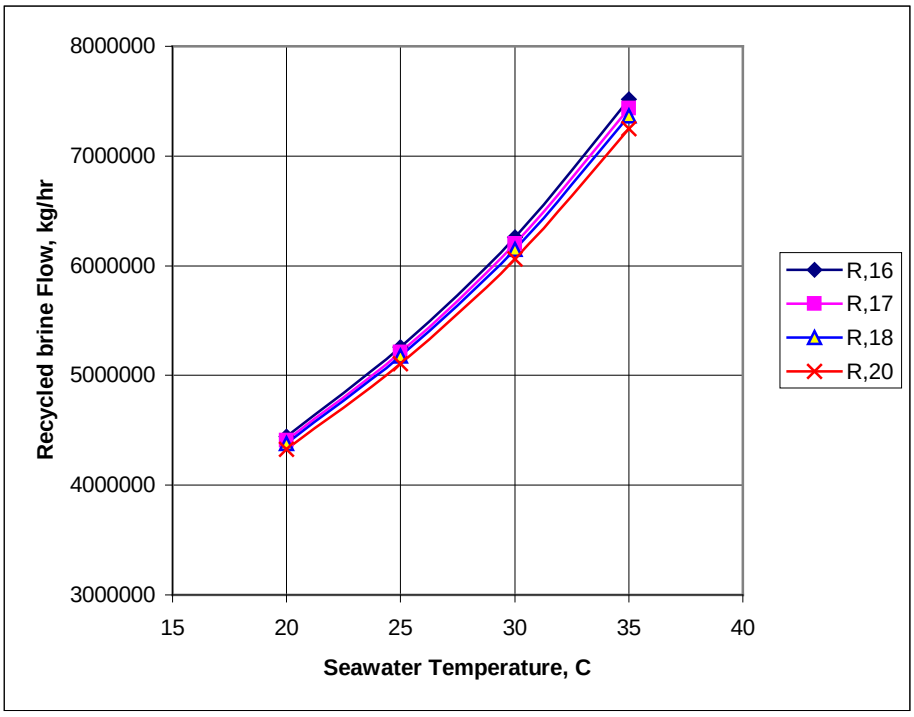

Fig. 5.8 Effect of Seawater Temperature on R for Different Number of Stages

5.6.3 Effect of heat exchange area and seawater temperature for fixed water demand

The heat exchange area of the brine heater (A_H) and of the Stages (A_j) is decreased by 10% (the base case values are shown in Table 5.2) to see its effect on the operation (Steam Flowrate, Steam Temperature, Bottom Brine Temperature, Recycled Brine Flowrate, etc.). The water demand (D_{NS}) was again fixed at 10^6 kg/hr and all other parameters were fixed as shown in Table5.2. The seawater temperature is also varied between 20 and 35 ^oC.

Figure 5.9 and 5.10 show the effect of heat exchange area on the steam flowrate and recycled brine flowrate at different seawater temperature respectively. For a given seawater temperature, while the steam flow increases by 6-7%, the recycled brine flow increases only by 1-2%. It is also noted that there is about 1-2% corresponding increase for steam temperature and bottom brine temperature. Although capital savings can be obtained by

reduced size heat exchangers, the operational cost will increase and the right balance between the design and operation has to be stricken.

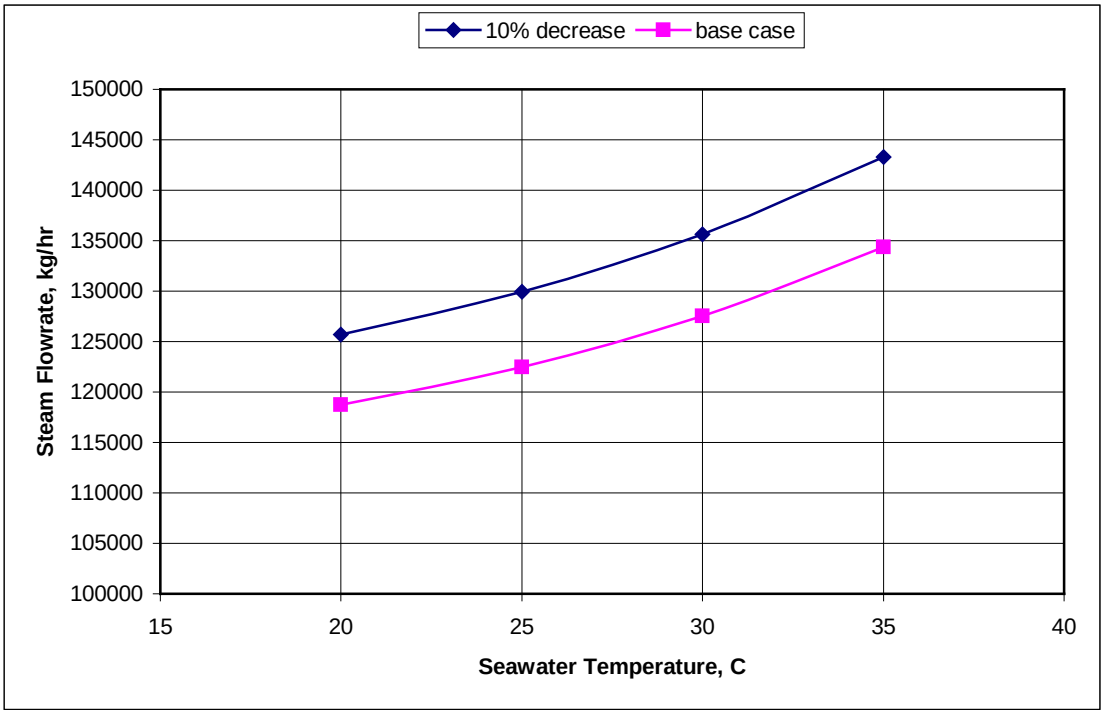

Figure 5.9 Effect of Heat Exchange Area on Steam Flowrate

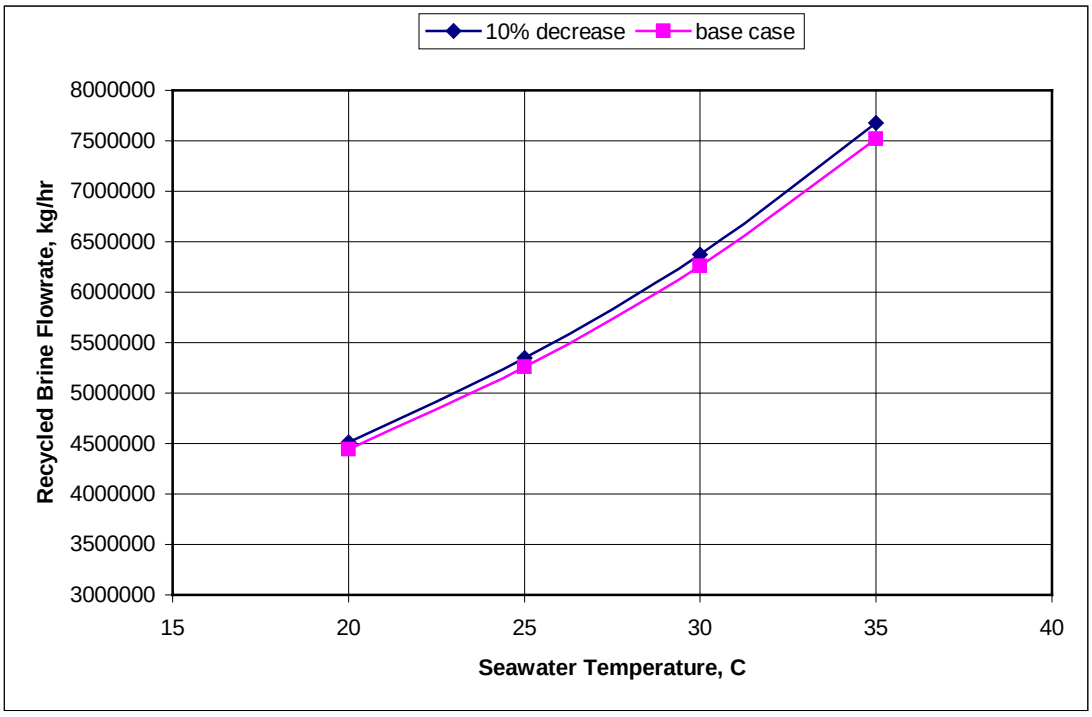

Figure 5.10 Effect of Heat Exchange Area on Recycled Brine Flowrate

5.7 Conclusions

Here, gPROMS modelling tool has been used to model an MSF process. A Neural Network based correlation NN_Cor_1 developed in earlier chapter for estimating *TE* is embedded within the gPROMS environment to develop the hybrid model. The predictions using the new model are in good agreement with the published results. The NN based correlation predicts *TE* very well even slightly outside the range of training.

The model is then used to study the sensitivity of two important operating parameters: the seawater temperature which is subject to seasonal variation, and the steam temperature in the brine heater which controls *TBT* of the process (indirectly controlling the design of the process). The results show that the steam temperature plays an important role to maintain

the production rate of freshwater at different seasons (however, may be at the expense of costly design).

In conclusion, over design is a possibility to accommodate this but an optimal design should be a way forward. Assuming the given design is flexible enough to accommodate all changes in operating conditions, the results show (qualitatively) that the cost of water production in summer will increase. The simulation also shows that for a fixed seawater temperature there might be a trade-off between design and operation.

The interaction of design (number of flash chambers, heat exchange areas) and operation (steam flowrate, steam temperature, recycled brine flowrate, bottom brine temperature) in the context of fixed fresh water demand and seasonal variation of seawater temperature is then studied here for MSF processes through modelling and simulation.

For a given design, the results show that some of the operating parameters such as recycled brine flowrate (R) will have to adjust by 70% for a seawater temperature rise of 15%. It is very important to note here that although 70% increase in R is possible in simulation, in practice, a given plant design may not be flexible enough to accommodate this huge change in operating condition.

The simulation results provide reasonable insight of the process performance and the next logical step would be to formulate an appropriate optimisation problem where design and operating parameters are simultaneously optimised subject to seasonal variation in seawater temperature.

Chapter 6

Simultaneous Optimisation of Design and Operation Parameters using MINLP Techniques

6.1 Introduction

Like other chemical process industries, desalination industries are also facing the challenges to improve the market shares (profitability) while meeting strict environmental constraints. While raw material costs are competitive in the global economy, the only way to achieve the target is by reducing the operational cost (labour, utility, etc.). The plant behaviour changes with time (due to corrosion, scaling, etc.). Therefore, use of one optimal set point operation decided at the time of commissioning the new plant will not guarantee the expected profitability while meeting the operational constraints. Now a day, it is necessary to determine the optimal set points of the individual control loops on a regular basis. Rather than playing with a running plant to determine the new set points, it is always economical to determine the optimal set points based on a rigorous process model and rigorous optimisation techniques before the operating set points are implemented in a real plant.

The degrees of freedom in terms of design and operating parameters are quite large for MSF processes (Figure 6.1) and an optimum combination of these parameters reduce the operating and investment costs of such plants thus significantly reducing the cost of fresh water.

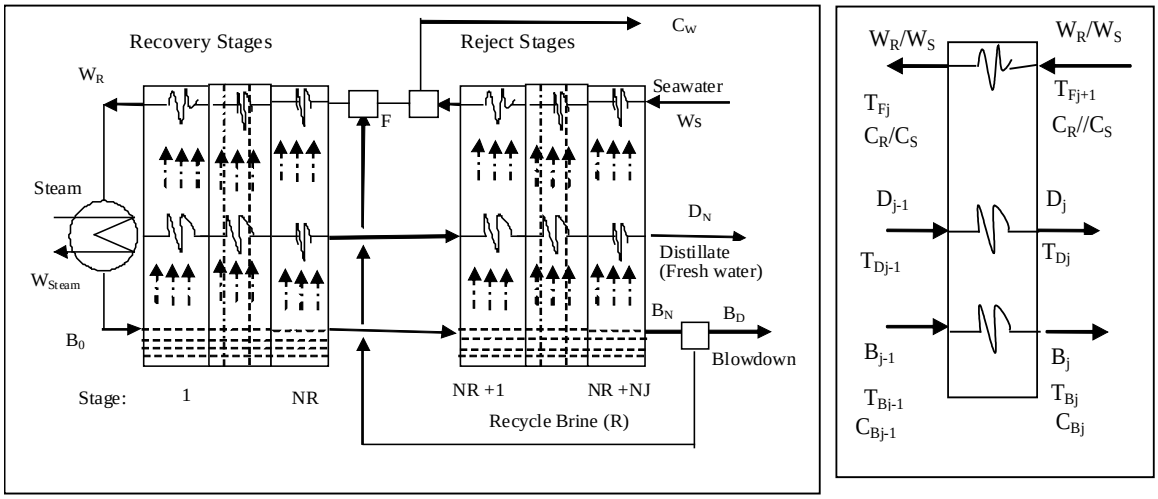

Figure 6.1 A typical MSF Process and Stage j

In the past, optimisation of design and operation of many chemical engineering problems has been optimised by continuous relaxation of Nonlinear Programming (NLP) and rounding off to the nearest integer for integer variables (such as number of plates in a distillation column) (Eliceche, 1981; Mujtaba and Macchietto, 1996). However, with recent developments in sophisticated numerical methods, for discrete systems with 0-1 option (i.e. a stage either exists or does not exist) use of Mixed-Integer Optimisation (MIO) such as MINLP, MILP techniques is most desirable (Mussati et al., 2005; Shah et al., 1993; Sharif, et al., 1998).

In chapter 5, the effects of design and operating parameters have been studied via repetitive simulation. In this chapter, simultaneous optimisation of design and operating parameters is considered using MINLP based optimisation problem formulation and solution within gPROMS. Two different types of optimisation problem formulations are considered with differing objective functions and constraints.

6.2 Optimisation within gPROMS

In OPTIMISATION Entity a subset of the ASSIGNed variables in the PROCESS Entity is used as optimisation decision (control) variables. An overview of the gPROMS Optimisation file for the MSF MINLP model is shown in Figure 6.2.

6.2.1 Different entry in optimisation section

gPROMS v2.3.4 supports continuous decision variables and four different types of discrete decisions variables ("mixed integer optimisation"). Types of discrete decisions variables can be specified in gPROMS:

- Binary variables
- General integer variables
- Enumerated variables and
- Special Ordered Sets one

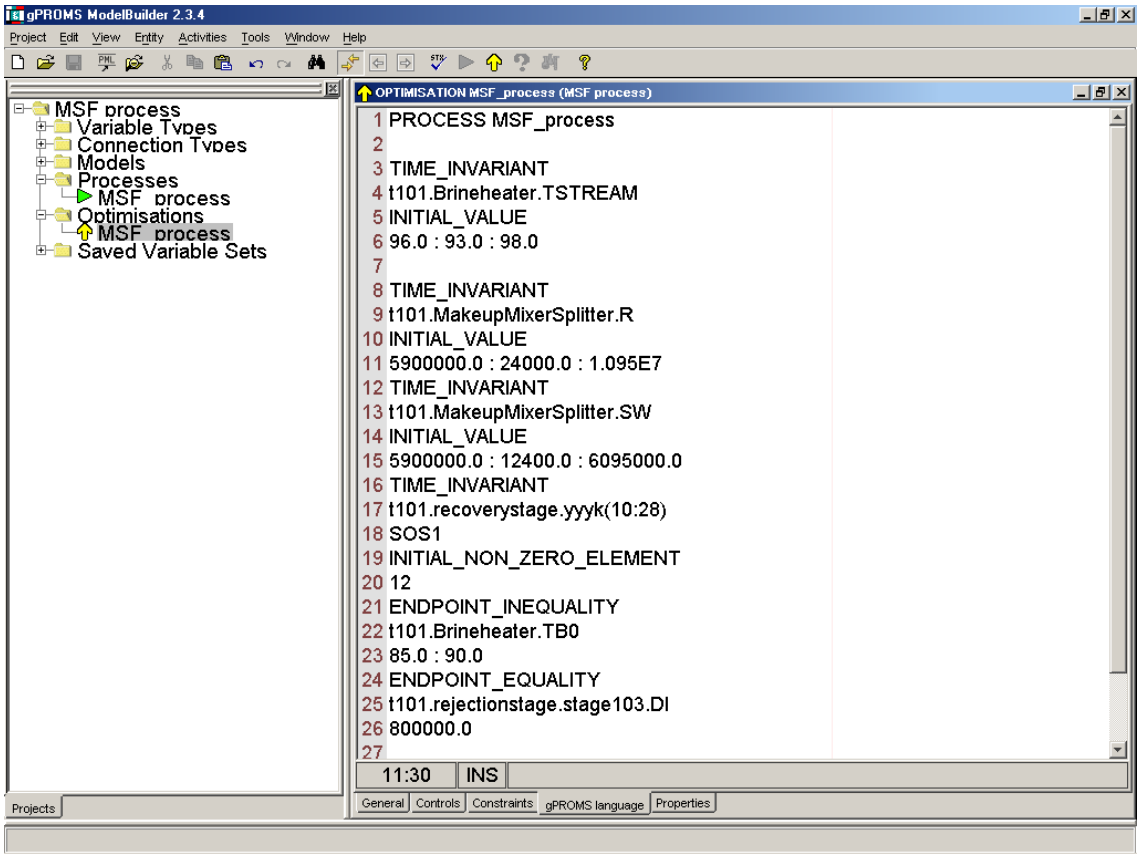

Figure 6.2 The snapshot of recovery section and different stage connection

The keyword BINARY, INTEGER, ENUM and SOS1 is used to specify above types of variables in the OPTIMISATION Entity. In gPROMS, the values of control variables are expressed in the form: [initial (guessed) value, lower bound, upper bound]; whereas the other variables limits are expressed in the form: [lower bound, upper bound] either in optimisation entry or process preset section or in the types of variables entry. In this work, Special Ordered Sets one and binary variables are used to develop the MINLP model.

6.2.2 MINLP gROMS optimiser solver

In gPROMS v2.3.4 the “CVP_SS” solver act as a single solver manager for the solution of both dynamic and steady state, continuous and mixed integer optimisation problems. In this work, MINLP based optimisation solver using outer approximation algorithm

(Viswanathan and Grossmann, 1990) called "OAERAP" tailored in "CVP_SS" solver is used to optimise the design and operating parameters. The "OAERAP" solver implements the outer approximation algorithm where SRQPD and GPLK are used as NLP and MIP solvers respectively (gPROMS, 2005). Figure 6.3 shows different steps of the optimisation algorithm.

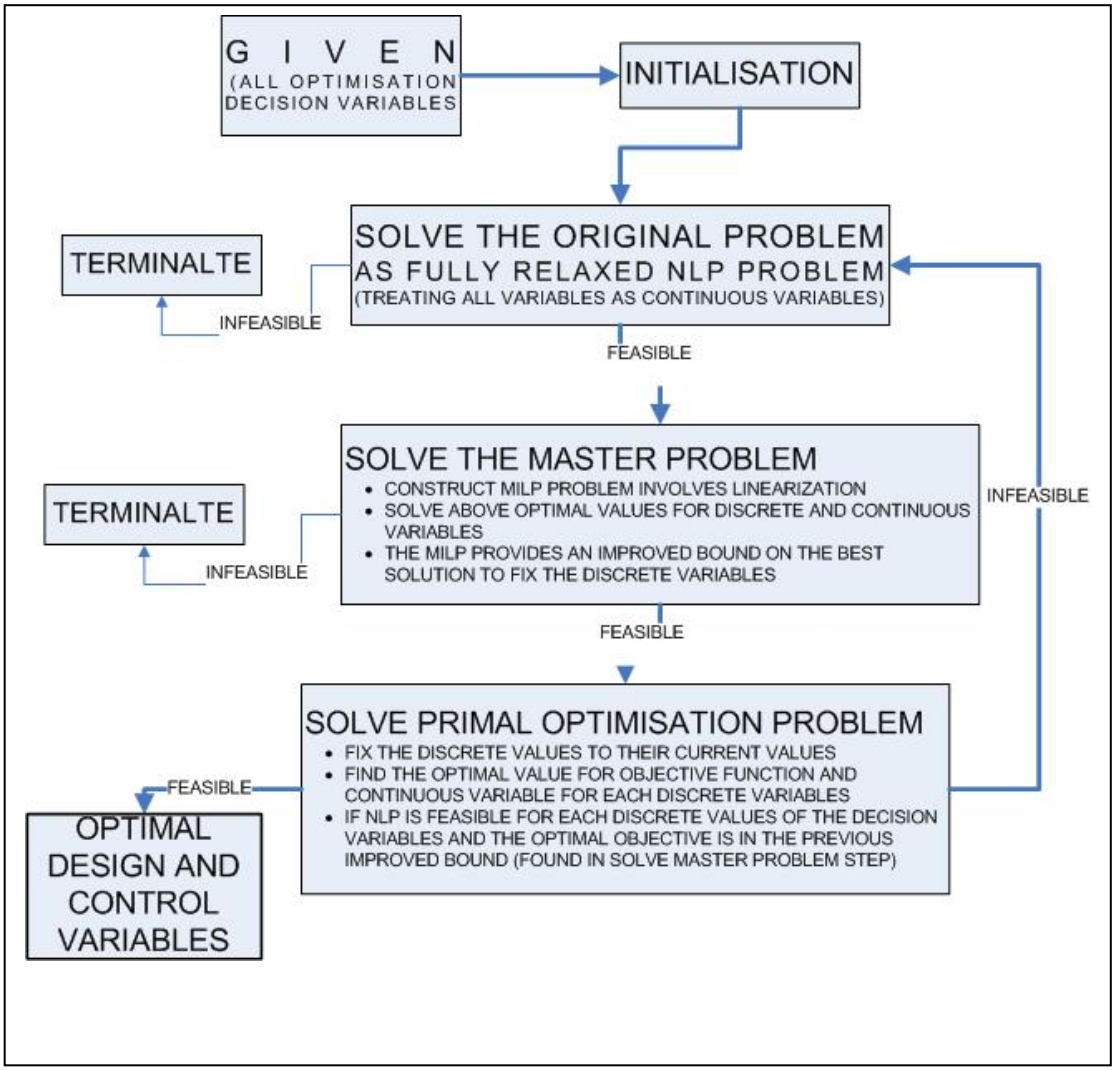

Figure 6.3 The Basic Steps of "OAERP" Optimisation Algorithm

6.3 Optimisation Problem Formulation

As mentioned in Chapter 5, the model equations for one recovery stage, one rejection stage, splitter, mixer, brine heater, etc. are written as unit models respectively. Note the number of rejection stage is fixed to three in this work. However, the number of recovery stage depends on the integer value for NR returned by the optimiser. For each optimisation iteration, depending on the value of NR, the recovery stages are connected automatically via the ports. The desalination plant components (named here as units), such as brine heater, flash chambers, mixer etc., are stored as icons. At the flowsheet level, the units are connected via ports automatically and the required set of model equations is generated.

6.3.1 Optimisation problem I: Performance optimisation

The amount of freshwater produced per unit of external heat input (steam) is generally termed as the 'Performance Ratio' in the literature (Hussain, 2003) which is often maximised. However, for a fixed freshwater demand this translates into minimising the external heat input.

In this work, for a fixed water demand the amount of external heating (supplied by steam) required is minimised while optimising the design parameter such as Number of Stages and operating parameters such at Steam Temperature, Recycled Brine Flowrate, Rejected Seawater Flowrate. Note external heat supply is a measure of operating cost and will thus reflect the cost of fresh water produced.

The optimisation problem is described as:

Given: Fixed water demand throughout the year, fixed number of rejection

stages, fixed amount of seawater flow, heat exchanger areas in stages, design specifications of each stages

***Optimise**:* The number of recovery stages, steam temperature, recycled brine flowrate, rejected seawater flowrate

So as to Minimise: the amount of external heat supplied via steam

Subject to: Process constraints: Equality constraints such as process model described in Chapter 5. Inequality constraints such as linear bounds on optimisation variables and other parameters.

The optimisation problem (***OP-1***) can be described mathematically by:

OP-1

$$\underset{NR,T_{steam},R,C_W}{Min} \quad Q_{steam}$$

$$\text{s.t.} \quad f(x,u,v)=0 \quad (\text{model equations})$$

$$D_{end} = D_{end}^{*}$$

$$(10)\ NR_L = NR = NR_U \ (28)$$

$$(93^oC)\ T_{steam}^L \le T_{steam} \le T_{steam}^U \ (95^oC)$$

$$(85^oC)\ TBT_L \le TBT \le TBT_U \ (90^oC)$$

$$(2.4\times10^4)\ R_L \le R \le R_U \ (1.095\times10^7)$$

$$(1.24\times10^4)\ C_W^L \le C_w \le C_W^U \ (6.095\times10^6)$$

D_{end} is the total amount of fresh water produced and D_{end}^{*} is the fixed water demand ($=7\times10^{5}$ kg/hr). *NR* is the number of recovery stages T_{steam} is the steam temperature. *TBT* is the Top Brine Temperature. R is the Recycle flowrate; C_w is the Rejected seawater flow rate. Subscripts/superscripts L and U refer to lower and upper bounds of the parameters. The bounds of the parameters are shown in brackets above.

The model equations presented in Chapter 5 can be described in a compact form by $f(x,u,v)=0$, where x ε R^n is the set of all algebraic variables, , u ε R^m is a vector of all optimisation variables, such as number of stages, steam temperature, etc., and v ε R^p is a vector of fixed parameters such as heat exchanger areas, design specification of stages, etc. The function $f: R^n \times R^m \times R^p \text{ -> } R^n$ is assumed to be continuously differentiable with respect to all its arguments.

6.3.2 Optimisation Problem II: Economic optimisation

In this work, for three different fixed water demand and for changing seawater temperature the total cost of the desalination (investment and operation cost) required is minimised while optimising the design parameter such as Number of Stages and operating parameters such at Steam Temperature (reflects utility cost), Recycled Brine Flowrate and Rejected Seawater Flowrate (reflect pumping cost). Note, some of the recent work (Mussati et al., 2005) also carried out optimisation using MINLP technique. However, their work was restricted to finding optimal design and operation for only one seawater temperature with a different objective function than what has been considered in this work. In addition,

sensitivity analysis of the cost parameters used in the objective function is provided for one set of water demand and seawater temperature.

The optimisation problem is described as:

Given: Fixed water demand throughout the year, fixed number of rejection stages, fixed amount of seawater flow, heat exchanger areas in stages, design specifications of each stages

Optimise: The number of recovery stages, steam temperature, recycled brine flowrate, rejected seawater flowrate

So as to Minimise: The total annualised cost of freshwater (or desalination)

Subject to: Process constraints: Equality constraints such as process model described in Figure 6.2. Inequality constraints such as linear bounds on optimisation variables and other parameters.

The optimisation problem (***OP-2***) can be described mathematically by:

OP-2

$$\underset{NR,T_{steam},R,C_w}{Min} \quad TAC$$

s.t. $\quad f(x,u,v)=0 \qquad (\text{model equations})$

$$D_{end} = D_{end}^{*}$$

$$(10)\ NR_L = NR = NR_U\ (28)$$

$$(93^oC)\ T_{steam}^{L} \le T_{steam} \le T_{steam}^{U}\ (98^oC)$$

$$(85^oC)\ TBT_L \le TBT \le TBT_U\ (90^oC)$$

$$\left(2.4\times10^{4}\right)\ R_L \le R \le R_U\ \left(1.095\times10^{7}\right)$$

$$\left(1.24\times10^{4}\right)\ C_W^L \le C_w \le C_W^U\ \left(6.095\times10^{6}\right)$$

D_{end} is the total amount of fresh water produced and D_{end}^{*} is the fixed water demand ($=8\times10^{5}, 7\times10^{5}$ and 9×10^{5} kg/hr). NR is the number of recovery stages T_{steam} is the steam temperature. TBT is the Top Brine Temperature. R is the Recycle flowrate and C_w is the rejected seawater flow rate. Subscripts/superscripts L and U refer to lower and upper bounds of the parameters. The bounds of the parameters are shown in brackets above.

The objective function, TAC (Total Annualised Cost) is defined as:

TAC = Total Annualised Cost, \$/yr = $ACC + ASC + APC$ **(6.1)**

Where, ACC = Annualised Capital Cost, \$/yr = $C_1 HN_{stage}^{x}$ (6.2)

ASC = Annualised Steam Cost, \$/yr = $C_2 HQ_{steam}$ (6.3)

APC = Annualised Pumping (operating) Cost, \$/yr = $C_3 HW_R$ (6.4)

With $x = 0.65$, $C_1 = 182$, $C_2 = 4\times10^{-5}$ and $C_3 = 2\times10^{-4}$. It is assumed that the plant runs for 8000 hr (=H) per year.

To increase the convergence of MINLP model, initialisation and scaling of the variables of the rigorous model is carried out as per guidelines in gPROMS to justify the global

optimum solution and to reduce the possibility of finding very near optimal solutions. In this work, the tolerance used for simulation is 10^{-8} and that for optimisation is 10^{-3}.

6.4 Results and Discussions

Table 6.1 lists all the constant parameters of the model equations including various dimensions of the brine heater and flash stages. As the temperature of the seawater varies with the season, instead of solving the optimisation problem ***OP*** for just one temperature, we have solved the problem for a set of seawater temperature (ranging from 20 to 40 deg C) demonstrating clearly the effect of this on the overall design and operation of the plant.

Table 6.1. Constant parameters

	A_j / A_H m^2	D_j^i / D_H^i m	D_j^o / D_H^o m	f_j^i / f_H^i $hm^{2o}C/Kcal$	w_j / L_j / L_H m	H_j m
Brine heater	3530	0.022	0.0244	$1.86x10^{-4}$	12.2	
Recovery stage	3995	0.022	0.0244	$1.4\ x10^{-4}$	12.2	0.457
Rejection stage	3530	0.024	0.0254	$2.33x10^{-5}$	10.7	0.457

6.4.1 Case 1: Performance optimisation

The optimisation results are summarised in Table 6.2.

Table 6.2. Summary of optimisation results of Case 1

T_{sea}	NR	R	C_w	TBT	T_{steam}	W_{steam}	Q_{steam}
40 (Summer)	21	2.40E+04	1.90E+06	90	93.01	54064.9	3.44E+07
35	19	2.40E+04	2.77E+06	90	93.02	55855.7	3.55E+07
30	17	2.40E+04	3.47E+06	90	93.10	58991.9	3.75E+07
25	16	2.40E+04	4.05E+06	90	93.09	60497.9	3.85E+07
20 (Winter)	15	2.40E+04	4.54E+06	90	93.12	62765.2	3.99E+07

The following observations are made from the results presented in Table 6.2.

- Steam can be supplied at the same temperature throughout the year. Smaller amount of external heat (also the amount of steam) is required in summer as the feed water is at higher temperature.

- TBT hit the upper bound in all cases. Therefore, all cases operate at the same TBT which is the inlet temperature of the feed in stage 1.

- Recycle flow in all cases hit the lower bound thus the cost of pumping this recycle stream will remain the same throughout the year.

- The amount of rejected seawater in winter is about 60% higher than in summer. The means during winter overall circulation of flow will be smaller thus reducing operating cost. This also demonstrates the possibility of using smaller feed seawater flow rate in winter.

- The number of stages in summer is higher than in winter. If the capital cost is charged based on the number of stages used, then the contribution of capital cost in winter will be lower compared to that in summer.

- For a fixed design and fixed water demand, in chapter 5 it is reported that both TBT and T_{steam} had to be increased by about 20% in summer (also recommended by El-Desousky and Ettourney, 2002). That would have considerable impact on the capital cost (different materials of construction) and operating cost (amount of anti-scaling and anti-corrosion materials) of the plant. However, in this work both TBT and T_{steam} remain almost constant at lower values throughout the season thus reducing capital cost of construction of flash units and operating costs

- Based on the results we can propose to design a plant based on summer condition, make the design of individual units as a stand-alone module and connect as many as of them as needed due to variation of weather condition while supplying a fixed amount of water throughout the year and irrespective of weather. This will result in flexible scheduling of the modules and will allow efficient maintenance of the modules without interrupting the production of water. In addition, there will be no requirement of full shut down of the plant.

Finally, summer demands higher capital cost contribution, higher pumping cost and lower energy cost. Winter demands lower capital cost contribution, lower pumping cost but higher energy cost.

6.5 Case 2: Cost optimisation

In addition, here we considered three different levels of water demand. For all cases, the feed seawater flow is 11.3×10^{6} kg/hr with salinity 5.7 wt %. The results are summarised in Table 6.3 and Figures 6.4-6.7.

Table 6.3. Summary of optimisation results (Case 2) for different fixed water demand

T_{sea} °C	*NR*	*R* Kg/hr	C_w Kg/hr	*TBT* °C	W_R Kg/hr	Q_{steam}	T_{steam} °C	W_{steam} Kg/hr	*TAC* $/yr
Case 2a: Water Demand, D_{end} = 700000 kg/hr									
20 (Winter)	15	2.40E+04	4.54E+06	90	6.78E+06	3.99E+07	93.12	62765	4.09E+03
25	16	2.40E+04	4.05E+06	90	7.27E+06	3.85E+07	93.09	60498	4.17E+03
30	18	2.40E+04	5.47E+06	90	7.85E+06	3.64E+07	93.00	57186	4.29E+03
35	19	2.40E+04	2.82E+06	90	8.56E+06	3.56E+07	93.02	55874	4.44E+03
40 (Summer)	21	2.40E+04	1.90E+06	90	9.42E+06	3.44E+07	93.01	54065	4.64E+03
Case 2b: Water Demand, D_{end} = 800000 kg/hr									
20 (Winter)	21	4.70E+05	4.01E+06	90	7.76E+06	3.65E+07	93.00	57415	4.40E03
25	22	5.18E+04	3.03E+06	90	8.33E+06	3.58E+07	93.01	56261	4.52E+03
30	24	2.19E+06	4.49E+06	90	9.00E+06	3.48E+07	93.00	54698	4.69E+03
35	26	1.94E+06	3.44E+06	90	9.80E+06	3.39E+07	93.00	53350	4.89E+03
40 (Summer)	28	5.62E+04	5.38E+05	90	1.08E+07	3.35E+07	93.04	52630	5.15E+03
Case 2c: Water Demand, D_{end} = 900000 kg/hr									
20 (Winter)	25	3.42E+04	2.57E+06	90	8.76E+06	3.73E+07	93.19	58619	4.78E+03
25	28	2.40E+04	1.93E+06	90	9.39E+06	3.49E+07	93.04	54799	4.91E+03
30	28	2.40E+04	1.14E+06	90	1.02E+07	3.60E+07	93.22	56602	5.12E+03
35	28	2.40E+04	1.68E+05	90	1.12E+07	3.77E+07	93.44	59163	5.38E+03
40 (Summer)	28	4.41E+06	3.38E+06	90	1.23E+07	4.08E+07	93.82	64086	5.74E+03

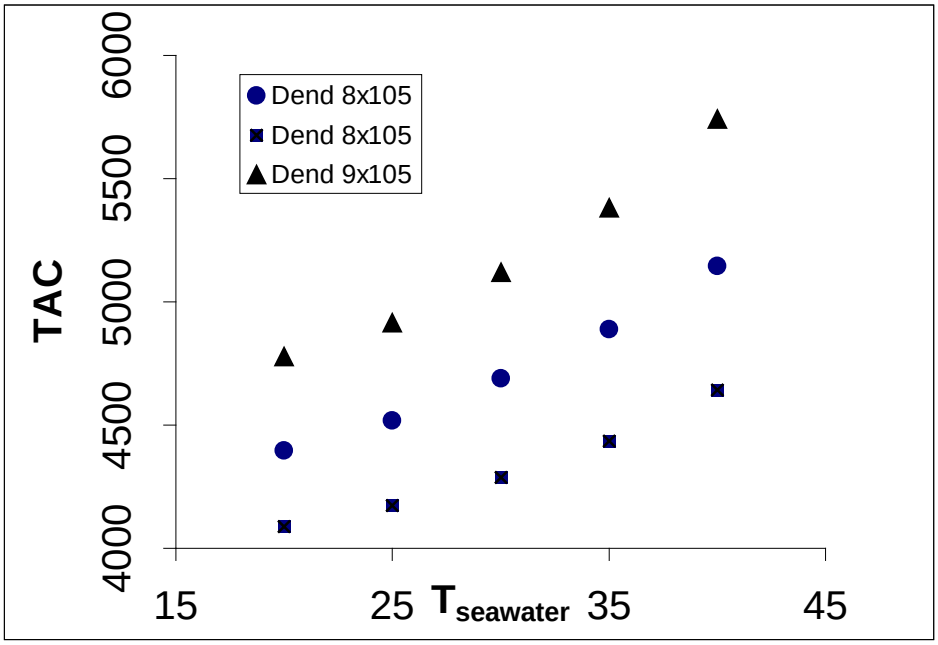

Figure 6.4 The Effects of Seawater Temperature on the Optimal Overall Costs for Different Fixed Water Demand

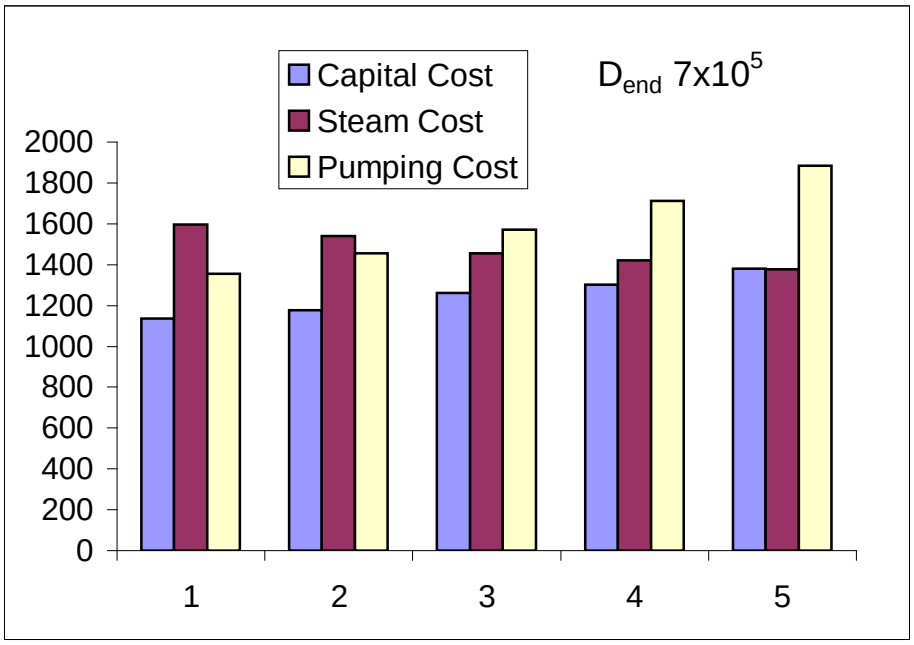

Figure 6.5 The Effects of Seawater Temperature on the Optimal Costs for Fixed Water Demand $7x10^5$ kg/h

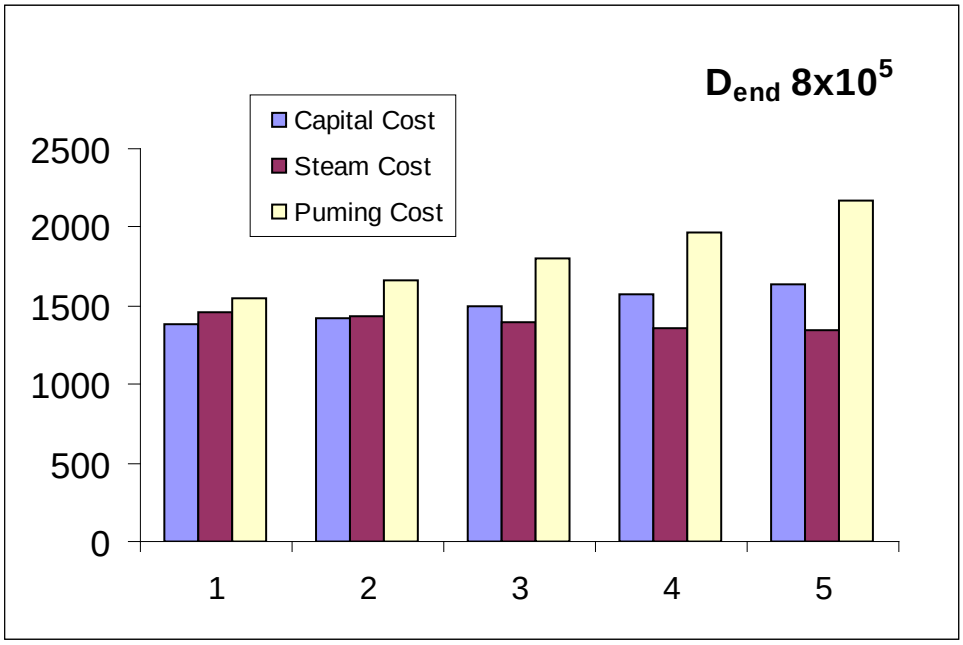

Figure 6.6 The Effects of Seawater Temperature on the Optimal Costs for Fixed Water Demand 8x10^5 kg/h

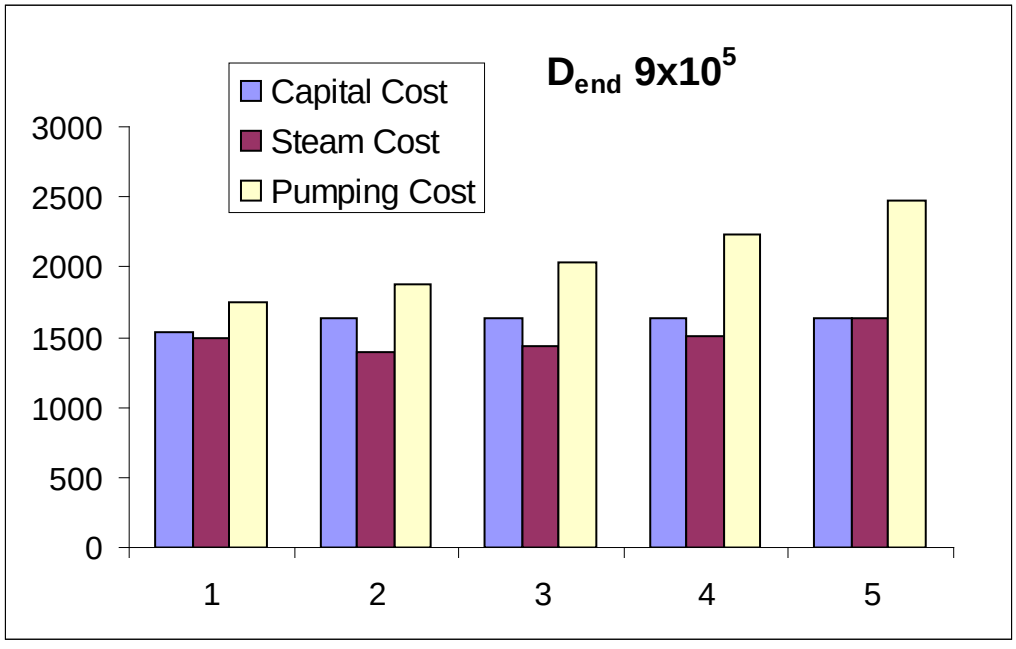

Figure 6.7 The Effects of Seawater Temperature on the Optimal Costs for Fixed Water Demand 9x10^5 kg/h

The following observations are made from the results presented in Table 6.3 and Figure 6.4-6.7:

- As the seawater temperature increases the total cost is increased for any fixed water demand. It is believed that due to decrease in temperature driving force in stages, the total number of stages and brine flowrate in recovery section increase. Although there is a decrease (only slightly) in steam cost, the contribution of the capital and pumping cost is higher. Note, however, for Case 3 (highest water demand), as the number of stages hit the upper bound, the only way the plant could fulfil the demand is by operating with higher amount of steam and brine flow rate.

- For a particular seawater temperature, when the water demand increases the total cost also increase due to increase in number of stages and brine flow (compare case 1-3 for any seawater temperature).

- Steam can be supplied at the same temperature throughout the year for any demand. However, for fixed design operation (see in Chapter 5) observed an increase in steam temperature and the amount of steam with increase in seawater temperature.

- The amount of steam varies within 9-17% for different water demands.

- The amount of brine flowrate (W_R) varies between for 38-40% for any fixed water demand for different seawater temperature.

- *TBT* hit the upper bound in all cases. Therefore, all cases operate at the same *TBT* which is the inlet temperature of the feed in stage 1.

- For case 1, recycle flowrate (*R)* hit the lower bound while for other cases this varies significantly. So the effect of seawater temperature on recycle flowrate is more

pronounced.

- For all cases, rejected seawater flowrate (C_w) varies significantly.
- El-Dessouky and Ettouney (2002) reported that operation at high temperature (specially in summer) requires larger amount of anti-scaling and anti-corrosion agents compared to the amount required at low temperature (winter). However, in this work both TBT and T_{steam} remain almost constant (the temperatures are also quite low, 90-94ºC) throughout the season thus reducing capital cost of construction of flash stages and operating costs. Similar, observation was noted for case 1 also.

6.5.1 Sensitivity of cost parameters

In the above, the cost parameters x, C_1 C_2 and C_3 were arbitrarily chosen. It would be interesting to see the effect of these parameters on the optimal design and operation. For this, we selected fixed water demand of 800000 kg/hr with seawater temperature 30 ºC. We vary x, C_1, C_2 and C_3 by + 20% as shown in Table 6.4.

Table 6.4. + 20% Variation in Cost Parameters

Run	
1 (base case)	$x = 0.65,\ C_1 = 182,\ C_2 = 4\times10^{-5},\ C_3 = 2\times10^{-4}$
2	$x = 0.65,\ C_1 = 145.6,\ C_2 = 4\times10^{-5},\ C_3 = 2\times10^{-4}$
3	$x = 0.65,\ C_1 = 218.4,\ C_2 = 4\times10^{-5},\ C_3 = 2\times10^{-4}$
4	$x = 0.52,\ C_1 = 182,\ C_2 = 4\times10^{-5},\ C_3 = 2\times10^{-4}$
5	$x = 0.78,\ C_1 = 182,\ C_2 = 4\times10^{-5},\ C_3 = 2\times10^{-4}$
6	$x = 0.65,\ C_1 = 182,\ C_2 = 3.2\times10^{-5},\ C_3 = 2\times10^{-4}$
7	$x = 0.65,\ C_1 = 182,\ C_2 = 4.8\times10^{-5},\ C_3 = 2\times10^{-4}$
8	$x = 0.65,\ C_1 = 182,\ C_2 = 4\times10^{-5},\ C_3 = 1.6\times10^{-4}$
9	$x = 0.65,\ C_1 = 182,\ C_2 = 4\times10^{-5},\ C_3 = 2.4\times10^{-4}$

Table 6.5. Sensitivity Analysis of Cost Parameters (case 2)

Run	T_{sea} oC	*NR*	*R* Kg/hr	C_w Kg/hr	*TBT* oC	W_R Kg/hr	Q_{steam}	T_{steam} oC	W_{steam} Kg/hr	*TAC* $/yr
1 (base)	30	24	2.19E+06	4.49E+06	90	9.00E+06	3.48E+07	93.00	5.47E+04	4.69E+03
2	30	24	2.19E+06	4.49E+06	90	9.00E+06	3.48E+07	93.00	5.47E+04	4.40E+03
3	30	24	2.19E+06	4.49E+06	90	9.00E+06	3.48E+07	93.00	5.47E+04	5.01E+03
4	30	24	2.19E+06	4.49E+06	90	9.00E+06	3.48E+07	93.00	5.47E+04	4.18E+03
5	30	23	4.96E+04	2.34E+06	90	9.01E+06	3.56E+07	93.07	5.59E+04	5.46E+03
6	30	23	4.67E+04	2.34E+06	90	9.01E+06	3.56E+07	93.07	5.59E+04	4.41E+03
7	30	24	2.19E+06	4.49E+06	90	9.00E+06	3.48E+07	93.00	5.47E+04	4.98E+03
8	30	24	2.19E+06	4.49E+06	90	9.00E+06	3.48E+07	93.00	5.47E+04	4.35E+03
9	30	24	2.19E+06	4.49E+06	90	9.00E+06	3.48E+07	93.00	5.47E+04	5.07E+03

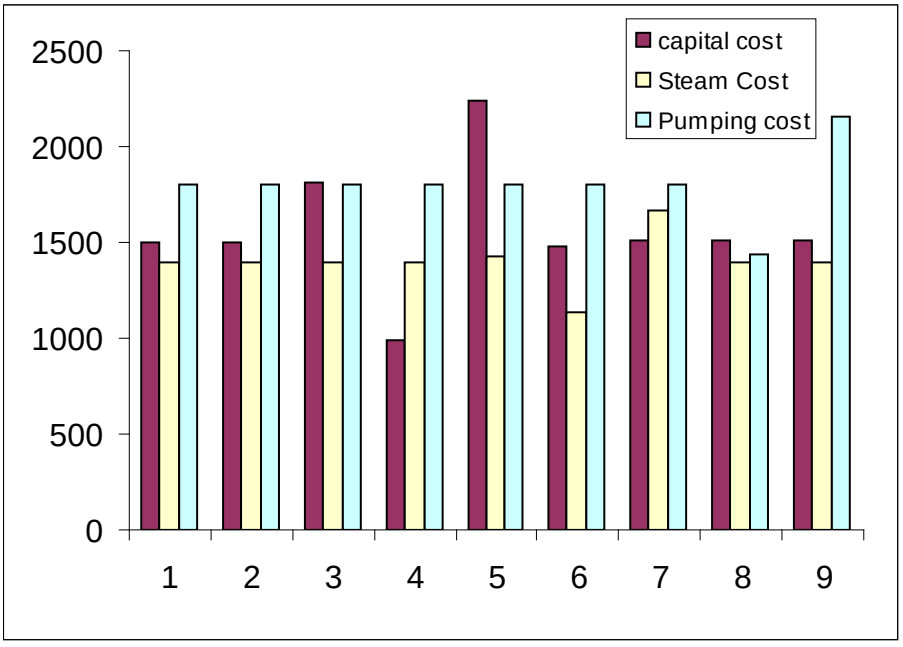

Figure 6.8 Individual Cost Components for Different Runs

The results are summarised in Table 6.5. The individual cost components for different runs are shown in Figure 6.8.

The following observations are made from the results presented in Table 6.4 and Figure 6.8:

- The effects x (index the number of stages), and C_2 (energy cost parameter) has significant effects (runs 4-7) on the design and operation variables (number of stages, recycle and rejected seawater flowrate).
- The effects C_1 (capital cost parameter) and C_3 (pumping cost parameter) has little effects on the design and operation variables (number of stages, recycle, and rejected seawater flowrate).
- Lower steam cost favours lower number of stages but higher amount of recycle flow to minimise the total cost (run 6) and the opposite is true for higher steam cost (run 7), although the pumping cost remains the same for both runs.

6.6 Flexible Scheduling

As the design/configuration of almost all industrial plants is fixed, even to supply fresh water at a fixed rate throughout the year or to increase the production at any time of the year, the common industrial practice is to operate the plant at high temperature (ElMoudir, 2007, 2008). However, this results in increased fouling and corrosion (Figure 6.9) of heat exchangers (and plant equipment) leading to frequent shut down of the plant (ElMoudir, 2007, 2008) interrupting freshwater supply or to the use of increased amount of anti-scalant (El-Dessouky and Ettouney, 2002) at high temperature operation increasing the cost.

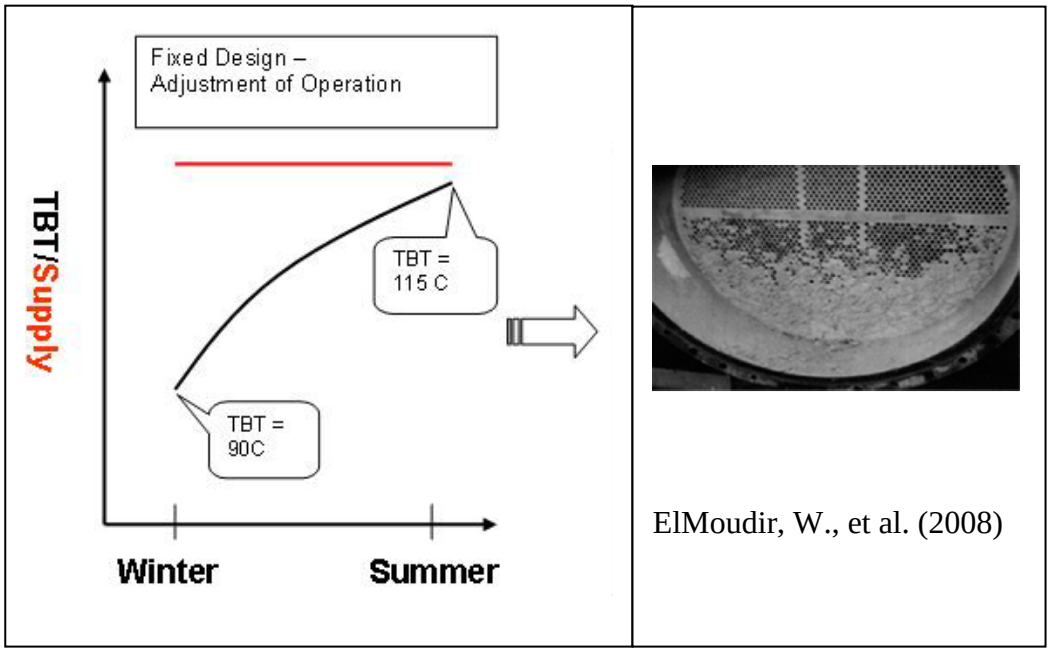

Figure 6.9 High Temperature Operation Leading to Heat Exchanger Corrosion

Based on the results (at least for cases 1 and 2 cost optimisation and performance optimisation) it is proposed to design a plant based on summer condition, making the design of individual units as a stand-alone module and connecting as many of them as needed due to variation in weather condition (Figure 6.10) while supplying a fixed amount of water throughout the year (and irrespective of weather). This will result in flexible scheduling of the modules and will allow efficient maintenance of the modules without interrupting the production of water. In addition, there will be no requirement of full shut down of the plant. A flexible design and operation at near constant temperature throughout the year or at peak demand period of the year would certainly address these issues.

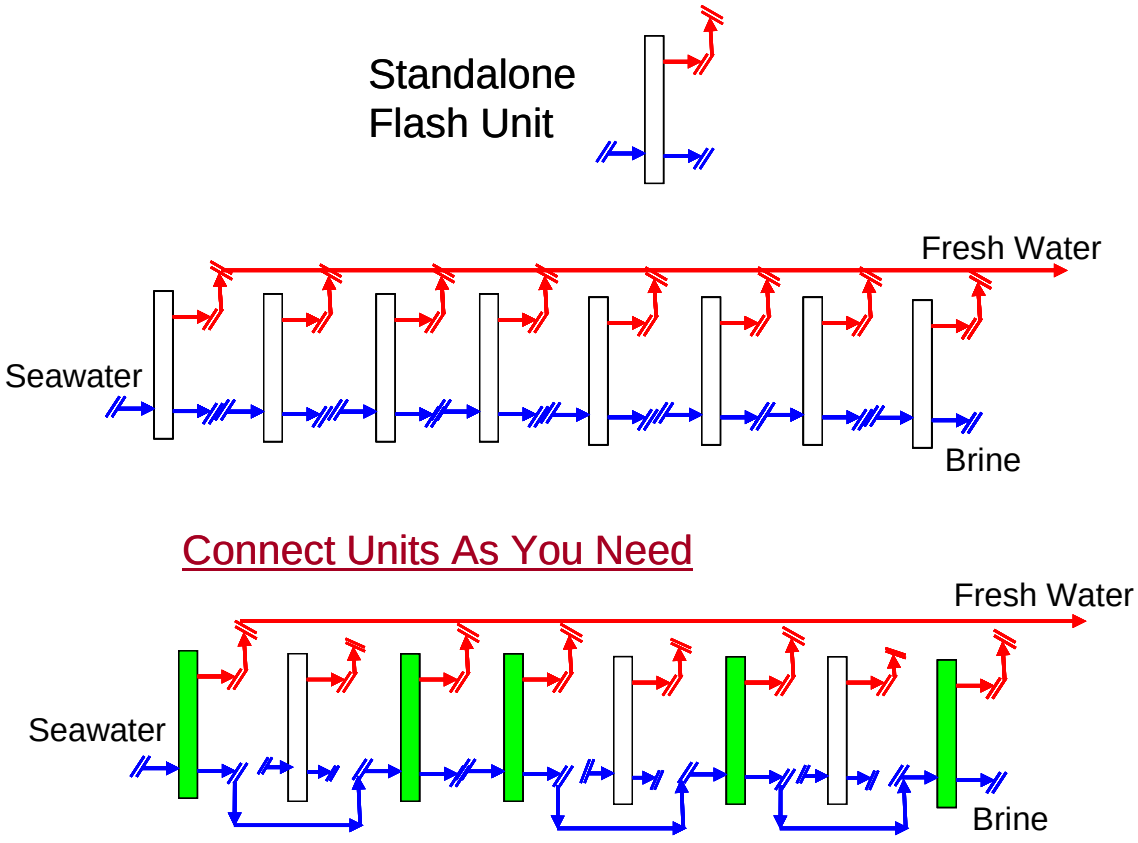

Figure 6.10 Flexible Design and Schedule

6.7 Conclusions

An MINLP based optimisation framework is developed for MSF desalination process using gPROMS 2.3.4 model builder. The flowsheet for the MSF process is developed by importing (from other sources) or drawing the icons for different units independently. Model equations for each unit are written separately. Graphical connections of each icon in the flowsheet automatically produce a Master Model (incorporating model equations for all the units). During optimisation when the number of stages is iterated, the model equations for all the stages with all the necessary internal connections are automatically generated.

A detailed model incorporating Neural Network based correlation for physical properties

estimation describes the process.

The number of flash stages (integer variable) and few significant operating parameters such as steam temperature, recycled brine flow and rejected seawater flow are optimised while minimising the total annualised cost (including capital, utility and pumping costs) of the process. The sensitivity analysis of the cost parameters shows that the optimal design and operation are sensitive to some of the parameters.

Some of the results cost optimisation and performance optimisation clearly show that a flexible scheduling of individual flash stages and operation is possible to supply fresh water at a fixed demand throughout the year with changing seawater temperature.

Also the operating conditions in terms of TBT and T_{steam} do not change much and thus the amount of anti-scaling and anti-corrosion agents does not have to change much with the weather condition.

Therefore, chances of fouling, corrosion and plant shutdown are reduced. Also the amounts of anti-scaling and anti-corrosion agents do not have to change much with the weather condition. This significantly reduced the operating cost. As the plant operates at low temperature the material of construction of the certain equipment will be reduced subsequently.

Simultaneous optimisation of design and operation achieves clear benefits over the earlier reported work on operation optimisation (by repetitive simulation) for a fixed design (Chapter 5).

Chapter 7

Hybrid Dynamic Modelling, Simulation and Optimisation

7.1 Introduction

In recent years, with the development sophisticated numerical methods for DAE (Differential Algebraic Equation) system, dynamic modelling, simulation and optimisation provided as a cost-effective tool to forecast feasible and sustainable design and operation of the process. Without conducting the lengthy and expensive tests on real plant, process dynamics are investigated by dynamic simulation and optimisation. Thus, dynamic modelling, simulation and optimisation provide a better insight into the process and provide optimal operation, control and design of the process.

Having presented a hybrid steady state model incorporating NN based correlations for physical property calculation, repetitive simulation and structured optimisation of MSF process in earlier chapters, it was attempted to present a dynamic model and demonstrate its capability with only preliminary simulation and optimisation results in this chapter. Note, study of design and operation optimisation and the design of control were beyond the scope of this research.

7.2 MSF Dynamic Process Model Development gPROMS

7.2.1 Model assumptions

The following assumptions are made

- The distillate from any stage is salt free

- Heats of mixing is negligible
- No sub cooling of condensate leaving the brine heater
- There are no heat losses and
- There is no entrainment of mist by the flashed vapour.
- The pumps are not considered

7.2.2 Model equations

The model equations for stage j (Figure 7.1) of the MSF process presented here are based on Helal et al. (1986), Rosso et al. (1996) and Husain et al. (2003).

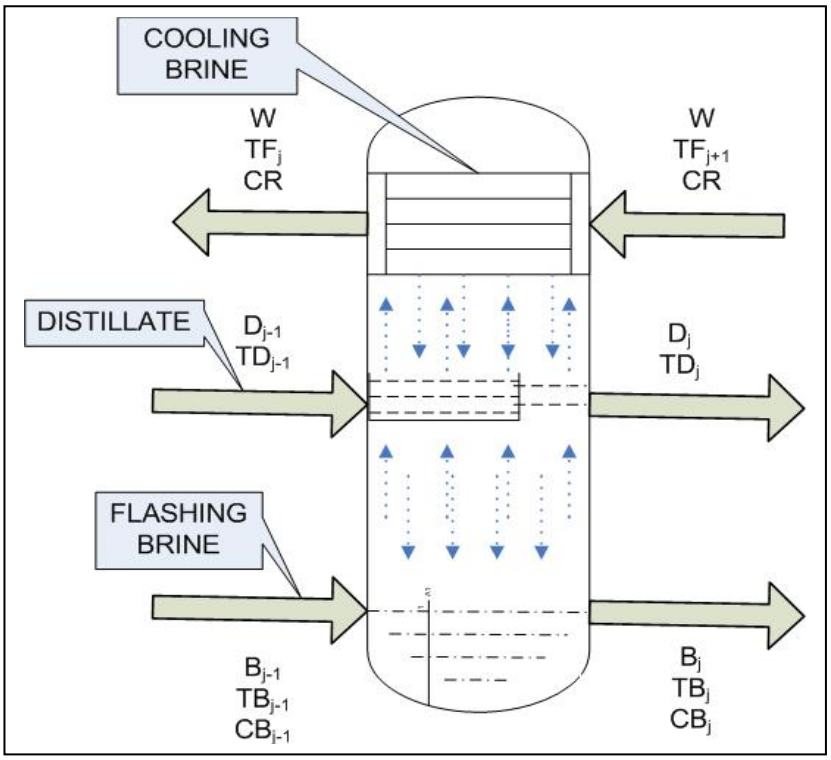

Figure 7.1 Schematic Representation of Stage-j

(a) Stage Model

The flashing brine model

Mass Balance

$$\frac{d}{dt}M_j^B = B_{j-1} + B_j - V_j \tag{7.1}$$

Salt Mass

$$\frac{d}{dt}\left(M_j^B \times X_j^B\right) = B_{j-1} \times CB_{j-1} - B_j \times CB_j \tag{7.2}$$

Enthalpy balance for the flashing brine

$$M_j^B \times h_j^B = B_{j-1} \times \left(h_{j-1}^B - h_j^B\right) - V_j \times \left(h_j^V - h_j^B\right) \tag{7.3}$$

Mass balance for the distillate tray:

$$\frac{d}{dt}M_j^D = D_{j-1} + D_j - V_j \tag{7.4}$$

$$h_{vj} = f(T_{Sj}) \tag{7.5}$$

$$h_{Bj} = f(C_{Bj}, T_{Bj}) \tag{7.6}$$

$$h_{Dj} = f(T_{Dj}) \tag{7.7}$$

The Cooling Brine Tube

Mass Balance

$$W_j = W_{j+1} = W_T \tag{7.8}$$

Salt Mass

$$W_{j-1} \times CF_{j-1} = W_j \times CF_j \tag{7.9}$$

Enthalpy Balance

$$M_j^F \frac{d}{dt} h_j^F = U_j \times A_j \times \frac{\left(T_j^F - T_{j+1}^F\right)}{\ln \frac{\left(T_j^D - T_{j+1}^F\right)}{\left(T_j^D - T_j^F\right)}} - W_T \left(h_j^F - h_{j+1}^F\right) \quad (7.10)$$

Overall Enthalpy Balance:

$$M_j^D \times \frac{dh_j^D}{dt} + \left(h_j^V - h_j^D\right) \times \frac{dM_j^B}{d} = D_{j-1} \times h_{j-1}^D + B_{j-1} \times h_{j-1}^B - D_j \times h_j^D - B_j \times h_j^B - W_T \times \left(h_j^F - h_{j+1}^F\right) \quad (7.11)$$

$$S_{Rj} = f\left(T_{Fj+1}, T_{Fj}, C_R\right) \quad \text{(Recovery/ Rejection stage)} \quad (7.12)$$

$$S_{Dj} = f\left(T_{Dj}\right) \quad (7.13)$$

$$S_{Bj} = f\left(T_{Bj}, C_{Bj}\right) \quad (7.14)$$

Overall heat transfer coefficient:

$$U_j = f\left(W_R, T_{Fj}, T_{Fj+1}, T_{Dj}, D_j^i, D_j^o, L_j^i, f_j^i\right) \quad \text{(Recovery stage)} \quad (7.14)$$

$$U_j = f\left(W_s, T_{Fj}, T_{Fj+1}, T_{Dj}, D_j^i, D_j^o, L_j^i, f_j^i\right) \quad \text{(Rejection stage)} \quad (7.15)$$

Distillate and flashing brine temperature correlation:

$$T_{Bj} = T_{Dj} + TE_j + EX_j + \Delta_j \quad (7.16)$$

Distillate and flashed steam temperatures correlation:

$$T_{Sj} = T_{Dj} + \Delta_j \quad (8.17)$$

Temperature drop due to demister correlation

$$\Delta_j = \exp\left(1.885 - 0.02063 \times T_j^D\right) \quad (7.18)$$

$$EX_j = f\left(H_j, w_j, T_{Bj}\right) \quad (7.19)$$

The relationship for the evaluation of the pressure (atm) of the stage P_j

$$\log 10 \frac{P_C}{P_j} = \frac{X}{T_j^V}\left(\frac{a + b \times X + c \times X}{d \times X}\right) \tag{7.20}$$

where $a = 3.2437814,\ b = 5.86826 \times 10^{-3},\ c = 1.1702379 \times 10^{-8}\ \ d\ = 2.1878462 \times 10^{-3}$

$X = T_c - T_j^S$, $P_c = 218.167\ atm$ and $T_c = 647.27K$ are the critical pressure and temperature of water, respectively.

Orifice equations for Distillate and Brine flow rate

Empirical relationship for orifice model is taken from (Lior et al.,1997; Reddy et al., 1995)

Empirical relationship between brine orifice and Brine flow rate

$$M_j^B = \rho_j^B \times Oh_j^B \times L_j \times V_j^B \tag{7.21}$$

$$V_j^B = \sqrt{\frac{2 \times g \times \left(L_j - L_{j+1} + \left(P_{j+1} - P_j\right)\right)}{1 - \left(\frac{Cc_j^B \times Oh_j^B \times Ow_j^B}{L_j \times Q_B}\right)}} \tag{7.22}$$

$$\Delta P = P_{j+1} - P_j + 0.098 \times (L_j - Cc_j^B \times Oh_j^B) \tag{7.23}$$

$$Cc_j^B = 0.61 + 0.18 \times r_{Bj} - 0.58 \times r_{Bj}^2 + 0.7 \times r_{Bj}^3 \tag{7.24}$$

$$r_{Bj} = \frac{g \times \frac{\rho_j^B}{1000} \times Oh_j^B}{100 \times \left(P_{j-1} - P_j\right) \times g \times \frac{\rho_j^B}{1000} \times L_j} \tag{7.25}$$

Empirical relationship between Distillate orifice and Distillate flow rate

$$M_j^D = \rho_j^D \times Oh_j^D \times L_j \times V_j^D \tag{7.26}$$

$$V_j^D = \sqrt{\frac{2 \times g \times \left(L_j - L_{j+1} + \left(P_{j+1} - P_j\right)\right)}{1 - \left(\frac{Cc_j^D \times Oh_j^D \times Ow_j^D}{L_j \times Q_D}\right)}} \tag{7.27}$$

$$\Delta P = P_{j+1} - P_j + 0.098 \times (L_j - Cc_j^D \times Oh_j^D) \tag{7.28}$$

$$Cc_j^D = 0.61 + 0.18 \times r_{Dj} - 0.58 \times r_{Dj}^2 + 0.7 \times r_{Dj}^3 \tag{7.29}$$

$$r_{Bj} = \frac{g \times \frac{\rho_j^D}{1000} \times Oh_j^D}{100 \times \left(P_{j-1} - P_j\right) \times g \times \frac{\rho_j^D}{1000} \times L_j} \tag{7.30}$$

$$M_j^F = \rho_j^F \times Oh_j \times A_j \tag{7.31}$$

(b)Brine Heater Model

Overall Mass Balance

$$B_{BH} = W_T \tag{7.32}$$

Salt mass Balance

$$C_{BH} = C_R \tag{7.33}$$

Enthalpy balance of the cooling brine

$$M_{BH} \times \frac{d}{dt} h_{BH} = U_H \times A_H \times \frac{T_{BH} - T_1^F}{\ln \frac{T_{steam} - T_1^F}{T_{steam} - T_{BH}}} - W_T \times \left(h_{BH} - h_1^F\right) \tag{7.34}$$

Enthalpy balance of the condensing vapour

$$W_{steam} \times \lambda_{steam} = U_H \times A_H \times \frac{T_{BH} - T_1^F}{\ln \frac{T_{steam} - T_1^F}{T_{steam} - T_{BH}}} \tag{7.35}$$

7.2.3 Physical and Chemical Properties Equations

The correlations for physical and chemical properties (except the calculation of TE) are

taken from (Helal et al., 1986; Rosso et al., 1996; Mazzotti et al., 2000 and Husain et al., 2003) are shown in Chapter 5. Instead of an empirical correlation an NN based correlation (NN_Cor_1, developed in Chapter 3) is used here to calculate the temperature elevation (TE) due to salinity.

7.2.4 Degrees of freedom analysis

The degrees of freedom (DOF) analysis for the dynamic model can be carried out in a similar way to those described in Chapter 5. However, note that the initial conditions (at time t = 0) of all the differential variables (such as $M_j^B, M_j^D, M_j^W, h_j^B, h_j^D, h_j^F, h_{BH}$) must be given.

7.3 Model Validation

7.3.1 Steady state

The dynamic model described above is first validated against the steady state results of Rosso et al. (1996) and by setting $\frac{dM_j^B}{dt}=0,\ \frac{dM_j^D}{dt}=0,\ \frac{dh_j^B}{dt}=0,\ \frac{dh_j^D}{dt}=0,\ \frac{dh_j^F}{dt}=0,$ $\frac{dh_{BH}}{dt}=0$ in the dynamic model. As before, there are 13 recovery stages and 3 rejection stages. Constant parameters and input variables of the process model are shown in Table 7.1. The results are reported in Table 7.2 (Rosso et al.'s results are shown in plain while the predictions by the dynamic model are shown in italic). Comparison of these results with those presented in Table 5.3 (Chapter 5) show a good agreement. The slight discrepancies are due to the addition of distillate and brine orifice models in the dynamic model. Clearly there is a need for better orifice models in future. The orifice heights are in the similar range (0.5 to 30 mm for the distillate and 105 to 180 mm for the flashing brine) of Mazzotti et al. (2000) and within this range the stage orifice height profile is taken from Thomas et

al. (1998) in this work.

Table 7.1. Constant Parameters and Input Data for Simulation and Model Validation

	A_j / A_H	D_j^i / D_H^i	D_j^o / D_H^o	f_j^i / f_H^i	w_j / L_j / L_H	H_j
Brine heater	3530	0.022	0.0244	$1.86*10^{-4}$	12.2	
Recovery stage	3995	0.022	0.0244	$1.40*10^{-4}$	12.2	0.457
Rejection stage	3530	0.024	0.0254	$2.33*10^{-5}$	10.7	0.457

W_S	T_{steam}	$T_{seawater}$	C_S	R	C_W
$1.131*10^8$ kg/h	97°C	35 °C	5.7 wt%	$6.35*10^6$ kg/h	$5.62*10^6$ kg/h

7.3.2 Dynamic behaviour

The model is acceptable to represents the dynamic behaviour of the MSF process in view of its qualitative agreement with those from the literatures.

The dynamic model is validated using the results of Table 5.5 of Chapter 5. The MSF

Table 7.2. Summary of the Simulation Results

F kg/h	B_D kg/h	W_R kg/h	W_{steam} kg/h	C_R wt/wt
$5.68*10^6$	$4.76*10^6$	$1.203*10^7$	$1.348*10^5$	$6.29*10^{-2}$
$5.68*10^6$	*$4.78*10^6$*	*$1.203*10^7$*	*$1.316*10^5$*	*$6.27*10^{-2}$*
Stage Profiles (Brine heater stage j =0; TBT = T_{B0})						
Stage	B_j kg/h	D_j kg/h	C_{Bj} wt/wt	T_{Fj} °C	T_{Dj} °C	T_{Bj} °C
0	$1.203x10^7$		0.0629			89.74
	$1.203\ x10^7$		*0.0627*			*88.66*
1	$1.197\ x10^7$	$5.94\ x10^4$	0.06295	83.68	86.04	85.58
	1.197 $x10^7$	*5.98* $x10^4$	*0.0632*	*83.33*	*85.75*	*86.89*
2	$1.191\ x10^7$	$1.19\ x10^5$	0.0635	80.76	83.17	84.27
	1.191 $x10^7$	*1.12* $x10^5$	*0.0635*	*80.41*	*82.87*	*84.01*
3	$1.186\ x10^7$	1.78E+05	0.0638	77.78	80.24	81.35
	1.185 $x10^7$	*1.80* $x10^5$	*0.0639*	*77.44*	*79.95*	*81.08*
4	$1.180\ x10^7$	$2.39\ x10^5$	0.0641	74.76	77.25	78.37
	1.179 $x10^7$	*2.40* $x10^5$	*0.0642*	*74.43*	*76.97*	*78.11*
5	$1.174\ x10^7$	$2.99\ x10^5$	0.0644	71.69	74.21	75.34
	1.173 $x10^7$	*3.00* $x10^5$	*0.0645*	*71.37*	*73.94*	*75.09*
6	$1.168\ x10^7$	$3.60\ x10^5$	0.0648	68.58	71.13	72.27
	1.167 $x10^7$	*3.59* $x10^5$	*0.0649*	*68.28*	*70.88*	*72.04*
7	$1.162\ x10^7$	$4.20\ x10^5$	0.0651	65.43	68.00	69.16
	1.161 $x10^7$	*4.18* $x10^5$	*0.0652*	*65.16*	*67.78*	*68.95*
8	$1.156\ x10^7$	$4.81\ x10^5$	0.0654	62.25	64.84	66.02
	1.155 $x10^7$	*4.77* $x10^5$	*0.0655*	*62.01*	*64.65*	*65.84*
9	$1.150\ x10^7$	$5.41\ x10^5$	0.0658	59.04	61.64	62.85
	1.149 $x10^7$	*5.35* $x10^5$	*0.0659*	*58.84*	*61.49*	*62.70*
10	$1.144\ x10^7$	$6.01\ x10^5$	0.0661	55.80	58.42	59.66
	1.143 $x10^7$	*5.92* $x10^5$	*0.0662*	*55.65*	*58.32*	*59.55*
11	$1.138\ x10^7$	$6.61\ x10^5$	0.0665	52.55	55.18	56.45
	1.138 $x10^7$	*6.48* $x10^5$	*0.0666*	*52.46*	*55.13*	*56.39*
12	$1.132\ x10^7$	$7.20\ x10^5$	0.0668	49.29	51.91	53.23
	1.133 $x10^7$	*7.04* $x10^5$	*0.0669*	*49.27*	*51.93*	*53.24*
13	$1.126\ x10^7$	$7.716\ x10^5$	0.0672	46.02	48.64	50.01
	1.127 $x10^7$	*7.780* $x10^5$	*0.0673*	*46.09*	*48.74*	*50.09*
14	$1.121\ x10^7$	$8.30\ x10^5$	0.0675	44.25	45.79	47.24
	1.122 $x10^7$	*8.06* $x10^5$	*0.0676*	*44.06*	*45.87*	*47.28*
15	$1.116\ x10^7$	$8.82\ x10^5$	0.0678	41.25	42.84	44.36
	1.118 $x10^7$	*8.55* $x10^5$	*0.0679*	*41.10*	*42.95*	*44.42*
16	$1.110\ x10^7$	$9.34\ x10^5$	0.0681	38.17	39.80	41.40
	1.113 $x10^7$	*9.04* $x10^5$	*0.0682*	*38.07*	*39.98*	*41.51*

The results of this work are shown in italic

process is assumed to be at steady state condition at $T_{seawater}$ = 23 ^{0}C and T_{steam} = 97 ^{0}C (case 1, Table 5.5) and the model is simulated at that condition for 5 seconds (by setting all differential variables of the model to zero). An external disturbance of seawater temperature is considered where it increases from 23 ^{0}C to 45 ^{0}C (Case 3, Table 5.5 and T_{steam} remaining at 97 ^{0}C). Note, in reality the plant will not experience such a big step change in a short period of time. However, this case is considered to test the robustness of the dynamic model in terms of handing large step change. With the change in proposed seawater change, the plant will reach to a different steady state condition.

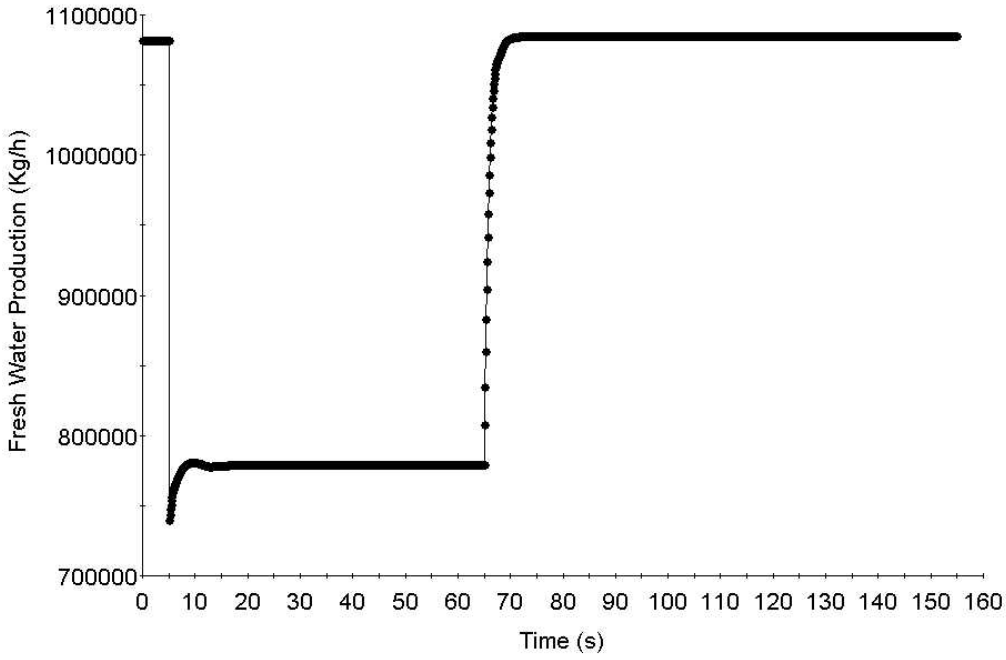

Figure 7.2 The Dynamic Model Prediction of Fresh Water Prediction to Seawater and Steam Temperature Disturbance

Figure 7.2 shows the steady state conditions in terms of freshwater production (the values are very close to those reported in Table 5.5). The dynamic model is now subjected to another step change but in terms of T_{steam} which is changed from to 97 ^{0}C to 116.5 ^{0}C (case

5, Table 5.5). This takes the freshwater production level back to the first steady state level (i.e. $T_{seawater}$ = 23 ^{0}C and T_{steam} = 97 ^{0}C) (as desired).

7.4 Dynamic Optimisation

Following on the example presented in section 7.3.2, it is decided to find out automatically (via dynamic optimisation within gPROMS) the desired steam temperature to maintain the fixed water demand while there is a step change in seawater temperature

Following optimisation problem is considered.

Given	A fixed fresh water demand, fixed seawater feed rate to MSF, fixed recycle flowrate, fixed rejected seawater flowrate, a given small but instantaneous step change in seawater temperature
Optimise	The steam temperature profile
So as to maximise	the Performance Ratio (PR) (defined as amount of freshwater per unit of energy consumption)
Subject to	Process constraints such as model equations and linear bounds of different variables

Mathematically, the optimisation problem can be written as:

OP

$$\underset{T_{steam},R,C_W}{Max} \quad PR$$

$$\text{s.t.} \quad f\left(x, \dot{x}, u, \dot{u}, v\right) = 0 \qquad \left(\text{model equations}\right) \qquad \left[t_0, t_f\right]$$

$$\left(93^o C\right)\ T_{steam}^L \le T_{steam} \le T_{steam}^U\ \left(101^o C\right)$$

$T_{seawater}$ = X1 (t <0, 8>

$T_{seawater}$ = X2 (t <10, 16>

$D^{end} = D^{*} = 9 \times 10^{6}$

R = 6.35×10^{6}

CW= 5.62×10^{6}

where X1 and X2 are seawater temperatures in the first and second intervals.

Control Vector Parameterisation (CVP) and SQP based dynamic optimisation techniques are used to solve the optimisation problem. Further details of the technique can be found in www.psenterprise.com and also in Mujtaba (2004).

7.4.1. Case Study

It is assumed that during a particular day of the spring season, the seawater temperature increases from 33 ^{0}C (9 am in the morning) to 39 ^{0}C (at 12 pm noon) and falls back to 33 ^{0}C (at 3pm in the afternoon) as shown in Figure 7.3. Although the temperature change will be gradual, but for the sake of convenience it is assumed that they change at discrete points as shown. It is also assumed that the steam temperature also changes at these discrete points. The purpose of this exercise is to find out optimum steam temperature at these discrete points which will be needed to off-set the change in seawater temperature while maintaining the same level of water demand and maximising the performance ratio (note, for a fixed water demand, steam temperature determines the amount of steam). The other input data are same as in Table 7.1.

The results are presented in Table 7.3. Note, it is assumed that the plant is operating at steady state right up to the point of changes of seawater temperature and reaches to the next steady state after 8s of the step change in the seawater temperature (as can be seen from Figure 7.4). Therefore, the results only include 16s operation prior and after the step

change. Basically, the second 8s operation is dynamic (as shown in Figure 7.4 for TBT). Figure 7.5 shows the dynamics of brine holdup of the first and last stage of the process for the seawater step change from 33 ^{0}C to 35 ^{0}C.

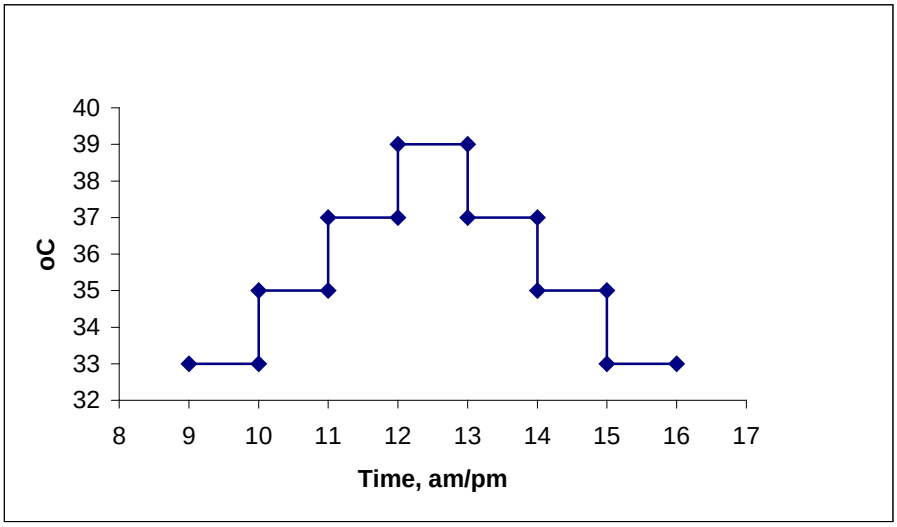

Figure 7.3 Discrete Seawater Temperature Profile during the Day

Table 7.3 Summary of the Results

Run	T_{steam}	$T_{seawater}$	PR
1	93.96	33	11.4481
$D^{end} = D^* = 9\times10^5$	95.76	35	
2	95.76	35	11.5376
$D^{end} = D^* = 9\times10^5$	97.55	37	
3	97.55	37	11.6261
$D^{end} = D^* = 9\times10^5$	99.35	39	
4	99.35	39	11.5376
$D^{end} = D^* = 9\times10^5$	97.51	37	
5 $D^{end} = D^* = 9\times10^5$	97.51	37	11.4481
	95.72	35	
6	95.72	35	11.3575
$D^{end} = D^* = 9\times10^5$	93.94	33	

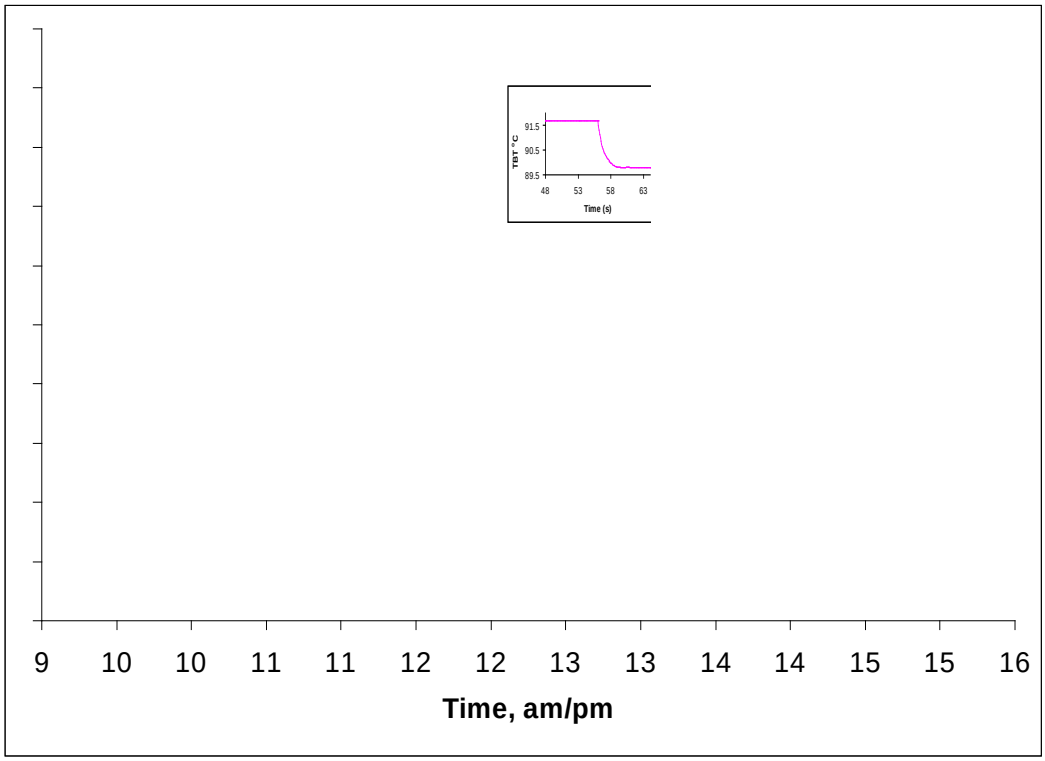

Figure 7.4 TBT Response of the Optimised Profile

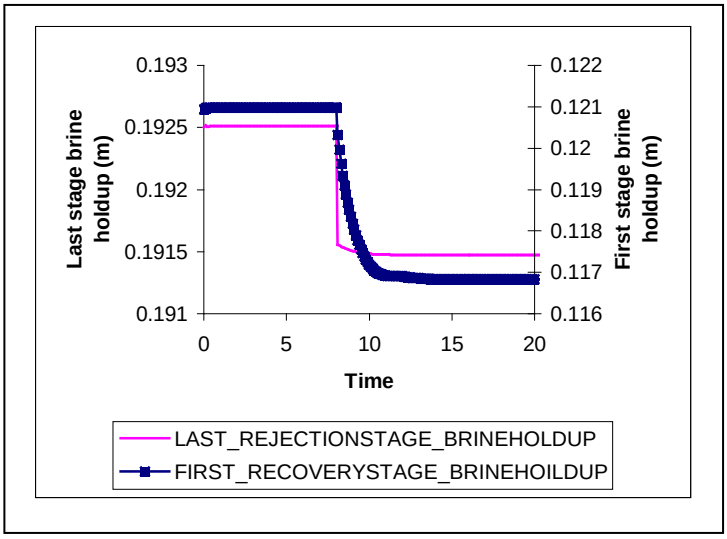

Figure 7.5 Brine Holdup Dynamics for Seawater Temperature Change from 33 C to 35^{O}C

The results clearly show that the change in steam temperature can off-set the change in seawater temperature while maintaining the fixed water demand. Also note, the PR values during the period (9 am to 3 pm) is almost constant.

7.5 Conclusions

A detailed dynamic MSF process model describing the physical behaviour of the plant and the operating procedures is presented. gPROMS software package has been used to construct the model. The model has considered non-equilibrium effects, demister pressure drop and the brine and distillate hold up equations. The model is validated using steady state condition and compared with the literature results. There is a close agreement between the predictions of the dynamic model at steady state condition with those presented by Rosso et al. (1996). The model is then used to simulate the process dynamics when subjected to seawater temperature change. The repetitive simulation confirmed the observed results obtained using the steady state model of Chapter 5.

Finally, the model is used within a dynamic optimisation framework to optimise steam temperature profile of the MSF process subject to several step changes in seawater temperature while ensuring fixed water demand and maximising the Performance Ratio.

In future, the dynamic model will be used for control study.

Chapter 8

Conclusions and Future Work

8.1 Conclusions

Desalination technology is the source of fresh water from sea, estuary or brackish water. As highlighted in Chapter 1 and 2, several desalination technologies exist in the world and among them MSF process produces 56% of the total fresh water (Husain, 2003)]. Simulation and optimisation help achieving better design and operation of MSF processes leading to low-cost production of fresh water. To carry out meaningful simulation and optimization to create alternative design and operation scenarios cheaply, development of a reliable process model is the first step (in the absence of a real plant).

Accurate estimation of Temperature Elevation (TE) due to salinity is important in developing reliable process model. Several empirical correlations exist in the literature to predict TE. However, in this work, several NN based correlations for predicting TE of seawater were developed. The NN based correlations predicted the experimental TE and TE obtained by using correlations form literature very closely. Predictions by different NN based correlations (for different salinity and BPT) within the training range followed the expected trends and it was within the engineering accuracy. For a given architecture, any correlation can be updated with additional data from other sources or a new correlation can be developed from the new source data.

In this work, gPROMS modelling tool has been used to model an MSF process

incorporating one of the NN based correlations developed earlier for estimating TE. The simulation results using the new model were in good agreement with the published results. NN based correlation predicted TE very well even slightly outside the range of training. The model was then used to study the sensitivity of two important operating parameters: the seawater temperature which is subject to seasonal variation, and the steam temperature in the brine heater which controls TBT of the process (indirectly controlling the design of the process). The results showed that the steam temperature played an important role to maintain the production rate of freshwater at different seasons (however, may be at the expense of costly design).

The interaction of design (number of flash chambers, heat exchange areas) and operation (steam flowrate, steam temperature, recycled brine flowrate, bottom brine temperature) in the context of fixed fresh water demand and seasonal variation of seawater temperature was then studied via repetitive simulation. For a given design, the results showed that some of the operating parameters had to be adjusted by 70% for a seawater temperature rise of 15%. It is very important to note here, in practice, a given plant design may not be flexible enough to accommodate this huge change in operating condition. Assuming the given design is flexible enough to accommodate all changes in operating conditions, the results showed (qualitatively) that the cost of water production in summer would increase. The simulation also showed that for fixed seawater temperature there might be a trade-off between design and operation.

The simulation results in Chapter 5 provided reasonable insight of the process performance and the next logical step was to formulate an appropriate optimisation problem where design and operating parameters were simultaneously optimised subject to seasonal variation in seawater temperature.

In Chapter 6, two MINLP based optimisation problems were considered for fixed water demand throughout the year. The number of flash stages (integer variable) and few significant operating parameters such as steam temperature, recycled brine flow and rejected seawater flow were optimised while minimising the external heat input to the process in the first optimisation problem while minimising total annualised cost in the second optimisation problem. The results from both optimisation problems clearly showed that a flexible scheduling of individual flash stages and operation was possible to supply fresh water at a fixed demand throughout the year with changing seawater temperature. Also the operating conditions in terms of TBT and T_{steam} did not change much and thus the amount of anti-scaling and anti-corrosion agents would not have to change with weather condition. Simultaneous optimisation of design and operation achieved clear benefits over the work on operation optimisation (by repetitive simulation) for a fixed or variable design (as in Chapter 5). In addition, the sensitivity analysis of the cost parameters showed that the optimal design and operation were sensitive to some of these parameters.

Finally, in Chapter 7, a dynamic MSF process model is presented which was validated using information form the literature. The model is then used to simulate the operation of MSF subject to step change in seawater temperature and steam temperature. The model is also used within dynamic optimisation framework to optimise steam temperature profile to maximise performance ratio subject to seawater temperature change of $6^{O}C$ over the period of 6 hrs.

8.2 Future Work

Following suggestions can be made for future work:

- As in Chapter 3, similar NN based correlations can be developed for other seawater properties such as density, viscosity, corrosion, scaling and other properties as well

as inter stage orifice model.

- Due to advancement of the microcomputer, plant automation becomes reliable means of plant maintenance. The intelligent system can be developed form the above control profiles using the neural network, neuro-fuzzy interface for supervision and control of the MSF desalination process.
- Neural network, neuro-fuzzy interface can be used to diagnose faults of MSF process.
- The model can be updated to include the degradation effects of scaling and corrosion with time and to reflect costing of different disposal methods.
- Also the MSF process model can be further developed incorporating the condensable and non-condensable gas behaviour, power devices such as pump, jet ejector, turbine.
- Hybrid desalination (Mixed MSF, MEE, RO) process can be considered, modelled and performance evaluated.
- Variable water demand (during the day and during the year) could be built up in optimisation framework considering intermediate storage.
- Detailed flexible scheduling of the unit modules can be designed to maintain efficiently for the MSF module without interrupting the production of water. This allows no requirement of full shut down of the plant. This needs detailed considerations by the designers, vendors, operators, etc.
- Dynamic model can be validated with real plant data by gPROMS validation tool (Experimental Design tools) or neural network based hybrid model (Mujtaba, 2004).
- Mixed integer dynamic optimisation can be studied of the MSF process for design and operation of the process.

- Controller design and controller study can be considered using the dynamic model developed in this work.

Nomenclature

A_H	Heat transfer area of brine	heater, m^2
A_j	Heat transfer area of stage j,	m^2
B_D	Blowdown mass flow rate,	kg/h
B_j	Flashing brine mass flow rate leaving stage j,	kg/h
B_o	Flashing brine mass flow rate leaving the brine heater,	kg/h
BBT	Bottom brine temperature =$T_{BNS,}$	^oC
C_{Bj}	Salt concentration in flashing brine leaving stage j,	wt/wt
C_B	C_{Bj} in	wt%
C_{BO}	Salt concentration in flashing brine in brine heater,	wt/wt
C_j	C_{Bj}	wt%
C_S	Feed seawater salt concentration,	wt/wt
C_R	Salt concentration in the cooling brine to the recovery section,	wt/wt
C_W	Rejected seawater mass flow rate,	kg/h
C_{xj}	Brine concentration,	g/l
D_H^i	Internal diameter of brine heater tubes,	m
D_H^o	External diameter of brine heater tubes,	m
D_j	Distillate flow rate leaving stage j,	kg/h
D^i	D_j^i	inch
D_j^i	Internal diameter of tubes,	m
D_H^o	External diameter of tubes,	m
EX_j	Non-equilibrium allowance,	^oC
F	Make-up seawater mass flow rate,	kg/h
f_H^i	Brine heater fouling factor	h m^2 ^oC/kcal
f_j^i	Fouling factor at stage j,	h m^2 ^oC/kcal
h_{Bj}	Specific enthalpy of flashing brine at stage *j*,	kcal/kg
h_f	Specific enthalpy of brine at T_F,	kcal/kg
h_{vj}	Specific enthalpy of flashed vapour at stage *j*,	kcal/kg
h_R	Specific enthalpy of brine at T_F,	kcal/kg
h_W	Specific enthalpy of brine at T_F,	kcal/kg
H_j	Height of brine pool at stage *j*,	m
L_H	Length of brine heater tubes,	m
L_j	Length of tubes at stage *j*,	m
$mean\_BPT$	Mean of the Temperature data for NN correlation,	^oC
$mean\_TE$	Mean of the Temperature elevation data for NN correlation,	^oC
$mean\_x$	Mean of the salinity data for NN correlation,	wt%
NS	Total number of stages, $N = NR + NJ$	

NJ	Number of stages in the heat rejection section	
NR	Number of stages in the heat recovery section	
R	Recycle stream mass flow rate,	kg/h
ρ	Brine density,	kg/m^3
S_{Bj}	Heat capacity of flashing brineleaving stage *j*,	kcal/kg/^oC
S_{Dj}	Heat capacity of distillate leaving stage *j*,	kcal/kg/^oC
S_{RH}	Heat capacity of brine in the brine heater,	kcal/kg/^oC
S_{Rj}	Heat capacity of cooling brine leaving stage *j*,	kcal/kg/^oC
std_BPT	Standard deviation of the boiling temperature data for NN correlation,	^oC
std_TE	Standard deviation of the temperature elevation data for NN correlation,	^oC
S_W	Mass flow rate to the reject seawater splitter	
std_x	Standard deviation of the salinity data for NN correlation,	wt%
T_{Bo}	Temperature of flashing brine leaving the brine heater,	^oC
T_{Bj}	Temperature of flashing brine leaving stage j,	^oC
T_B	T_{Bj}	^oF
T_{Dj}	Temperature of distillate leaving stage j,	^oC
T_D	T_{Dj}	^oF
TE_j	Boiling point elevation at stage j,	^oC
T_{Fj+1}	Temperature of cooling brine leaving stage j,	^oC
T_F	T_{Fj+1}	^oF
T_{sj}	Temperature of flashed vapour at stage j,	^oC
T_s	T_{sj}	^oF
T_{FNS+1}	Seawater temperature,	^oC
T_{Steam}	Steam temperature,	^oC
U_H	Overall heat transfer coefficient at the brine heater	
U_j	Overall heat transfer coefficient at stage j	
v	Linear velocity of stage,	ft/s
V_j	Flashed vapour mass flow rate at stage,	kg/h
w	w_j	ft
w_j	Width of stage,	m
W_s	Seawater mass flow rate to the heat rejection section,	kg/h
W_{steam}	Steam mass flow rate,	kg/h
W_s	Seawater mass flow rate	
x	salt concentration,	wt%
Δ_j	Temperature loss due to demister between demister and condenser tube,	^oC
λ_s	Latent heat of steam to the brine heater,	kcal/kg

INDEX

H	Brine heater
j	Stage index
*	Reference value

Reference

Al-Anezi, K. and Hilal, N. (2007) Scale formation in desalination plants: effect of carbon dioxide solubility, *Desalination,* **204**, 385-402.

Alasfour, F.N., Darwish, M.A. and Bin Amer, A.O. (2005) Thermal analysis of MEE-TVC+MEE desalination system, *Desalination,* **174**, 39-61.

Aldrich, C. and Slater, M. J. (2001) Simulation of liquid-liquid extraction data with artificial neural networks. In: *Application of neural networks and other learning technologies in process engineering*. (Eds, Hussain, M. A. and Mujtaba, I. M.) Imperial college pres,London: World Scientific Pub Co Inc.

AWWA (American Water Works Association) (2004) *Water Desalting Planning Guide for Water Utilities.* Hoboken, New Jersey: John Wiley and Sons.

Aziz, N., Mujtaba, I. M. and Hussain M. A. (2001) Set point tracking in batch reactors: use of PID and generic model control with neural network techniques. In: *Application of neural networks and other learning technologies in process engineering*. (Eds, Hussain, M. A. and Mujtaba, I. M.) Imperial college press, London: World Scientific Pub Co Inc.

Badger, W. L. (1959) Critical review of literature on formation and prevention of scale. Michigan: Office of saline water research and development for US department of the interior.

Beamer J.H. and Wilde, D.J. (1994) The simulation and optimization of a single effect multi-stage flash desalination plant. *Desalination,* **9** (3)**,** 259-275.

Bejan, A. (1996) *Thermal Design and Optimization.* New York: John Wiley & Sons.

Bhat, N. and McAvoy, T. J. (1990) Use of neural nets for dynamic modeling and control of chemical process systems. *Computers & Chemical Engineering,* **14**(4-5)**,** 573-582.

Borchers,B. and Mitchell, J. E. (1994) An improved branch and bound algorithm for mixed integer nonlinear programs. *Computers & Operations Research,* **21**(4)**,** 359-367.

Bomberger, J. D., Seborg, D.E. and Ogunnaike B.A. (2001) RBFN identification of an industrial polymerization. In: *Application of neural networks and other learning technologies in process engineering*. (Eds, Hussain, M. A. and Mujtaba, I. M.) Imperial college press, London: World Scientific Pub Co Inc.

Bromley, L. A., Singh, D., Ray, P., Sridhar, S. and Read S.M. (1974) Thermodynamic properties of sea salt solutions. *AIChE,* **20**(2)**,** 326 - 335.

Brooke (1992) *GAMS 2.25 User's Guide.* Scientific Press.

CAPE OPEN (2007) www.colan.org

Cardona, E., Culotta, S. and Piacentino, A. (2003) Energy saving with MSF-RO series desalination plants. *Desalination,* **153**(1-3)**,** 167-171.

Darwish, N.A. et al. (2007) Neural networks simulation of the filtration of the sodium chloride and magnesium chloride solutions using nanofiltration membranes. *Chemical Engineering Research and Design,* **85,** (A4)**,** 417-430.

Delene, J.G. and Ball, S.G. (1971) A digital computer code for simulating large multistage flash evaporator desalting plant dynamics, ORNL Report# ORNLTM_2933

Duran, M. A. and Grossmann I.E. (1986) An outer approximation algorithm for a class of mixed-integer nonlinear programs. *Math Progg.,* **36** (2)**,** 307-339.

Edgar, T. F., Himmelblau, D. M. and Ladson. L. S.. (2001) *Optimization of chemical processes.* Boston: McGraw-Hill.

Eikens, B., Karim, M.N. and Simon L. (2001a) Combining neural networks and first principle models for bioprocess modelling. In: *Application of neural networks and other learning technologies in process engineering*. (Eds, Hussain, M. A. and Mujtaba, I. M.) Imperial college pres, London: World Scientific Pub Co Inc.

Eikens, B., Karim, M.N. and Simon L. (2001b) Process identification with self -organizing networks. In: *Application of neural networks and other learning technologies in process engineering*. (Eds, Hussain, M. A. and Mujtaba, I. M.) Imperial college pres,London: World Scientific Pub Co Inc.

El-Dessouky, H. and Bingulac, S. (1996) Solving equations simulating the steady-state behavior of the multi-stage flash desalination process. *Desalination,* **107**(2)**,** 171-193.

El-Dessouky, H. T. and Ettouney, H. M. (2002) *Fundamentals of salt water desalination.* Amsterdam: Elsevier Science Ltd.

El-Dessouky, H., Shaban H. I. and Al-Ramadan H. (1995) Steady-state analysis of multi-stage flash desalination process. *Desalination,* **103** (1-3)**,** 271-287.

Eliceche, A. and Sargent, R. W. H. (1981) IChemE Symposium Series No 61, 1.

ElMoudir, W., ElBousiffi, M. and Al-Hengari S. (2007) Process modelling in desalination plant operations, In: *the Desalination and the Environment Conference* Halkidi:. 22-25 April

ElMoudir, W., ElBousiffi, M. and Al-Hengari S (2008) Process modelling in desalination plant operations. *Desalination,* **222,** 431-440.

Fabuss, B. M. (1980) Principles of desalination. Vol. 1 (Eds, Spiegler, K. S. and Laird, A. D. K.) New York: Academic Press.

Floudas, C. A. (1995) *Nonlinear and mixed-integer optimisation: Fundamentals and Applications.* USA: Marcombo.

Foust, A. S., Wenzel L. A., Clump C. W., Maus Louis and L. Bryce Andersen. (1980) *Principles of unit operations.* New York: Wiley.

Georgiadis, M.C., Giovanoglou, A., Pistikopoulos, E.N., Palacin-Linan, J. and Pantelides, C.C. (2005) gPROMS: An advanced tool for research and teaching on process modelling, simulation, design, control and optimisation. In Proceedings of PRES'05, Giardini Naxos, Sicily Italy ,15-18 May 393-398

Gille, D. (2003) Seawater intakes for desalination plants. *Desalination,* **156** (1-3)**,** 249-256.

Gosling, I. (2005) Process simulation and modelling for industrial bioprocessing tools and techniques. *Ind. Biotechnology,* **1** , (2), 106-109

gPROMS (2005) *gPROMS User Guide. 2005*: Process System Enterprise Ltd (PSE).

Griffin, W. and Keller, R., (1965) *Report ORNLL-TM- 1299.*

Glueck, A.R. and Bradshaw, R.W. (1970) A mathematical model for a multistage flash distillation plant, 3rd symposium on fresh water from the sea, **1**, 95-108.

Gupta, O.K. and Ravindran, A. (1985) Branch and bound in convex nonlinear integer programming. *Management Science,* **31** (12)**,** 1533-1546.

Hagan, M. T., Demuth, H.B. and Beale, M. (1996) *Neural Network Design.* Boston: PWS.

Hayakawa K., Satori, H., and Konishi, K. (1973) Process simulation of a multistage distillation plant, In *Proceedings 4th international symposium on fresh water from the sea*, **1**, 303.

Helal, A. M. (1985) Mathematical modelling and simulation of multistage flash (MSF) desalination plants. PhD Thesis, University of Leeds, UK.

Helal, A. M., Medani, M. S., Soliman M. A. and Flower J. R. (1986) A tridiagonal matrix model for multistage flash desalination plants. *Computers & Chemical Engineering,* **10**(4)**,** 327-342.

Husain, A. (Ed.) (2003) *Integrated power and desalination plants.* Oxford: Eolss.

Husain, A., Hassan, A., Al-Gobaisi, D. M. K., Al-Radif, A., Woldai, A.and Sommariva C. (1993) Modelling, simulation, optimization and control of multistage flashing (MSF) desalination plants Part I: Modelling and simulation. *Desalination,* **92** (1-3)**,** 21-41.

Husain, A., Woldai, A., AI-Radif, A., Kesou, A., Borsani, R., Sultan, H. and Deshpandey P. B. (1994) Modelling and simulation of a multistage flash (MSF) desalination plant. *Desalination,* **97** (1-3)**,** 555-586.

Ingham, J. (2000) *Chemical Engineering Dynamics: An Introduction to Modelling and Computer*. Weinheim; Chichester: Wiley-VCH.

Kondili, E. Pantelides, C.C. and Sargent, R.W.H. (1993) General algorithm for short-term scheduling of batch operations-I. MILP formulation. *Computers & Chemical Engineering,* **17**(2)**,** 211 -227.

Leyffer, S (1996) Integrating SQP and branch-and-bound for Mixed Integer Nonlinear Programming. *Computational Optimization and Applications,* **18,** 295-301.

Lior, N., Lizee, V. and Miyatake, O. (1997) Correlations for predicting the flow through MSF plant interstage orifices In: *IDA Madrid Proceedings,* Vol. V ,169-182 Madrid, Spain: IDA.

Maniar, V. M. and Deshpande, P. B. (1996) Advanced controls for multi-stage flash (MSF) desalination plant optimization. *Journal of Process Control,* **6**(18)**,** 49-66.

Marcovecchio, M. G., Mussati, S. F., Aguirre, P. A. and Scenna, N. J. (2004a) Optimization of hybrid desalination processes including multi stage flash and reverse osmosis systems. *Desalination,* **182** , 111–122.

Mazzotti, M., Rosso, M., Beltramini, A. and Morbidelli,M. (2000) Dynamic modeling of multistage flash desalination plants. *Desalination,* **127,** 207-218.

Mujtaba and Macchietto (1996) Simultaneous optimisation of design and operation of multicomponent batch distillation column--single and multiple separation duties. *Journal of Process Control,* **6**(10)**,** 27 -36.

Mujtaba, I. M. (2004) *Batch distillation: design and operation.* London: Imperial College Press.

Mujtaba, I. M. and Hussain, M. A. (Eds.) (2001) *Application of neural networks and other learning technologies in process engineering.* London: Imperial College Press.

Mussati, S. F., Marcovecchio, M. G. P.A. and Scenna, N.J.. (2004a) A new global optimization algorithm for process design: its application to thermal desalination processes. *Desalination,* **166** , 129-140.

Mussati, S. F., Aguirre, P.A. and Scenna, N.J. (2004b) A rigorous, mixed integer, nonlinear programming model (MINLP) for synthesis and optimal operation of cogeneration seawater desalination plants. *Desalination,* **166** , 339-345.

Mussati, S. F., Aguirre, P.A. and Scenna, N.J. (2005) Optimization of alternative structures of integrated power and desalination plants. *Desalination,* **182**(1-3)**,** 123-129.

M.W. Kellog Co. 1965. Saline Water Conversion Engineering Data Book. New York: Office of Saline Water Engineering Data Book, US Department of the Interior, on sale from the Superintendent of documents, Washington, D. C.

Nada, N. (2002) A thermodynamic assessment for the top brine temperature in MSF evaporator In: *Bahrain Proceedings*, Vol. CD Bahrain: IDA.

Oh, M. and Pantelides, C.C. (1996) A modelling and simulation language for combined lumped and distributed parameter systems. *Computer and Chemical Engineering*, **20**, 611-633.

Pantelides, C.C., Gritsis, D., Morison, K.R. and Sargent, R.W.H. (1988) The mathematical modelling of transient systems using differential-algebraic equations. Computer and Chemical Engineering, **12**(5), 449-454.

Pardoe, J. (1990) Optimisation strategies and methods for thermal desalination process flowsheets. PhD Thesis, University of Leeds, UK.

Papageogiou, L.G., Rotstein, G.E. and Shah, N. (2001) Strategic supply chain optimisation for the pharmaceutical industries. *Ind. Eng. Chem. Res.,* **40**(1)**,** 275 -286.

Pearce, N. (2004) Desalination- the solution for the water crisis? *The Chemical Engineering.,* **757,** 34-35.

Raman R. and Grossmann I.E. (1994) Modelling and computational techniques for logic based integer programming. Computers and & Chemical engineering **18,** 563-578

Reddy, K.V., Husain, A., A Woldai, A., Al-Gopaisi, D.M.K. (1995) Dynamic modelling of the MSF desalination process In: *IDA Abu Dhabi Proceedings*, Vol. IV ,227-224 Madrid, Spain: IDA.

Rimawi, M. A., Ettouney H. M.and Aly G. S. (1989) Transient model of multistage flash desalination. *Desalination,* **74,** 327-338.

Rosso, M., Beltramini, A., Mazzotti, M. and Morbidelli,M. (1997) Modeling multistage flash desalination plants. *Desalination,* **108** (1-3)**,** 365-374.

Shah, N. ,Pantelides, C. C. and Sargent, R. W. H. (1993) General algorithm for short-term scheduling of batch operations-II. Computational issues. *Computers & Chemical Engineering,* **17**(2)**,** 229 -244.

Sharif, M., Shah, N. and Pantelides, C. C. (1998) On the design of multicomponent batch distillation colums. *Computers & Chemical Engineering,* **22**(Supplement 1)**,** 69 - 76(8).

Scheffer, R. and Filho, R. M. (2001) Process identification of a fed-batch penicillin production process- training with the extended kalman filter. In: *Application of neural networks and other learning technologies in process engineering*. (Eds, Hussain, M. A. and Mujtaba, I. M.) Imperial college pres,London: World Scientific Pub Co Inc.

Spiegler, K. S. (1977) *Salt-water purification.* New York: Plenum Press.

Spiegler, K. S. and Laird, A. D. K. (Eds.) (1980) *Principles of desalination.* New York: Academic Press.

Tarifa, E.E., Humana,D., Franco,S., Martínez, S. L., Núñez, A. F. and Scenna, N. J. (2002) Fault diagnosis for a MSF using neural networks, *Desalination,* **152,** 215-222.

Thomas, P.J., Bhattacharyya, S. , Patra, A. and Rao G. P.. (1998) Steady state and dynamic simulation of multi-stage fash desalination plants: A case study. *Computers & Chemical. Engineering,* **22** (10)**,** 1515-1529.

Tijl, P. (2005) Assessment of the parameter estimation capabilities of gPROMS and Aspen Custom Modeler, using the sec-butyl-alcohol stripper kinetics case study. Graduation report, Eindhoven Technical University, Amsterdam

Valero, A., Lozano, M.A., Serra, L., Tsatsaronis, G. (1993) CGAM Problem: Definition and Conventional Solution. *Energy,* **19,** 279-286.

Van Roy, T.J. and Wolsey, L.A. (1986) Valid Inequalities for Mixed 0-1 Programs. *Discrete AppliedMathematics*, **14,** 199-213.

Vassiliadis, V.S., Sargent, R.W.H. and Pantelides, C.C., (1994) Solution of a Class of Multistage Dynamic Optimization Problems. 1. Problems without Path constarint. Industrial & Engineering Chemistry Research, **33**, 2111-2122.

Villafafila, A. and Mujtaba, I. M. (2005) Fresh water by reverse osmosis based desalination: simulation and optimisation. *Desalination,* **155(**1**),** 1-13.

Viswanathan, J. and Grossmann, I. E. (1990) A combined penalty function and outer-approximation method for MINLP optimization. *Computers & Chemical Engineering*, **14**(7)**,** 769-782.

Wagnick, K. (1991) 1990 worldwide desalting plants inventory the development of the desalination market. Mediterranean Conference Centre, Malta: Institution of Chemical Engineers.

Yee, T. F., Grossmann, I. E. and Kravanja Z. (1990) Simultaneous optimization models for heat integration-III. Process heat exchanger. *Computers & Chemical Engineering,* **14,** 1185-1200.

Zupan, J. and Gasteiger, J. (1999) *Neural Networks in Chemistry and Drug Design.* Weihein, Germany: Wiley-VCH.